NPS-58DW9072A

UNITED STATES
NAVAL POSTGRADUATE SCHOOL

THE T-S GRADIENT METHOD, A NEW METHOD OF COMPUTING GEOSTROPHIC CURRENTS OVER LARGE OCEAN AREAS

by

Warren Wilson Denner

June 1969

NAVAL POSTGRADUATE SCHOOL
Monterey, California

Rear Admiral R. W. McNitt, USN
Superintendent

R. F Rinehart
Academic Dean

ABSTRACT:

Requirements for indirect computation of geostrophic surface currents over large ocean areas are discussed. These requirements point to a need to simplify standard geostrophic computations, and to separate the first order thermal and haline contributions to geostrophic flow.

The equations of motion for geostrophic flow are reviewed and the standard geostrophic computations discussed. Errors and limitations in the geostrophic method are reviewed. Previous attempts to simplify geostrophic computations are discussed and shown to be inadequate for synoptic computation over hemispheric ocean areas.

It is shown that the Helland-Hansen equation can be rewritten such that the geostrophic velocity is composed of a temperature structure term and a salinity structure term. In order to apply this modified equation to hemispheric synoptic geostrophic computations, simple expressions are required for the dependence of specific volume on temperature at constant salinity and pressure, $(\partial\alpha/\partial T)_{S,P}$, and on salinity at constant temperature and pressure, $(\partial\alpha/\partial S)_{T,P}$. Two approaches are explored to derive these expressions, using:

1) Experimental P-V-T-S data collected in the laboratory.
2) P-V-T-S data derived from an equation of state for sea water.

Numerical fitting of the experimental P-V-T-S data shows that the dependence of specific volume on temperature, $\alpha(T)_{S,P}$, can be expressed by a quadratic equation and the dependence of specific volume on salinity, $\alpha(S)_{T,P}$, can be expressed by a linear equation. The coefficients in the temperature dependence equation are a function of salinity and pressure, and the coefficient in the salinity dependence is a function of temperature and pressure. However, it is shown that the lack of experimental data and the presence of small errors in the data lead to inconsistencies in the values of the coefficients derived. This difficulty is corrected using Ekman's equation of state for sea water to generate P-V-T-S data.

Using derived expressions for $(\partial\alpha/\partial T)_{S,P}$ and $(\partial\alpha/\partial S)_{T,P}$ an equation is derived from the Helland-Hansen relationship and is called the Temperature-Salinity Gradient scheme for computing geostrophic currents, or simply T-S Gradient scheme. This scheme gives equivalent results to the standard geostrophic computations, yet is computationally much simpler and faster than the standard scheme. Other advantages are (1) the variables observed in the ocean, temperature and salinity structure are used directly in the computations (2) no other quantities such as σ_o and σ_t need be computed, and

(3) thermal and haline contributions to the geostrophic flow can be expressed independently.

The T-S Gradient scheme is applied to existing hemispheric fields of T and S data. It is shown that in the expressions for $(\partial\alpha/\partial T)_{S,P}$ and $(\partial\alpha/\partial S)_{T,P}$ the use of fixed coefficients over the entire Pacific Ocean relative to a reference level of 1000 db, introduces less than five percent error in the surface velocity. This application shows the feasibility of making geostrophic computations by the T-S gradient scheme. Unfortunately, it also shows the deficiencies of the available fields for hemispheric computations by any scheme. These deficiencies are (1) the inaccuracy of the data, (2) the large grid spacing, and (3) the inconsistency of the temperature and salinity fields. These must be corrected before hemispheric geostrophic computations can be made. The construction of new fields to meet the requirements of geostrophic computations using available data is discussed.

Two other aspects of current computation were investigated. First, using the capability of the T-S Gradient scheme to separate flow into thermal and haline components, the relationship between the thermal component and the total geostrophic surface current in the Gulf Stream water mass in the Grand Banks was studied. Results show that these quantities are satisfactorily related by a linear expression which allows the determination of the total geostrophic surface flow in this water mass using only temperature measurements. Such techniques may be useful in reducing survey time of the Coast Guard Ice Patrol in this region.

A second aspect investigated is the relationship between the indirectly computed currents and measured currents in the California current. Two experiments were performed in which drogue-measured surface currents were compared to indirectly computed currents given by the Fleet Numerical Weather Central and those computed by the Helland-Hansen and T-S Gradient schemes using standard hydrographic data. This investigation points out the significant need for more work on this aspect.

This task was supported by: Fleet Numerical Weather Central
Monterey, California

WARREN W. DENNER
Assistant Professor of Oceanography

Approved by:

D. F. LEIPPER, Chairman
Department of Oceanography

Released by:

for C. E. MENNEKEN
Dean of Research Administration

The T-S Gradient Method, A New Method of Computing Geostrophic Currents over Large Ocean Areas

by

Warren Wilson Denner

Department of Oceanography
Naval Postgraduate School
Monterey, California

A REPORT

submitted to

Fleet Numerical Weather Central
Monterey, California

in fulfillment of Work Request 9-00111

June 1969

ACKNOWLEDGEMENTS

I would like to acknowledge the contribution of my colleagues and the students at the Naval Postgraduate School, whose interest and discussions have encouraged me in my work. In particular, I would like to acknowledge the efforts of Dr. Glenn Jung who read my report in an early stage and made so many helpful suggestions. I would also like to acknowledge the aid in computer programming provided by Mr. Robert Middelburg.

Finally, I would like to acknowledge the support of Fleet Numerical Weather Central, Monterey, California for making it possible to complete this work.

TABLE OF CONTENTS

LIST OF FIGURES

LIST OF TABLES

THE T-S GRADIENT METHOD, A NEW METHOD OF COMPUTING GEOSTROPHIC CURRENTS OVER LARGE OCEAN AREAS

I. INTRODUCTION

The purpose of the research reported in this study is to improve the contemporary techniques of computing synoptic geostrophic ocean surface currents over large ocean regions. Techniques that are used today are either gross approximations with little scientific basis or applicable to only small regions, or both. Yet knowledge of surface currents is important, and in some cases essential to public, commercial, and military use of the sea.

The U. S. Coast Guard uses surface current information in search and rescue, as well as in the forecasting of iceberg drift for the shipping lanes in the Northwest Atlantic (Lenczyk, 1964). The U. S. Navy Fleet Numerical Weather Central, Monterey, California, computes surface currents every 12 hours over the Northern Hemisphere principally to aid in thermal structure forecasting (Hubert and Laevastu, 1967). The U. S. Naval Oceanographic Office computes surface currents in the ASWEPS (Antisubmarine Warfare Environmental Prediction System) area of the Northwest Atlantic for thermal structure forecasting (James, 1966).

Mariners have been using knowledge of ocean currents probably

since the beginning of navigation. As early as 600 BC the east to west circum-navigation of Africa may have been aided by favorable winds and currents (von Arx, 1962). Early Greek and Arab traders could penetrate the Arabian Sea and Bay of Bengal because of favorable currents under the influence of the monsoon winds. Spanish trade between Mexico and the Philippines was also aided by knowledge of the winds and currents (Jones, 1939). The Spanish captains would take advantage of the North Equatorial Current on their westerly journey, and return to Mexico along a more northerly route reaching land fall around Cape Mendocino. An early chart of the Gulf Stream was published by Benjamin Franklin in 1770. This chart is said to have improved mail service from England to the American Colonies by two weeks per crossing (Groen, 1967). Pilot charts, published by the Naval Oceanographic Office, provide monthly summaries of wind and surface current conditions. Surface current atlases giving the monthly mean values are also available from the Naval Oceanographic Office.

Flow in the surface layers of the deep ocean is influenced by several forces: the most important are the horizontal pressure gradient and viscous forces within the fluid, the action of wind stress, tidal forces, and the Coriolis force. Today incomplete knowledge of ocean dynamics and lack of suitable available data restricts the indirect determination of surface currents to the computation of the

geostrophic and wind driven components (Hubert, 1965).

Computation of geostrophic flow over a large ocean area on a synoptic basis are facilitated if the computations be as simple and as fast as possible. Standard geostrophic computations are unsuitable for many reasons:

1) The computations are numerous and consume more computer time than is available for this task.

2) Several quantities must be computed that are not used beyond the analysis of currents.

3) The temperature and salinity data that are required for standard geostrophic computations are not yet available in the necessary accuracy and density.

4) It would be useful to compute the temperature and salinity structure contributions to the geostrophic current independently. This is difficult by the standard method.

Further explanation of the last two points is in order. Because of the relative ease of measuring temperature structure over the salinity structure, temperature is a much more commonly observed variable in the ocean. Until the recent development of in situ conductivity measurement, rapid determination of salinity structure was not possible. For this reason, while nearly synoptic thermal structure information may be available from many areas of the oceans, salinity structure is available only from the historical records

contained in oceanographic data centers and various atlases derived from this historical data. It will probably be several years before salinity structure is as commonly observed as thermal structure. It is because of this compatability that it is desirable to compute the temperature and salinity contributions to the geostrophic flow separately. Furthermore, salt is not as easily exchanged between the air and sea as is heat, and therefore, it may be more acceptable to use historical data for salinity information than for temperature information. By directly computing the thermal and haline components of the geostrophic flow the significance of air-sea heat exchanges on thermohaline flow may be more easily examined.

To summarize, the purpose of this thesis is to study a simplified method of computing geostrophic surface currents over large ocean areas that gives essential agreement with currents computed by the standard geostrophic method. The derived method must be computationally faster on digital computers than the standard method. Furthermore, that the method ought to express, at least to first order, the thermal and haline components separately.

II. THE GEOSTROPHIC CURRENT

The Equations of Motion for Geostrophic Flow

Fluid is said to be in geostrophic balance if the flow is unaccelerated and the horizontal pressure gradient is balanced by the Coriolis force. The simplified equations of motion for geostrophic flow in rectangular coordinates (x axis east, y axis north and z axis positive down from the sea surface) are:

$$f\hat{k} \times \vec{V}_H = \alpha \overrightarrow{\nabla_H P} \tag{1}$$

$$\vec{g} = \alpha \frac{\partial \vec{P}}{\partial Z} \tag{2}$$

where

$f = 2\omega \sin \phi$ is the Coriolis parameter (1/ sec)

ω = the angular velocity of the earth (radians/sec)

ϕ = the geographic latitude (degrees)

$\vec{V}_H$ = the horizontal velocity (cm/sec)

$\vec{g}$ = the local acceleration of gravity (cm/sec^2)

α = specific volume (cm^3/gm)

$\overrightarrow{\nabla_H P}$ = the horizontal pressure gradient ($dynes/cm^2$)

$\frac{\partial \vec{P}}{\partial Z}$ = the vertical pressure gradient ($dynes/cm^2$)

$\hat{k}$ = the vertical unit vector

Given the horizontal pressure gradient along a level surface the geostrophic flow along the surface could be determined directly from Equation 1. However, direct measurement of the horizontal pressure gradient in the sea has not been achieved. Several schemes have been developed to compute the horizontal pressure gradient from the mass distribution as determined from the measured temperature and salinity distributions.

The Helland-Hansen Equation

Geostrophic computations, also often referred to as dynamic computations or the dynamic method, are discussed in any elementary physical oceanography text, for example Neumann and Pierson (1967). Fomin (1964) discusses in considerable detail the application and the limitation of the dynamic method. Yao (1967) gives an excellent review of various computational schemes for computing geostrophic currents. What might be called the standard or classical method is based on an equation originally derived from Bjerknes' circulation theorem (1900) by Sandstrom and Helland-Hansen (1903), (as cited by Proudman, 1953). However, the resulting equation is commonly referred to in the literature as the Helland-Hansen equation. The Helland-Hansen equation, written in terms of the horizontal gradient of the geopotential between two levels P_1 and P_2 is,

$$\hat{fk} \times (\overrightarrow{V_1 - V_2}) = \overrightarrow{\nabla_H \int_{P_1}^{P_2} a(x, y, p)dp} \qquad (3)$$

where

$\int_{P_1}^{P_2} a(x, y, p)dp$ = the geopotential of level P_1 with respect to P_2 $(cm/sec)^2$

$(\overrightarrow{V_1 - V_2})$ = the horizontal velocity at P_1 relative to the level P_2 (cm/sec)

The geopotential difference between two levels in the ocean is determined by the integral in the right-hand term of Equation 3. The integral is numerically evaluated (using the trapazoidal rule) from computed vertical density distributions, determined from the measured vertical temperature and salinity structure. Using two stations the measured temperature and salinity structure can be used to compute the horizontal gradient in geopotential along an isobaric surface, and Equation 3 can be evaluated to give the geostrophic flow between the two stations.

The Limitations of the Dynamic Method

Use of Helland-Hansens'formula suffers from several limitations (Fomin, 1964). The feasibility of computing ocean currents using the dynamic method is based on the following assumptions:

1) The horizontal velocity and the horizontal pressure gradient is balanced by the Coriolis force.

2) The horizontal velocity and the horizontal pressure gradient become negligible at a moderate depth below the sea surface.

3) The field accelerations and frictional forces can be neglected (Sverdrup, 1947).

That these assumptions are realistic for the large scale motions, at least sometimes, has been illustrated by Stommel (1965). Even when the assumptions of geostrophy are satisfied, the necessary measurements are difficult to obtain to the desired accuracy.

Errors in the Dynamic Method

Errors in the dynamic method have been estimated by many authors, however, no completely satisfying error analysis of geostrophic procedures is available. The errors in computing the geostrophic current from standard hydrographic measurements (temperature and salinity at discrete levels) can be divided into the two categories, measurement errors and computational errors.

Errors in the geostrophic current due to errors in the hydrographic measurements have been discussed by Wooster and Taft (1958), Reid (1959) Fomin (1964), and others. Following Reid (1959) the measurement errors in classical hydrographic work are summarized below:

1. Incorrect temperatures due to errors in temperature readings.
2. Incorrect temperatures due to errors in the location of the measurement.
3. Incorrect salinities due to errors in the salinity readings.
4. Incorrect salinities due to errors in the location of the measurement.
5. Incorrect temperature due to time and space variability.
6. Incorrect salinity due to time and space variability.

The errors in computing geostrophic currents due to computational procedures have been discussed by Rattray (1961), Fomin (1964), Yao (1967) and others. These errors are summarized below:

1. Errors in interpolation of point hydrographic data between sampling levels.
2. Rounding and truncation errors in the numerical integration.

Due to the dependence of the measurement and computational errors on one another, no completely rigorous analysis is yet available for the accumulated error in determining geostrophic currents by the dynamic method. The analysis by Fomin (1964) appears to be the most complete to date, but his discussion is not fully documented. The magnitude of the total error in dynamic height due to measurement and computational errors has been estimated independently by

several authors. Some of the available estimates are presented in Table 1. Error in the geostrophic current due to the indicated error in dynamic height is given in Table 1 for stations separated by 100 km at 45° latitude.

Table 1. Estimates of the error in the dynamic height and geostrophic surface current relative to 1, 000 db.

Author	Dynamic Height Error (dynamic meters)	Velocity Error (cm/sec)
Wooster and Taft (1958)	0. 011	1. 1
Reed and Laird (1966)	0. 003	0. 3
Kollmeyer (1964)	0. 018	1. 8
Fomin (1964)	0. 004	0. 4

The significance of these errors on geostrophic computations depends on the magnitude of the current. Certainly if the currents at mid-latitudes are only a few cm/sec then the relative error may be 50 to 100 percent. Fomin (1964) states in his conclusions concerning the accuracy of the geostrophic current computations that, "computational errors may completely distort the result." Reid (1960) estimates that the combined error in salinity, temperature, pressure and position are on the order of 20 percent. While these relative errors seem prohibitive, an important point must be made here: from a practical point of view it is significant to know that

the geostrophic currents are weak. Therefore, if the currents are less than a few centimeters per second, this fact can be determined even if the relative error is large.

Verification of Geostrophic Surface Currents

A few direct current measurements have been collected in support of geostrophic computations from hydrographic measurements. The classic case is a comparison reported by Wust (1924) of Pillsbury's current observations (1885-1889) in the Straits of Florida to geostrophic currents computed from hydrographic data collected in 1888 and 1912. Observed currents are in remarkable agreement with the computed geostrophic currents. von Arx (1962) reports a comparison of currents observed with the geomagnetic electrokinetograph (GEK) and dynamic topography showing substantial agreement in the Gulf Stream. Broida (1966) made simultaneous measurements of currents and hydrographic casts in the Florida Straits. His measured surface currents were in fair agreement with the computed geostrophic surface currents. Reed (1965) compared geostrophic currents and currents measured by parachute drogue in the Alaska Stream and found excellent agreement between the two values for the surface current. Smith (1931) showed a definite association between the geopotential topography in the Grand Banks Region and

the drift paths of icebergs that established the basis for the U. S. Coast Guard hydrographic surveys of this region which continue today.

III. STANDARD GEOSTROPHIC COMPUTATIONS

Prior to exploring attempts to simplify the standard geostrophic computations these computations should be reviewed. Several schemes have been suggested for computing geostrophic currents: (1) the geopotential scheme using the Helland-Hansen formula (Equation 3), (2) the acceleration potential scheme of Montgomery and Stroup (1962), and (3) the isanosteric contour slope scheme of Werenskjold (1935, 1937). These three methods have been reviewed by Yao (1967). Only the geopotential scheme will be reviewed here, because of its role in later sections of this thesis, and its more frequent use over the other methods.

The standard computations in the geopotential scheme as expressed by the Helland-Hansen equation are expressed in the following equation:

$$(V_1 - V_2) = \frac{(\Delta D_A - \Delta D_B)}{f\Delta n} \qquad (4)$$

where

$\Delta D_A - \Delta D_B$ = the difference in the anomaly of dynamic height at stations A and B $(cm/sec)^2$

ΔD = $\sum_i \bar{\delta}_i \Delta P_i$, where $\bar{\delta}_i$ is the average specific volume anomaly in the i^{th} pressure interval $(10^{-5}\ cm^3/gm)$

$(V_1 - V_2)$ = the magnitude of the relative current normal to a line joining the two stations (cm/sec)

In order to carry out geostrophic computations with Equation 4 several complicated formulae must be used, or the empirical expression of these formulae in tables (LaFond, 1951). The formulae necessary to calculate in situ specific volume anomaly from measured or interpolated temperature and salinity are summarized by Yao (1967).

Salinity as a function of chlorinity is given by Knudsen's (1901) equation:

$$S = 0.030 + 1.805\ Cl \quad \text{(Knudsen, 1901)} \tag{5}$$

where

S = salinity (‰)

Cl = chlorinity (‰)

If the measurement of electrical conductivity is to be used to determine salinity or chlorinity then other formulae or tables must be used.

Given the chlorinity the quantity σ_o can be computed.

$$\sigma_o = -0.069 + 0.4708Cl - 0.001570Cl^2 + 0.0000398Cl^3 \tag{6}$$

And with σ_o the quantity σ_t can be computed.

$$\sigma_t = \Sigma_T + (\sigma_o + 0.1324)[1 - A_T + B_T(\sigma_o - 0.1324)] \quad (7)$$

where

$$\sigma_t = (\rho_{S,T,O})10^3 \qquad \text{(Bjerknes and Sandstrom, 1910)}$$

and

$\rho_{S,T,o}$ = the *in situ* density at atmospheric pressure

$\sigma_o = \sigma_t$ if $T = 0°C$

$$\Sigma_T = \left[\frac{(T - 3.98)^2}{503.570}\right]\left[\frac{T + 283}{T + 67.26}\right]$$

$$A_T = T(4.7867 - 0.09815T + 0.0010843T^2)10^{-3}$$

$$B_T = (18.030 - 0.8164T + 0.01667T^2)10^{-6}$$

T = temperature (°C)

The specific volume of a sea water sample *in situ* can then be computed from the equation of state (Ekman, 1908)

$$a_{S,T,P} = a_{S,T,o} - Pa_{S,T,o}10^{-9}\left\{\frac{4886}{1 + 0.000183P} - [227 + 28.33T \quad (8)\right.$$

$$- 0.551T^2 + 0.004T^3] + P10^{-4}[1055 + 9.50T - 0.158T^2]$$

$$- 1.5P^2T\,10^{-8} - \frac{\sigma_o - 28}{10}[147.3 - 2.72T + 0.04T^2$$

$$-P10^{-4}(32.4 - 0.87T + 0.002T^2)] + \left(\frac{\sigma_o - 28}{10}\right)^2[4.5$$

$$\left. + 0.1T - P10^{-4}(1.8 - 0.6T)]\right\}$$

where

$a_{S, T, P}$ = *in situ* specific volume (cm^3/gm)

$a_{S, T, o}$ = specific volume at atmospheric pressure (cm^3/gm)

P = pressure (decibars)

Frequent oceanographic practice uses the specific volume anomaly rather than the specific volume.

$$\delta = a_{S, T, P} - a_{35, O, P} \tag{9}$$

where

δ = specific volume anomaly (cm^3/gm)

$a_{35, O, P}$ = specific volume at S = 35‰, T = 0° C, and P decibars (cm^3/gm)

the latter quantity is computed from the following equation:

$$a_{35, O, P} = a_{35, O, O} - Pa_{35, O, O}\left[\frac{4886}{1 + 0.0000183P} - 227 + 0.01055P - (\sigma_{35, O, O} - 28)(14.73 - 0.0000324P)\right] 10^{-9} \tag{10}$$

where

$a_{35, O, O} = 0.972643\ cm^3/gm$

$\sigma_{35, O, O} = 28.126$

Specific volume is often expressed in the following way:

$$\delta = \Delta_{S,T} + \delta_{S,P} + \delta_{S,T,P} \quad \text{(Sverdrup, 1933, cited (11) by LaFond, 1951)} \qquad (11)$$

where

$\Delta_{S,T} = \delta_S + \delta_T + \delta_{S,T}$ and is called the thermosteric anomaly (cm^3/gm) (Montgomery and Wooster, 1954)

$$\Delta_{S,T} = 0.0273596 - 10^{-3}\sigma_t/(1 - 10^{-3}\sigma_t)$$

$$= \alpha_{S,T,O} - \alpha_{35,O,O}$$

$$\delta_{S,P} = \delta_{S,O,P} - \delta_{35,O,O}$$

$$\delta_{T,P} = \delta_{35,T,P} - \delta_{35,O,O}$$

$\delta_{S,T,P} = \delta - \Delta_{S,T} - \delta_{S,P} - \delta_{T,P}$ ($\delta_{S,T,P}$ is an order of magnitude smaller than any of the other terms and normally neglected in geostrophic calculations.)

The individual terms in Equation 11 are given in tables (Sverdrup et al., 1942 and LaFond, 1951).

These formulae illustrate the computational complexity of standard geostrophic computations. To carry out these computations synoptically, on a hemispheric grid such as that used by the U. S. Navy Fleet Numerical Weather Central is not desirable if it can be avoided. The question remains can geostrophic computations be simplified, without giving up necessary accuracy?

IV. PAST EFFORTS TO SIMPLIFY GEOSTROPHIC COMPUTATIONS

Several attempts have been made to simplify geostrophic computations. The attempts can be divided into three categories: those which (1) neglect the pressure dependent terms in the specific volume anomaly, (2) assume a simple relationship between the density of sea water and the variables (temperature, salinity, and pressure), and (3) determine the correlation function between two of the variables in particular water masses. The first approach is the most direct and will be the most generally applicable, and is discussed in the following section.

Thermosteric Anomaly

Montgomery and Wooster (1954) showed that the "thermosteric anomaly," $\Delta_{S,\,T}$, can be substituted for the specific volume anomaly in geostrophic computations under some conditions without significant loss of accuracy. One condition is that the computations be limited to the upper layers, above 1,000 db where the pressure terms ($\delta_{S,\,P}$ and $\delta_{T,\,P}$) are not large; thus the thermosteric anomaly is a good approximation to the specific volume anomaly.

Performing geostrophic computations on 47 hydrographic stations from the Atlantic and Pacific oceans, using both the complete specific volume anomaly and the thermosteric anomaly, Montgomery

and Wooster showed that, except for one station in the Atlantic Ocean, the pressure terms contribute at most five percent to the station to station difference in the anomaly of dynamic height. These authors stated (page 66):

> The conclusion is reached that for hydrostatic computation limited to the upper 500 db or 1,000 db, especially in the Pacific Ocean, if extreme precision is not required and if significant convenience is gained, the pressure terms may be neglected; in other words the thermosteric anomaly $\Delta_{S,T}$ may be used in place of the complete specific volume anomaly δ.

While this is clearly a simplification of the standard geostrophic computations, the use of the thermosteric anomaly requires determination of σ_o and σ_t. Since the sole purpose for determining these quantities is to evaluate the thermosteric anomaly in geostrophic computations, a scheme which would allow geostrophic computations without the determination of these preliminary quantities would be more efficient. An interesting point made by Montgomery and Wooster is that for all practical purposes the pressure terms are nearly linear from the surface to the 2,000 db level or deeper.

Temperature-Salinity Correlation Methods

One of the earliest attempts to simplify dynamic computations is that of Stommel (1947) through the use of temperature and salinity correlation. Since specific volume is a function of

temperature, salinity and pressure, all three of these variables must be accurately known in order to compute this quantity. However, if a correlation exists between any two of the independent variables, say temperature and salinity, then the specific volume anomaly could be expressed in terms of only two quantities, since the correlation function determines the relationship between the other two quantities. Since temperature as a function of depth is an easier and more common measurement, Stommel suggested geostrophic computations could be made from temperature structure measurements alone using the temperature-salinity correlation to determine the salinity; from this the specific volume anomaly and then the dynamic height could be evaluated. Oceanographers have long recognized that temperature and salinity are correlated in certain water masses (Sverdrup et al., 1942). That is, for each temperature there will be a small range of salinity in a given water mass.

Assuming that a satisfactory temperature-salinity correlation exists in a given water mass, then using this temperature-salinity correlation a new set of tables can be constructed giving the specific volume anomaly as a function of only two terms:

$$\delta = [T] + [T, P] \tag{12}$$

The first term on the right-hand side, $[T]$, is in reality the thermosteric anomaly, $\Delta_{S,\,T}$, which is a function of the temperature only

because of the established temperature-salinity correlation. The second term, $[T, P]$, includes $\delta_{S, P}$ and $\delta_{T, P}$, but is fully determined from temperature and depth in the given water mass because of the established temperature-salinity correlation. It is clear that the accuracy of the temperature-salinity correlation method is dependent on the nature of the temperature-salinity correlation. For each temperature there will be a certain finite range of salinity (R_s) which will represent the uncertainty in specifying the salinity from the temperature-salinity correlation. The uncertainty in salinity decreases with the slope of the temperature-salinity curve on the temperature-salinity diagram. Obviously this is due to the fact that for small slopes a small error in the temperature leads to a large change in the implied salinity. The uncertainty in salinity will also be large whenever seasonal variation and mixing lead to a poor temperature-salinity correlation. Values of R_s can be determined at each level from the scatter of temperature-salinity pairs around the mean. Associated with the value of R_s at each level for a given water mass is an uncertainty in specific volume R_δ. Summation of the values of R_δ over the water column during the computation of dynamic height gives a measure of the uncertainty in the calculated dynamic height introduced by the uncertainty in the temperature-salinity correlation.

Stommel applied the temperature-salinity correlation technique

to stations of the International Ice Patrol (3275 to 3278) off the Grand Banks, ATLANTIS stations 1637 to 1642 across the Gulf Stream, and some stations (unidentified) from the Sargasso Sea. He found that the use of temperature-salinity correlation was unsuited off the Grand Banks as the temperature-salinity correlation is poor in this region. His results are not surprising since the Grand Banks region is a mixing region for water masses of the Labrador Current and Gulf Stream (Kollmeyer, 1966). In the Gulf Stream he found that the temperature-salinity correlation method can be applied, but only if the stations are grouped, as the temperature-salinity correlation changes across this current. However, in the Sargasso Sea where temperature-salinity correlation is excellent the method seems well suited. Stommel concludes (page 91):

> As a result it appears that in certain restricted regions the temperature-salinity diagram may be used for rough dynamic computations. For more details survey work where great accuracy of the results is desired the method using the temperature-salinity diagram is clearly unsuitable.

LaFond (1949) applied the temperature-salinity correlation scheme in the Marshall Island region in an attempt to determined the geostrophic flow in this region using bathythermograms. He used existing hydrographic data to establish the temperature-salinity correlation function for this region. LaFond's conclusion (page 236) summarizes the results of his studies:

To use bathythermograms in determining relative currents, there are several prerequisites which must be met: (1) the bathythermogram must extend at least to 900 ft., (2) the temperature-salinity relation must be established, with consideration of seasonal and geographic effects, and (3) the effects of internal waves must be largely eliminated. If these conditions are attainable the direction of relative currents can be established from bathythermograms. The results of this test indicate that the speed of the current (0/305 db) can be within 25 percent of those obtained from Nansen bottle and reversing thermometer data (0/1, 000 db).

Yausi (1955) used temperature-chlorinity correlation in the Kuroshio Current, and later (1957) in the adjacent seas of Japan to determine the dynamic height anomaly from measurement of temperature alone. Approximating σ_t by the following expression:

$$\sigma_t = A + BT + CT^2 + DCl \tag{13}$$

and using the temperature-chlorinity relationship to express chlorinity as a function of temperature for the water mass he developed an approximate equation for the dynamic height anomaly.

$$\Delta D = 0.016 - 0.000241033 \int_0^{1,000} T\,dZ + 0.000010461 \int_0^{1,000} T^2\,dZ - 0.00000033426 \int_0^{1,000} T^3\,dZ \tag{14}$$

Yausi further simplified this expression by determining the linear correlation function between the first integral, and the second and

third integral. Using the derived correlation function, Equation 9 can be written:

$$\Delta D = (0.2637 \pm 0.0182) + (0.0001543 \pm 0.0000015) \int_0^{1,000} TdZ \qquad (15)$$

Comparing the dynamic height anomalies computed using Equations 14 and 15 to those computed by the standard method Yausi found standard deviations of 0.0484 dynamic meters and 0.0772 dynamic meters respectively. These are at least four and seven times the accepted error in the standard method of dynamic computations (Wooster and Taft, 1958). Computing the surface currents through a section extending south off Shionomisaki along approximately 135.7° E, Yausi found good agreement between the geostrophic surface currents found from Equation 14 and those computed by the standard dynamic computations.

Yausi attempted to achieve further simplification of Equation 14 by expressing the dynamic height at the sea surface relative to 1,000 db in terms of the dynamic height of the surface relative to shallower levels, i.e. 300, 400, 500, and 600 db. Again the linear correlation function was determined as the relationship between the quantities. The error in determining ΔD_{1000} from the thermal structure above 600 db was 0.048 dynamic meters, above 500 db was 0.051 dynamic meters, above 400 db was 0.081 dynamic meters,

and above 300 db was 0. 129 dynamic meters. He concluded that a reasonably accurate measure of the geostrophic surface currents could be obtained by using only the thermal structure above 500 db.

Yausi (1957) attempted to apply these methods to the adjacent seas of Japan, east of Honshu. While the patterns of dynamic topography obtained by the standard dynamic method and using the simplified equations of the form of Equation 14 and 15 were similar, an uncertainty of 0. 08 dynamic meters was inherent in the simple method due to poor temperature-chlorinity correlation. This is not unexpected because of the nature of the temperature-chlorinity correlation curve in the adjacent seas and the strong seasonal variability in this region.

Attempts were made to apply the method over other parts of the North Pacific using stations 100 to 150 in the seventh cruise of the CARNEGIE. The difference between the dynamic height computed by Equation 14 and the standard method was less than 0. 06 dynamic meters, except for stations 126 and 131 off the west coast of the United States where the difference between the two methods reaches 0. 18 dynamic meters.

One concludes that the temperature-salinity or temperature-chlorinity methods are applicable in specific regions. However, it is not suited to other regions where the temperature-salinity curves have small slopes or in regions where seasonal variations and mixing

lead to a large scatter of temperature-salinity pairs. Furthermore, temperature-salinity correlations would have to be established for each water mass, and the correlation functions altered at water mass boundaries. Since water mass boundaries are not fixed such correlation will be difficult to determine.

U. S. Navy Schemes

Two groups in the U. S. Navy make ocean surface current computations on a synoptic basis over large ocean regions. One group uses techniques developed at the Naval Oceanographic Office (NAVOCEANO) principally for application in the Northwest Atlantic Ocean (James, 1966). The other group, Fleet Numerical Weather Central (FNWC), computes surface currents over the Northern Hemisphere every 12 hours (Hubert, 1964). Both groups rely on synoptic thermal structure data transmitted from ships at sea. The density and accuracy of thermal structure data has been discussed by Wolff (1964).

NAVOCEANO Scheme

NAVOCEANO techniques were originally reported by Gibson (1962). The technique is based on a relationship between the horizontal surface temperature gradient and the surface current speed. Discussing a hydrographic section along the 50th meridian Gibson

summarizes (page 4) the basis for the scheme:

> These data and sections for other ocean areas (not shown) form the basis for the analytical approach described below. Symmetrical undulation of the isotherms indicates four major water masses.
>
> Upon crossing each mass the surface current changes direction in an orderly manner; that is, the circulation is cyclonic for cold waters and anticyclonic for warm waters. There is also general agreement between the magnitude for temperature gradients and current velocity.
>
> If $\vec{V}$ is the surface current velocity, $\hat{k}$ a vertical vector, positive outwards, and ΔT is grad T, the relation, $\vec{V} = \hat{k}$ cross ΔT holds in principle. This relation, analogous to that which applies for straight air flow suggests that water bands can be treated as greatly elongated air masses.

James (1966) discusses the application of Gibsons' suggestion to synoptic analysis of ocean surface currents. Plotting observed currents against observed horizontal surface temperature gradients in the Northwest Atlantic, a set of curves is derived giving the surface current as a function of horizontal surface temperature gradient. The curves are shown in Figure 1 for the Gulf Stream, Sargasso and Labrador water masses for summer and winter conditions. The surface current is obtained by determining the sea surface temperature gradient and reading current speed from the appropriate curve. Direction of flow is assumed to be parallel to the isotherms. James states (page 60):

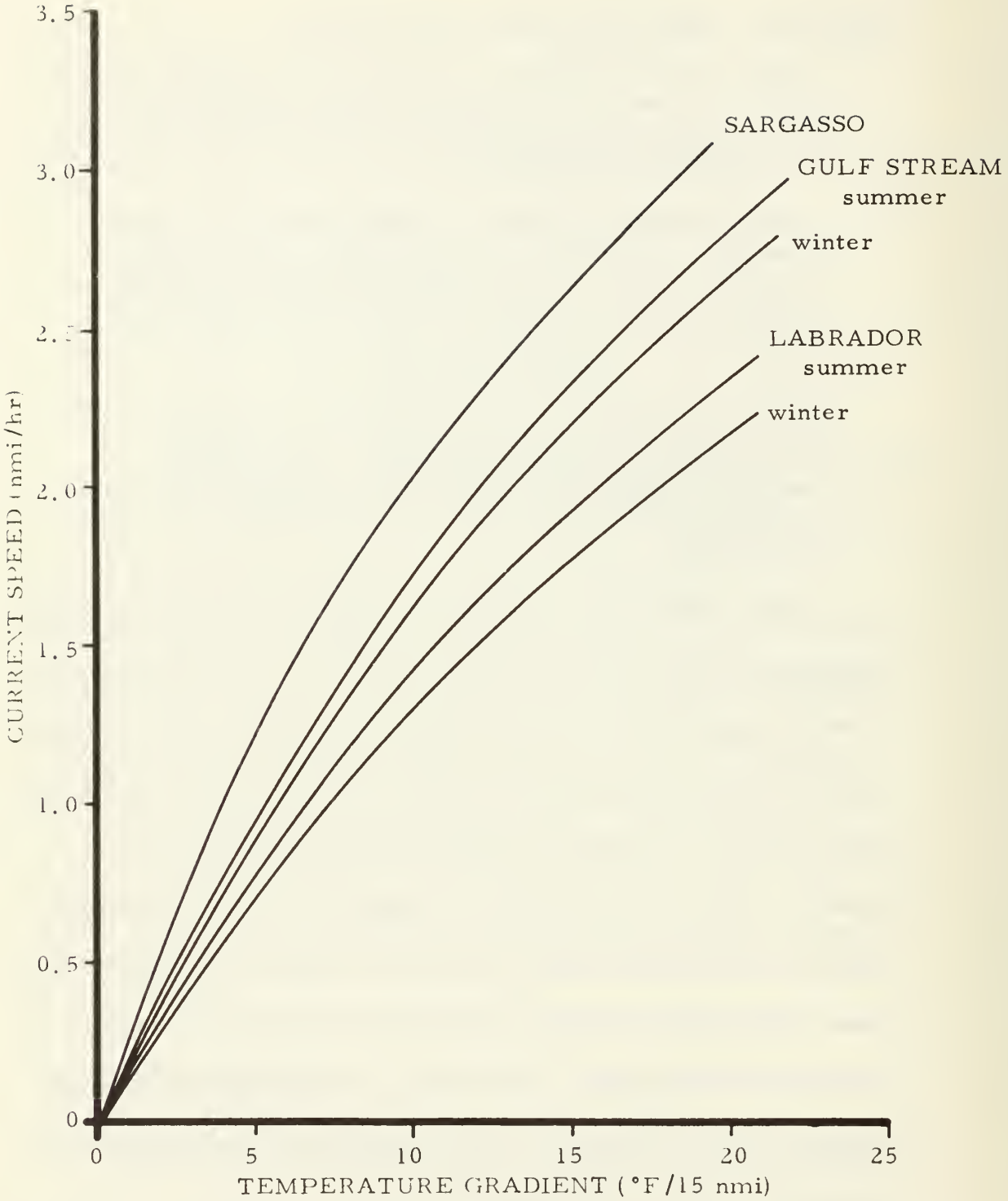

Figure 1. NAVOCEANO relationship between surface current speed and horizontal surface temperature gradient in the Northwest Atlantic (James, 1966).

> This system, aside from the ease of computation, has two advantages: (1) use of input based on synoptic temperature data is apt to be more reliable than the use of climatological means, and (2) the direction of the flow is fairly accurate.

Interstate Electronics Corporation (1968) made an evaluation of the geostrophic prediction techniques used by NAVOCEANO. In this study 7,000 hydrographic station pairs were selected from the archives of the National Oceanographic Data Center. Only those station pairs were selected that were consecutive and separated in time less than 24 hours. Geostrophic computations were carried out for the 0 db and 125 db levels relative to the 1,000 db level. The geostrophic currents at 0 db and 125 db between station pairs were correlated with the horizontal temperature gradient at these levels. The 125 db computation should have overcome local effects due to heat exchange across the sea surface. The results of the study were negative showing no correlation between the horizontal temperature gradient at the surface or at 125 db and the geostrophic current at these levels.

NAVOCEANO determines the wind drift component of the surface current independently and adds this to the geostrophic component to obtain the total surface current. Other forcing factors are not considered. Wind drift is determined from curves relating the surface drift to wind speed, duration and fetch (James, 1966).

FNWC Scheme

Hubert (1964) presents the equation used by FNWC to compute surface geostrophic flow over the Northern Hemisphere oceans on a synoptic basis.

$$(V_1 - V_2) = \frac{g\Delta Z}{f\overline{T}} \nabla_H \overline{T} \qquad (16)$$

where

ΔZ = the depth of the level of no motion

$\nabla_H \overline{T}$ = the horizontal gradient of $\overline{T}$

$\overline{T} = K_1 T_{sfc} + K_2 T_{200}$, where K_1 and K_2 are "tuning constants"

T_{sfc} and T_{200} = the surface and 200 meter temperatures respectively.

Hubert (1964) does not develop Equation 16, nor can this investigator find the development for application to the ocean. However, Equation 16 is of the same form as the thermal wind equation (Haltiner and Martin, 1957). Development of the thermal wind equation requires that there be a linear relationship between the temperature and density, that is, the thermal wind is parallel to the mean virtual isotherms with low temperature on the left. Such a relationship cannot exist in the sea since the density of sea water is a nonlinear function of temperature, salinity and pressure. Hubert points out

that the coefficients K_1 and K_2 can be adjusted in areas where salinity gradients are known to be significant.

The use of only the surface and 200 meter temperature fields cannot be justified over much of the ocean, as these two fields are not necessarily representative of the fields at other levels. Clearly, more of the water structure than just the sea surface temperature and 200 meter temperature is necessary to make meaningful geostrophic computations.

The wind drift is computed from Wittings (1909) formula

$$W = K_3\sqrt{V} \tag{17}$$

where

W = the current velocity (cm/sec)

V = the 24 hour mean geostrophic wind speed (M/sec)

K_3 = "wind factor"

The factor K_3 is adjusted to account for the mass transport associated with waves and the change of velocity with depth. For the surface wind drift K_3 is taken to be 4.8, and the surface wind drift current is assumed to be parallel to the geostrophic wind.

Both the geostrophic current and the wind drift current computations are carried out on a 63 x 63 linear grid system on a polar stereographic projection over the Northern Hemisphere (Figure 2). The grid point separation is given by the following expression:

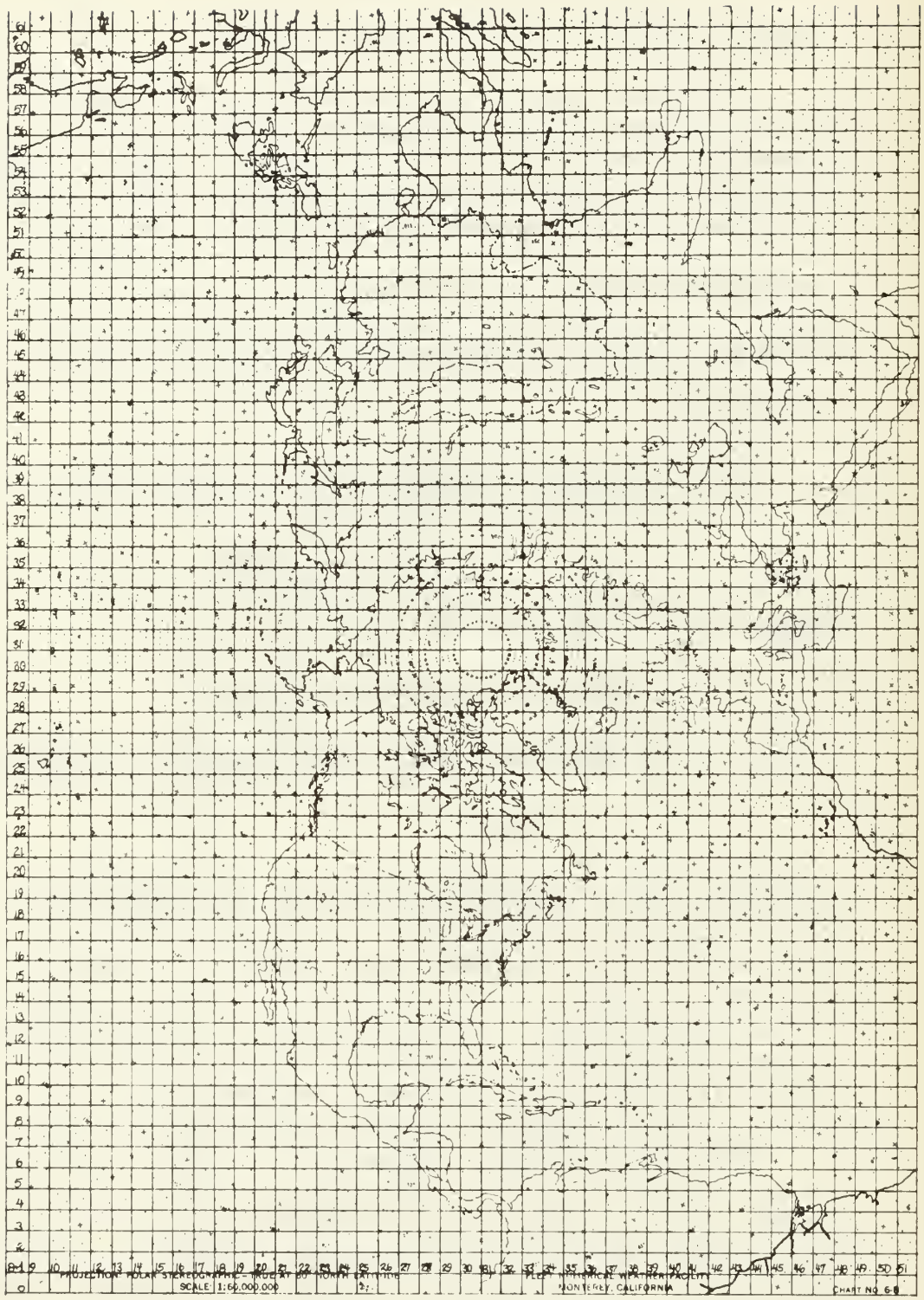

Figure 2. FNWC polar stereographic projection and grid.

$$X = \frac{[1 + \sin 60^\circ]}{[1 + \sin \phi]} \times 200 \qquad (18)$$

The projection is true at 60° N where the grid spacing is 200 nautical miles.

The wind drift and geostrophic surface current components (i and j) are computed independently at each grid point, and these components are added to arrive at the combined wind and geostrophic u and v components. From these components the current magnitude and current direction are determined. The isotachs are contoured resulting in a total transport (Figure 3).

In order to obtain a single chart containing both speed and direction the components are used to obtain the vorticity of the current flow and the stream function ψ is obtained by a relaxation solution of Poisson's equation (Hubert and Laevastu, 1965).

$$\nabla^2 \psi = \frac{\partial v}{\partial x} - \frac{\partial u}{\partial y} \qquad (19)$$

However, this stream function analysis is only applicable to non-divergent irrotational flow. The stream function field corresponding to the current transport field shown in Figure 3 is shown in Figure 4.

Direct verification of FNWC computed surface currents has not been possible. Indirect verification of surface currents has been made through the verification of sea surface temperature analysis

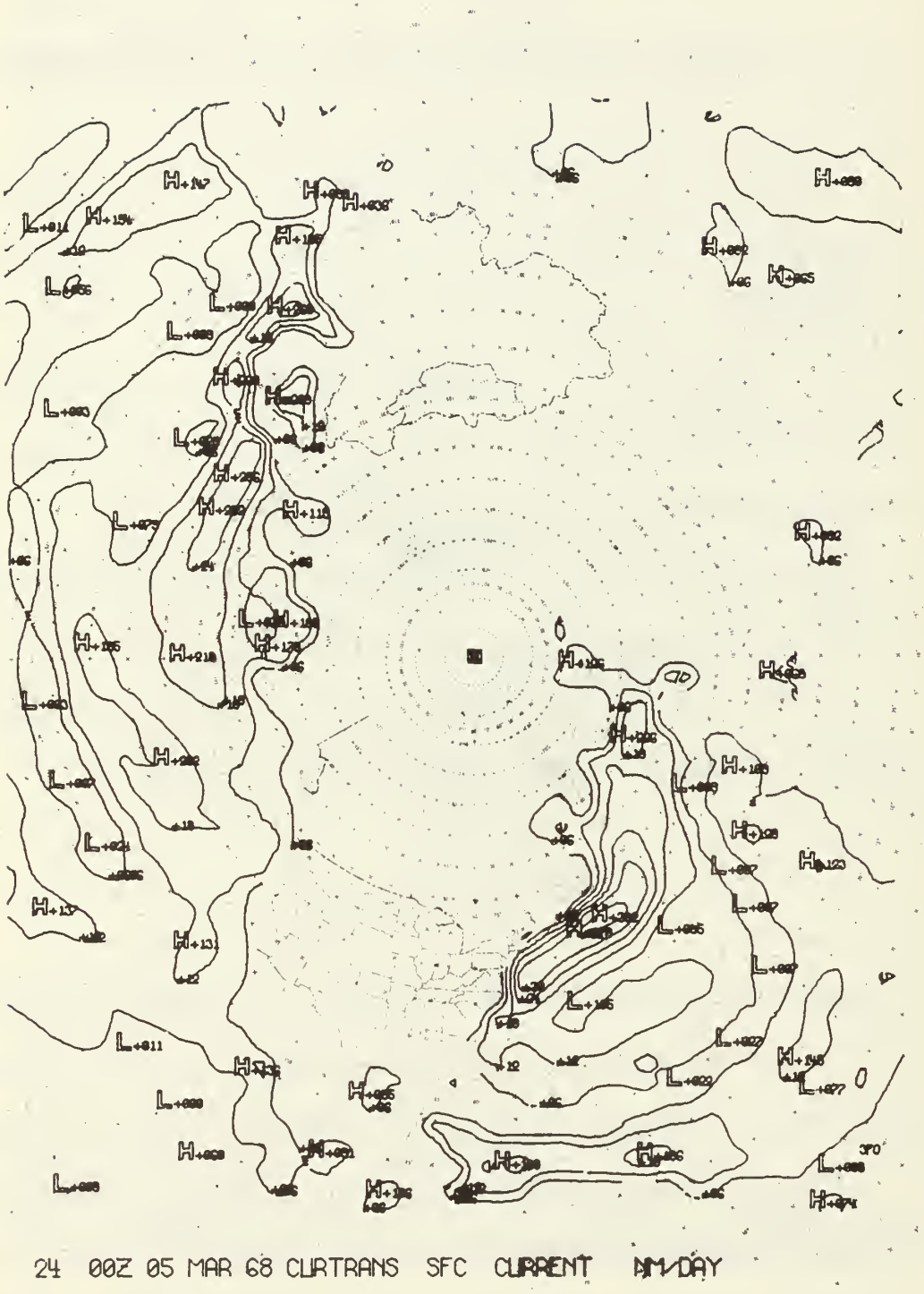

Figure 3. FNWC current transport

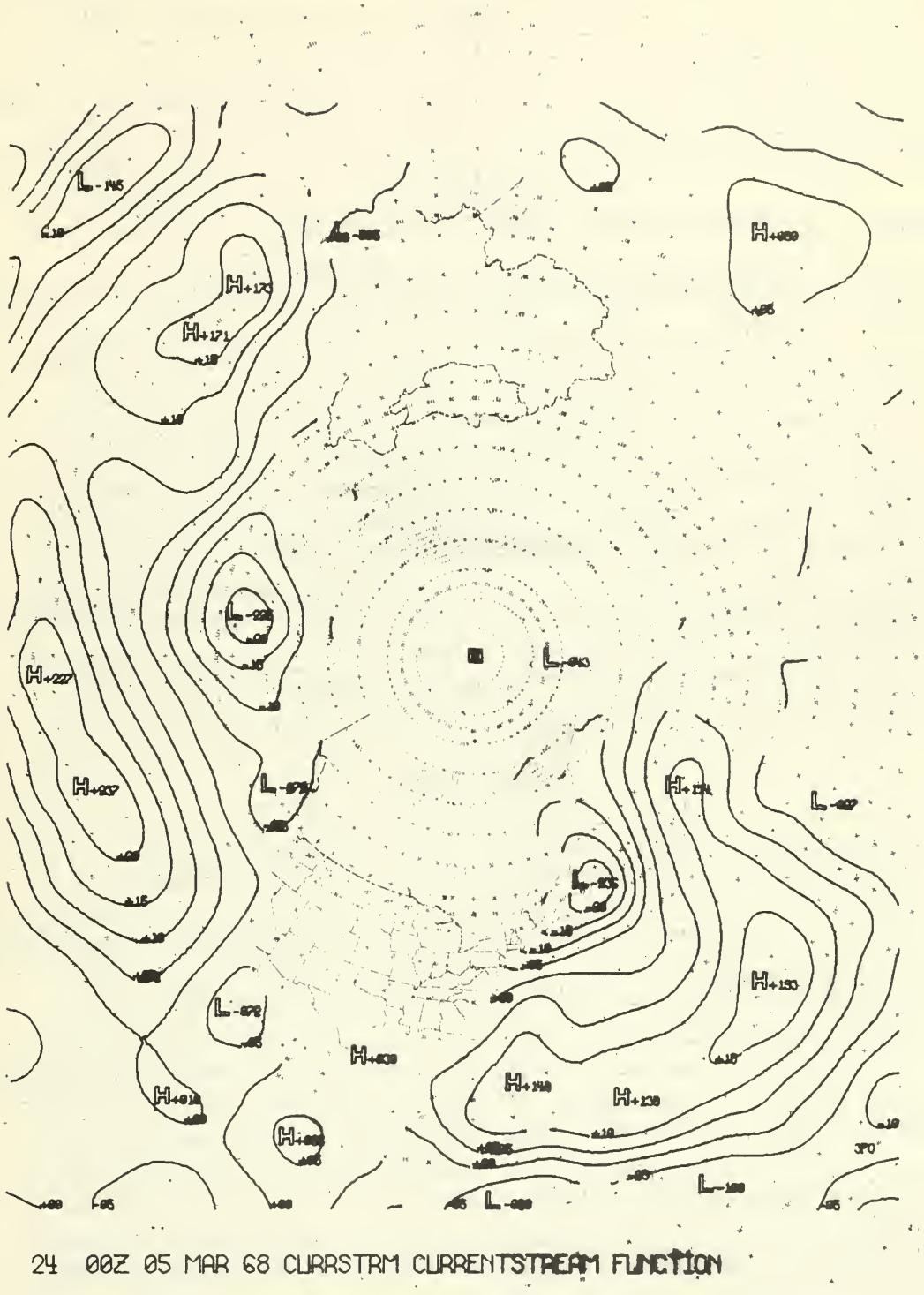

Figure 4. FNWC stream function analysis

(Hubert and Laevastu, 1965). Sea surface temperature analyses are made twice a day at FNWC over the Northern Hemisphere (Wolff, 1964). Sea surface temperature changes computed from the air-sea heat exchange are subtracted from the analysis. If the residual correlates with the temperature advection field determined from the surface current analysis then the currents are assumed to be correct. If the residual does not correlate with the temperature advection field then the currents can be "tuned" to achieve agreement. It should be noted that the air-sea heat exchange formulae used in this procedure are generally empirical and have not been subjected to widespread rigid verification. This indirect verification procedure may be questioned seriously when used for quantitative results.

Discussion

The methods for determining geostrophic flow described in this section represent attempts to simplify geostrophic computations. Each model had some success but all suffer from certain deficiencies. The temperature-salinity correlation schemes of Stommel, LaFond, and Yausi greatly reduce the number of computations required to determine geostrophic currents. These methods could also reduce sharply the field measurements, allowing geostrophic surface currents to be determined from temperature measurements alone. However, temperature-salinity correlation is a regional

parameter, varying from water mass to water mass; and in individual water masses it varies in both time and space. Furthermore, in regions of intense mixing such as the Kuroshio-Oyashio confluence (Tully, 1964), temperature-salinity curves are so variable that correlation approaches are not applicable.

Use of the thermosteric anomaly $\nabla_{S,T}$ instead of the specific volume anomaly reduces the number of computations, or number of tables, that need to be interpolated in geostrophic computations. The error introduced by this simplification is acceptable if the computations are limited to the upper 1,000 db. However, even in this simplified procedure the quantities σ_o and σ_t must be determined; since these are not used beyond the geostrophic computations, their determination represents unnecessary expenditure of computation time.

NAVOCEANO correlation curves between current and surface temperature gradient may provide adequate synoptic current information in some regions where strong surface temperature gradients are dynamically sustained, such as in the Gulf Stream. Over the world oceans this is not the case; the surface temperature gradients are small and often are determined by the local heat exchange and mixing processes. In fact no definite relationship was found between the surface current and the horizontal temperature gradient in 7,000 selected hydrographic station pairs in the Northwest

Atlantic where the NAVOCEANO curves (Figure 1) were derived (Interstate Electronics Corporation, 1968).

The application of the thermal wind equation to the ocean has no foundation. The simplifying assumption that the density of sea water is a linear function of temperature cannot be accepted (Fofonoff, 1962). The adjustment of the coefficients used by FNWC on the basis of sea surface temperature analysis verification must be questioned. Since the sea surface temperature field is developed using the surface current field to compute the advected heat the use of sea surface temperature in surface current verification is not an independent verification.

Geostrophic surface currents are most valuable if determined over a short period of time, say over a seven day period (Lenczyk, 1964). This will be possible only when synoptic fields of temperature and salinity are available. While such fields are not available at the present time, a more scientifically sound scheme of computing geostrophic currents must be available when these fields do become available. Any scheme used must yield surface currents that are in agreement with observed surface currents or at least those computed by the standard geostrophic method. Every effort should be made to verify by direct measurements any scheme of indirectly computing surface currents.

V. TEMPERATURE-SALINITY GRADIENT SCHEME

Development of the T-S Gradient Equation

Consider the Helland-Hansen equation, Equation 3, for geostrophic flow where the horizontal gradient is expressed in differential notation and n is perpendicular to $(v_1 - v_2)$ in the horizontal plane.

$$(V_1 - V_2) = \frac{1}{f}\left[\frac{d}{dn}\int_{P_1}^{P_2} \alpha(n, P)\, dp\right] \tag{3}$$

Equation 3 can be rewritten:

$$(V_1 - V_2) = \frac{1}{f}\int_{P_1}^{P_2}\left[\frac{d}{dn}\,\alpha(n, P)\right]_p dp \tag{20}$$

where the subscript p indicates the bracket quantity is evaluated at constant pressure.

Assuming that sea water can be regarded effectively as a binary fluid system whose specific volume is a function of the three independent variables, temperature, salinity and pressure.

$$\alpha = f(T, S, P) \tag{21}$$

Then Equation 22 can be written in the following form carrying out

the indicated differential operation (Reid, 1959).

$$(V_1 - V_2) = \frac{1}{f} \int_{P_1}^{P_2} [(\frac{\partial a}{\partial T})_{S, P} \frac{dT}{dn} + (\frac{\partial a}{\partial S})_{T, P} \frac{dS}{dn}]_p \, dp \qquad (22)$$

Note that there is no term representing the compressibility of sea water because the operation in brackets is carried out at a constant pressure.

Equation 22 gives the geostrophic velocity in terms of the horizontal gradients of temperature and salinity; a quantity $(\partial a/\partial T)_{S, P}$ specifying the dependence of specific volume on temperature at a given salinity and pressure, and a quantity $(\partial a/\partial S)_{T, P}$ specifying the dependence of specific volume on salinity at a given temperature and pressure. These latter quantitites become the coefficient of thermal compressibility and saline contraction if each is divided by the specific volume. Note that the compressibility of sea water enters Equation 22 indirectly through the dependence of these quantities on pressure.

The question then arises, as to whether or not simple expressions be found for $(\partial a/\partial T)_{S, P}$ and $(\partial a/\partial S)_{T, P}$ such that Equation 22 represents a substantial simplification over standard geostrophic computations without significant loss in accuracy. Two possible ways of expressing $(\partial a/\partial T)_{S, P}$ and $(\partial a/\partial S)_{T, P}$ are: (1) to use empirical data giving the specific volume as a function of temperature, salinity and pressure, such as Newton and Kennedy (1965) or (2) to use one of the available equations of state, such as that of

Ekman (1908), that have been numerically fitted to the available empirical data.

Determination of $(\partial\alpha/\partial T)_{S, P}$ and $(\partial\alpha/\partial S)_{T, P}$

Empirical Data

The most widely used P-V-T (pressure, specific volume, temperature) data for sea water are based primarily on Ekman's (1908) compression determinations. He measured the specific volume of a sample of sea water taken from 3,000 m at a station off Portugal, at two different salinities; 31.13 ‰ and 38.83 ‰, obtained by dilution and evaporation of the sample, and at three pressures; 200, 400 and 600 bars. V-T data often used is that of Forsch, et al. (1902) for different salinities at atmospheric pressure. Forsch, et al. used a total of 24 samples collected entirely from the surface, mainly from the Baltic, North Sea and the North Atlantic Ocean.

A more recent and extensive set of measurements are those of Newton and Kennedy (1965). They carried out measurements of specific volume for three salinities (31.52, 34.99 and 41.03 ‰) at temperatures from 0 to 25°C in 5°C steps, and at pressures from 1 to 1,000 bars in 100-bar steps. The precision of the measurements is reported to be better than seven parts in 10^5. Because of the time lapse of about six decades between the measurements of

Ekman and Forsch, and those of Kennedy and Newton, the latter measurements should reflect any advance in technique and apparatus in that interval. Furthermore, P-V-T-S data available prior to Newton and Kennedy is not sufficient to determine the quantities $(\partial\alpha/\partial T)_{S,P}$ and $(\partial\alpha/\partial S)_{T,P}$ over the range of temperature, salinity, and pressure of interest in the ocean without extensive interpolation of the data. However, Ekman's compressibility data is internally consistant to a remarkable degree (Eckart, 1958; Li, 1967).

The dependence of specific volume on temperature, $\alpha(T)_{S,P}$ at fixed salinity and pressure, and the dependence of specific volume on salinity, $\alpha(S)_{T,P}$, at fixed temperature and pressure are illustrated in Figures 5 and 6 respectively (Newton and Kennedy, 1965). Figure 5 shows that $\alpha(T)_{S,P}$ is a nonlinear function over the range of variables shown, and of practical interest in this study. However, $\alpha(T)_{S,P}$ is a continuously increasing function over these ranges. Figure 6 shows that $\alpha(S)_{T,P}$ is nearly a linear function over the range of variables of interest in this study.

The quantities of interest, $(\partial\alpha/\partial T)_{S,P}$ and $(\partial\alpha/\partial S)_{T,P}$, can be determined by direct differentiation of $\alpha(T)_{T,P}$ and $\alpha(S)_{T,P}$ if suitable expressions can be found for these functions. Polynomials of progressively higher degree (first through fifth) were fit in the least square sense to Newton and Kennedy's data to determine $\alpha(T)_{S,P}$ over the three salinities, at pressures of 1, 100, and 200

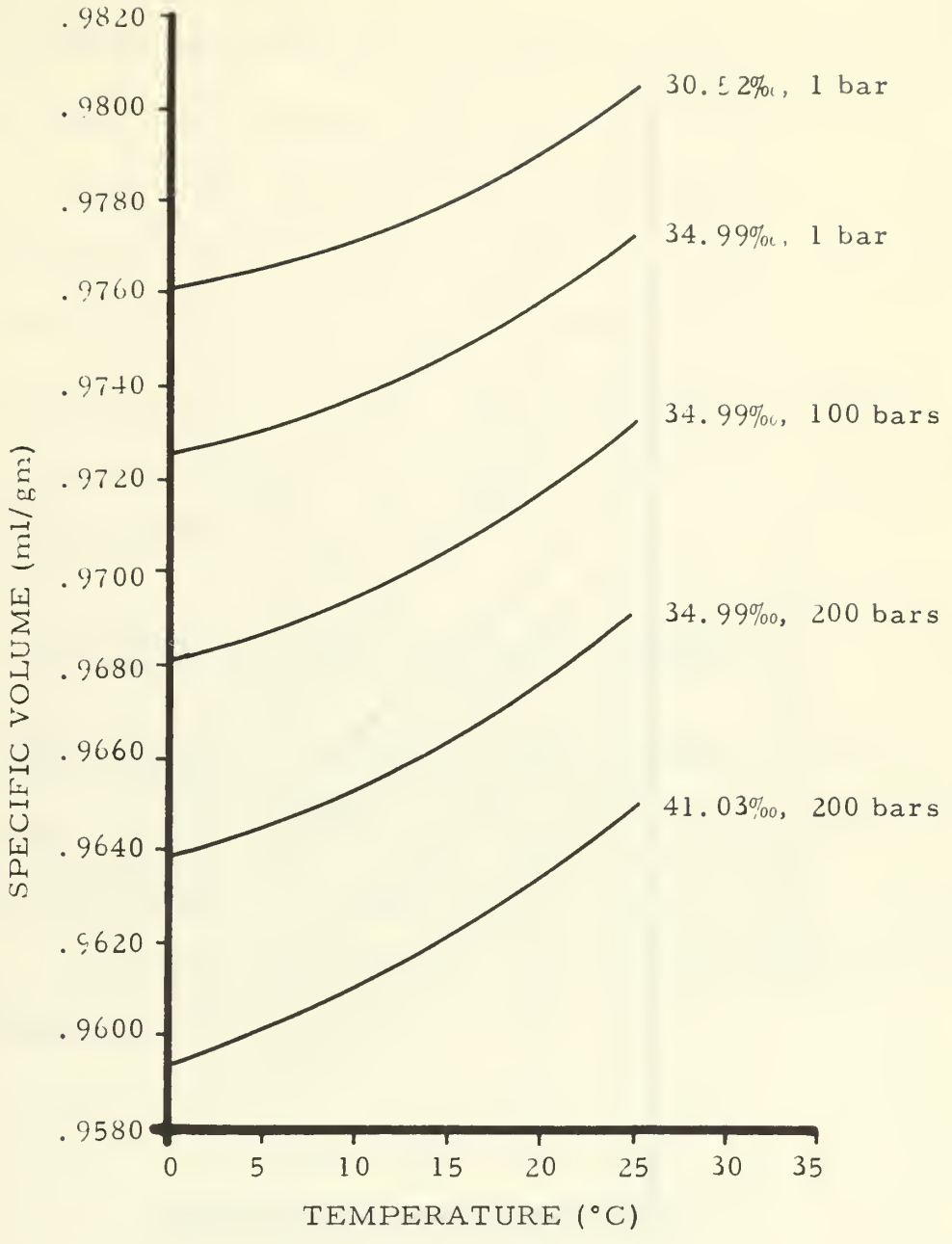

Figure 5. The dependence of specific volume as a function of temperature at fixed salinity and pressure

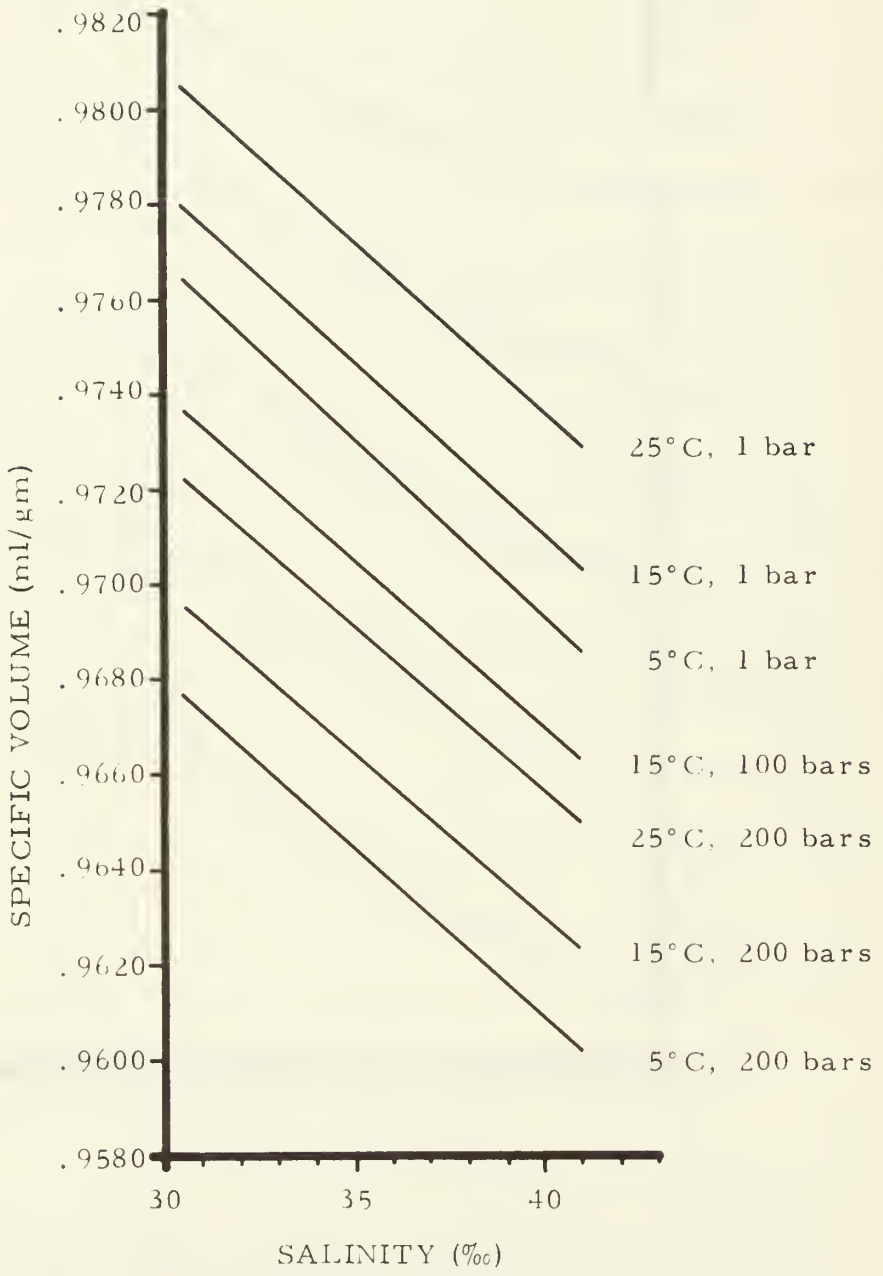

Figure 6. The dependence of specific volume as a function of salinity at fixed temperature and pressure

bars. The fitting was performed on the Naval Postgraduate School IBM/360 digital computer using the program LSQPOL (Jordan and Vogel, 1961). This program computes the coefficients of the polynomial, an estimate of the error in the coefficients, and the standard deviation of the computed points from the fitted points. The standard deviation of the computed points was less than the precision of the original data points for a second degree polynomial. Therefore, $\alpha(T)_{S,P}$ can be expressed to the accuracy of the original data points by an expression of the form:

$$\alpha(T)_{S,P} = \alpha_o(S,P) + A(S,P)T + B(S,P)T^2 \qquad (23)$$

The values of $\alpha_o(S,P)$, $A(S,P)$, and $B(S,P)$ are given in Table 2. A similar procedure was followed to determine $\alpha(S)_{T,P}$ over the range of temperature and the pressure previously given for $\alpha(T)_{S,P}$. $\alpha(S)_{T,P}$ was expressed to the precision of the original data points by a polynomial of first degree.

$$\alpha(S)_{T,P} = \alpha_o(T,P) - C(T,P)S \qquad (24)$$

The values $\alpha_o(T,P)$ and $C(T,P)$ are presented in Table 3.

Examining the values in Tables 2 and 3 inconsistencies are noted for which no physical reason is available. For example, in Table 2 the values of A(30. 52 ‰, 100 bars) and B(30. 52 ‰, 100 bars) are less than the values of these coefficients at 100 bars and

Table 2. $a_o(S, P)$, $A(S, P)$ and $B(S, P)$ as function of salinity and pressure in cgs units. (From Newton and Kennedy, 1965).

Salinity (‰)	Pressure (bars)	$a_o(S, P)$	$A(S, P) \times 10^6$	$B(S, P) \times 10^7$
30.52	1	0.9761	48.71	50.00
30.52	100	0.9715	89.14	40.00
30.52	200	0.9672	99.93	40.71
34.99	1	0.9726	67.28	47.14
34.99	100	0.9682	88.21	43.57
34.99	200	0.9639	109.91	40.00
40.03	1	0.9680	90.78	40.71
40.03	100	0.9637	111.71	37.14
40.03	200	0.9595	126.07	36.43

Table 3. $a_o(T, P)$ and $C(T, P)$ as a function of temperature and pressure in cgs units (From Newton and Kennedy, 1965).

Temperature (°C)	Pressure (bars)	$a_o(T, P)$	$C(T, P) \times 10^5$
0	1	0.9996	-77.02
0	100	0.9942	-74.23
0	200	0.9895	-73.24
5	1	0.9993	-75.13
5	100	0.9943	-73.24
5	200	0.9895	-71.35
10	1	0.9997	-74.14
10	100	0.9948	-72.25
10	200	0.9904	-71.35
15	1	1.0000	-72.34
15	100	0.9955	-71.35
15	200	0.9910	-70.36
20	1	1.0014	-73.24
20	100	0.9965	-70.80
20	200	0.9920	-69.46
25	1	1.0025	-72.34
25	100	0.9977	-70.45
25	200	0.9934	-69.46

34.99 ‰ This is opposite to the trend in the other data. Similar inconsistencies are found in Table 3 for the C(S, P) coefficients. These inconsistencies are not unexpected. They are due to the fact that few data points are used and small errors in the data points fit lead to large errors in the coefficients. However, such inconsistencies in the coefficients makes interpolation of coefficients from Newton and Kennedy's data to other temperatures, salinities and pressures impossible. The use of additional data points would overcome this difficulty. Additional data points smoothed to compensate experimental error can be computed from the equation of state for sea water.

Equations of State for Sea Water

Several equations of state have been suggested for sea water. The earliest equation (Equation 8) is that suggested by Ekman (1908) (Bjerknes and Sandstrom, 1910) for existing P-V-T-S data.

$$\alpha = \alpha_o(1 + \mu p) \tag{25}$$

where

α = specific volume, (ml/gm)

α_o = specific volume at atmospheric pressure

p = pressure, in decibars

$$\mu = 10^{-9}\{[4886/(1 + 1.83 \times 10^{-5}p)] - (227 + 28.33T - 0.551T^2 + 0.004T^3) + 10^{-4}p\,(105.5 + 9.50T - 0.158T^2) - 1.5 \times 10^{-8}TP^2 - 10^{-1}(\sigma_o - 28[(147.3 - 2.72T + 0.04T^2) - 10^{-4}p(32.4 - 0.87T + 0.02T^2)] + 10^{-2}(\sigma_o - 28)^2[4.5 - 0.1T - 10^{-4}p(1.8 - 0.06T)]\}$$

Ekman's work would indicate that Equation 25 would be applicable over the following ranges in the variables:

Temperature	-2° C to 26° C
Salinity	31.13 ‰ to 38.53 ‰
Pressure	0 bars to 600 bars

LaFond (1951), however, gives the range of application as:

Temperature	-2° C to 30° C
Salinity	21 ‰ to 38 ‰
Pressure	0 bars to 1,000 bars

Eckart (1958) carefully studied the available P-V-T-S data for pure water and sea water. He concluded that the equation of state is represented to the accuracy of the available data (2×10^{-4} ml/gm) by the Tumlirz equation.

$$(P + P_o)(a - a_o) = \lambda \qquad (26)$$

where

P = total pressure in atmospheres

$P_o = 5890 + 38T - 0.375T^2 + 3S$

$a_o = 0.6980$

$\lambda = 1779.5 + 11.25T - 0.0745T^2 - (3.80 + 0.01T)S$

Eckart indicates that Equation 26 is a satisfactory fit of the available data over the following range:

Temperature	0° C to 40° C
Salinity	0 ‰ to 40 ‰
Pressure	0 bars to 1,000 bars

Fofonoff (1962) compared the Ekman expression to the Tumlirz equation and found that the maximum disagreement between the two equations was less than 2×10^{-4} ml/gm over nearly the entire range of salinity, temperature, and pressure in the sea. Only at unusually high ocean temperatures (greater than 29° C) with salinities of 36 ‰ did the disagreement reach 3×10^{-4} ml/gm. However, while specific volumes computed by the two equations agree to within the accuracy of measurements, quantities derived from the equation of state, such as the coefficient of thermal expansion, are in serious disagreement.

Li (1967) reviewed the available P-V-T-S data and suggested

the Tait-Gibson equation as an equation of state. The Tait-Gibson equation is given by Li as:

$$a = a_{S, T, 1} - (1 - S \times 10^{-3})C \text{ Log } [\frac{B^* + P}{B^* + 1}] \qquad (27)$$

where

$$C = 0.315\, a_{o, T, 1}$$

$$B^* = (2670.8 + 6.89056S) + (19.39 - 0.0703178S)T - 0.223T^2$$

Equation 27 is a satisfactory fit to existing P-V-T-S data over the following range of variables:

Temperature	0° C to 20° C
Salinity	30 ‰ to 40 ‰
Pressure (absolute)	1 bar to 100 bars

Equation 27 gives results that are in agreement with measurements to the experimental error in the P-V-T-S data. The difference between the Tait-Gibson equation and Ekman's equation for sea water of 35 ‰, 0° C from 1 to 1,000 bars is no more than 1×10^{-5} ml/gm. At atmospheric pressure the agreement between the density of sea water from Knudsen's tables (1901), in common usage in oceanography, and Equation 27 is less than 3×10^{-5} gm/ml over the chlorinity range of 15 to 22 ‰ and temperature range of 0 to 20° C. Li concludes (page 2073): "Ekman's very involved equation of state of sea water is equivalent to the much simpler expression given here." However, as the Tumlirz equation proposed by Eckart did

not give the same values as the Ekman equation for derived properties such as the coefficient of thermal expansion, the Tait-Gison equation gives again different values.

The dependence of specific volume on temperature $a(T)_{S, P}$ is a function of temperature, salinity and pressure according to the three proposed equations of state discussed above. In each case the functional relationships are markedly different. Furthermore, quantities derived from these expressions such as the coefficient of thermal expansion , $1/a(\partial a/\partial T)_{S, P}$, may differ significantly. Fofonoff (1962) compared the coefficient of thermal expansion of sea water 35 ‰ salinity at atmospheric pressure computed from the Ekman and Eckart relationships. The results are given in Table 4.

Table 4. A comparison of the coefficient of thermal expansion of sea water $1/a(\partial a/\partial T)_{S, P} \times 10^6$ at 35 ‰ salinity and atmospheric pressure computed from the Ekman and Eckart equations of state (from Fofonoff, 1962).

Temperature (°C)	Ekman	Eckart
0	52	80
5	114	121
10	167	161
15	214	201
20	256	237
25	297	274
30	335	311

While the coefficient of thermal expansion computed by the two equations are not significantly different at temperatures around 10°C

these differences increase significantly at higher and lower temperatures.

Equation 22 requires the value of $(\partial\alpha/\partial T)_{S, P}$ before it can be used for geostrophic computations. To illustrate how this quantity changes between the three equations of state, Ekman, Eckart, and Tait-Gibson, the value of $(\partial\alpha/\partial T)_{S, P}$ as a function of pressure for a salinity of 34 ‰ for temperatures 0, 10, 20, and 30° C is plotted in Figure 7. The three proposed equations of state yield values for $(\partial\alpha/\partial T)_{S, P}$ in closest agreement at temperatures near 10° C at pressures near one atmosphere. However, the values diverge toward higher and lower temperatures and higher pressures. There is no clear cut way to specify which equation of state would yield the best value of $(\partial\alpha/\partial T)_{S, P}$. Furthermore, direct differentiation of the Ekman, Eckart or the Tait-Gibson equations leads to rather complicated expressions for $(\partial\alpha/\partial T)_{S, P}$ as well as $(\partial\alpha/\partial S)_{T, P}$. Such complicated expressions would give Equation 22 no advantage over the Helland-Hansen equation, Equation 4.

Fofonoff (1962) has examined the coefficients of saline contraction, $(\partial\alpha/\partial S)_{T, P}$, as computed from the Ekman and Eckart relationships and found that they differ by less than one percent. Therefore, in geostrophic computations using Equation 22 there is little advantage in either expression for $(\partial\alpha/\partial S)_{T, P}$. Thus, while the value of $(\partial\alpha/\partial T)_{S, P}$ differs significantly between equations of state

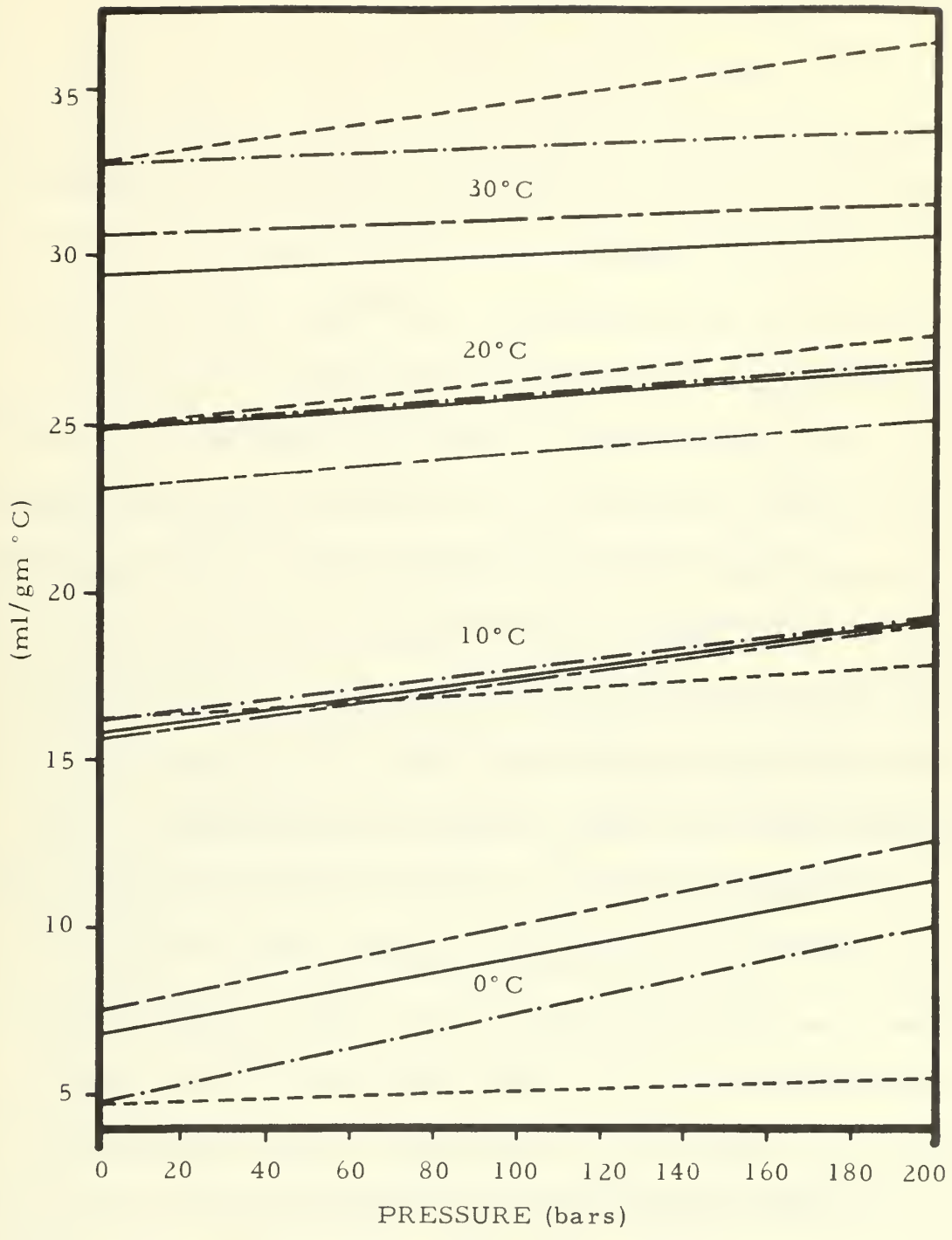

Figure 7. Variation of $(\partial\alpha/\partial T)_{S,P}$ as a function of pressure for a salinity of 34‰ according to the Ekman (— · —), Eckart (—— –), Tait-Gibson (— – —) equations of state and Equation 23 with coefficients derived from the Ekman equation of state (———)

the value of $(\partial\alpha/\partial S)_{T,P}$ does not.

Another approach to the determination of $(\partial\alpha/\partial T)_{S,P}$ and $(\partial\alpha/\partial S)_{T,P}$ would be to compute specific volume at sufficient values of temperature, salinity, and pressure using one of the equations of state, and fitting the resulting values with polynomials as was attempted with the Newton-Kennedy P-V-S-T data. This would overcome the difficulty encountered in directly fitting the empirical P-V-S-T data caused by experimental errors in the few data points as the equations of state would smooth individual inconsistent points. The question is which equation of state to use to compute the specific volume? There is little evidence that any of the expressions gives more reliable values of specific volume over the range of variables of interest in computing geostrophic currents in the upper few thousand meters of the ocean (Wilson and Bradley, 1968; Li, 1967).

The Ekman equation (Equation 25) has been the principle equation of state used by oceanographers (LaFond, 1951). Tables by Bjerknes and Sandstrom (1910), Sverdrup (1942) and LaFond (1951) are based on this expression. Since these tables have been and continue to be so widely used in oceanography the Ekman equation of state is selected to determine $\alpha(T)_{S,P}$ and $\alpha(S)_{T,P}$.

Specific volume was computed using Equation 25 over the range of temperature, salinity, and pressure of interest in this study:

Temperature	0°C to 30° C
Salinity	30 ‰ to 40 ‰
Pressure	0 bars to 200 bars

Values of specific volume were computed for all possible combinations of the variables at intervals of 2° C for temperature, 2 ‰ for salinity and 10 bars for pressure.

Second degree polynomials were fit to the specific volume as a function of temperature at fixed salinity and pressure to yield $a(T)_{S, P}$, and first degree polynomials were fit to specific volume as a function of salinity at fixed temperature and pressure to give $a(S)_{T, P}$. Again the fitting was accomplished on the Naval Postgraduate School IBM/360 digital computer using the program LSQPOL. The values of the coefficients A(S, P) and B(S, P) as in Equation 23 and C(T, P) as in Equation 24, are given in Appendix I as a function of their respective independent variables. The errors determined for these coefficients and the standard deviation of the computed versus the original data points is also given in Appendix I.

The standard deviation of the goodness of fit of the computed to original data points, is always less than 2×10^{-5} ml/gm. Since Eckart (1958) contends specific volume is not known any better than 2×10^{-4} ml/gm the use of higher degree polynomials is not justified. Direct differentiation of $a(T)_{S, P}$ (Equation 23) with respect to temperature yields the following expression:

$$\left(\frac{\partial \alpha}{\partial T}\right)_{S, P} = A(S, P) + 2B(S, P)T \qquad (28)$$

The values $(\partial \alpha / \partial T)_{S, P}$ from this equation were compared to the values given by the Ekman, Eckart, and Tait-Gibson equations of state in Figure 7. The quadratic expression of $\alpha(T)_{S, P}$ leads to as good agreement with the commonly accepted Ekman equation of state as do either of the other proposed equations of state (Equation 26 or Equation 27).

In the same way differentiation of $\alpha(S)_{T, P}$ (Equation 24) with respect to salinity yields:

$$\left(\frac{\partial \alpha}{\partial S}\right)_{T, P} = - C(T, P) \qquad (29)$$

Linear interpolation of the computed values of the three coefficients leads to Figures 8, 9 and 10 for $A(S, P)$, $2B(S, P)$ and $C(T, P)$ respectively.

Temperature-Salinity Gradient Scheme

Recall Equation 22.

$$(V_1 - V_2) = \frac{1}{f} \int_{P_1}^{P_2} \left[\left(\frac{\partial \alpha}{\partial T}\right)_{S, P} \frac{dT}{dn} + \left(\frac{\partial \alpha}{\partial S}\right)_{T, P} \frac{dS}{dn}\right]_P dP \qquad (22)$$

Substitution from Equation 28 and Equation 29 for $(\partial \alpha / \partial T)_{S, P}$ and $(\partial \alpha / \partial S)_{T, P}$ respectively in Equation 22 yields the following

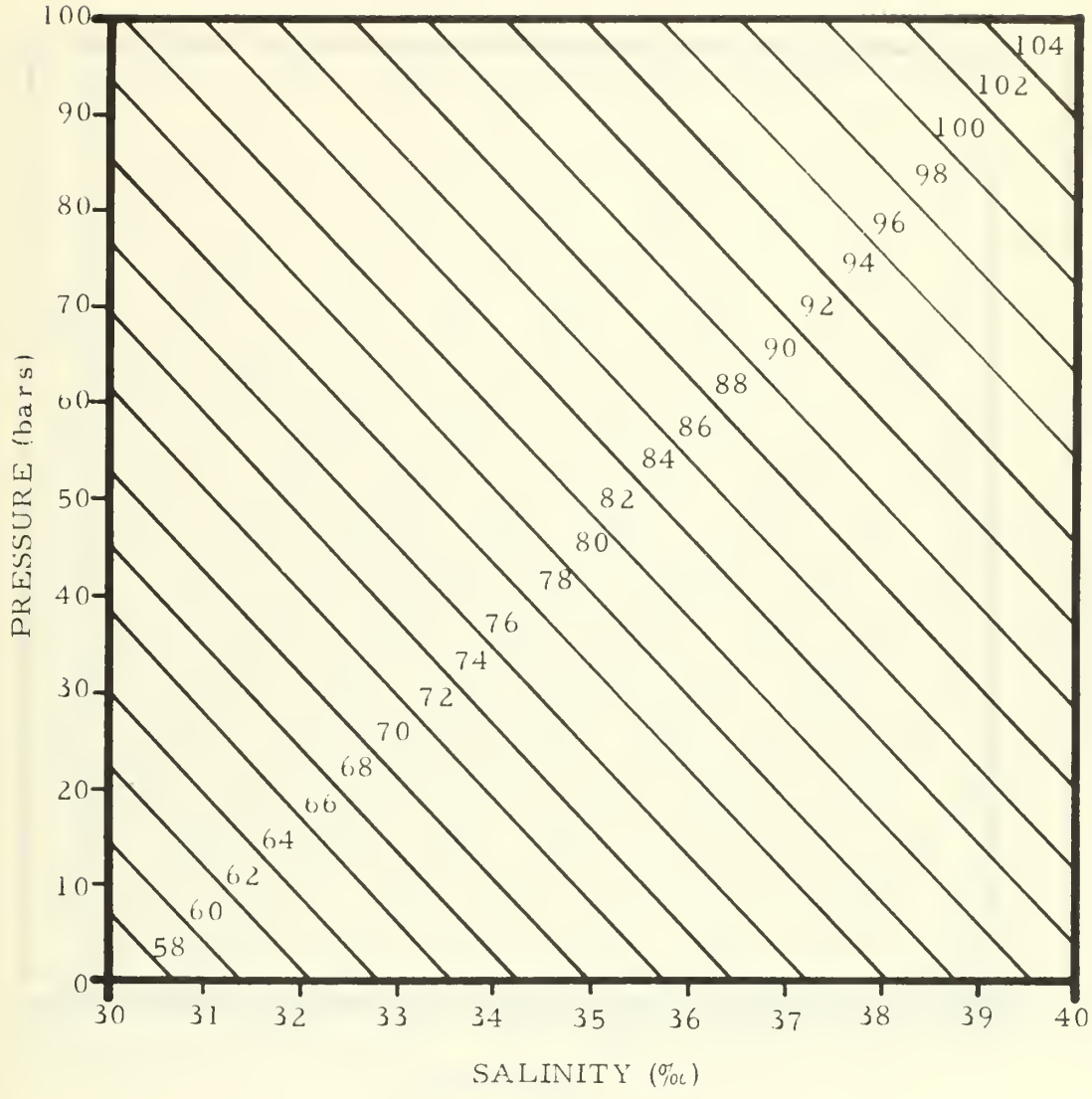

Figure 8. A(S, P) as a function of salinity and pressure

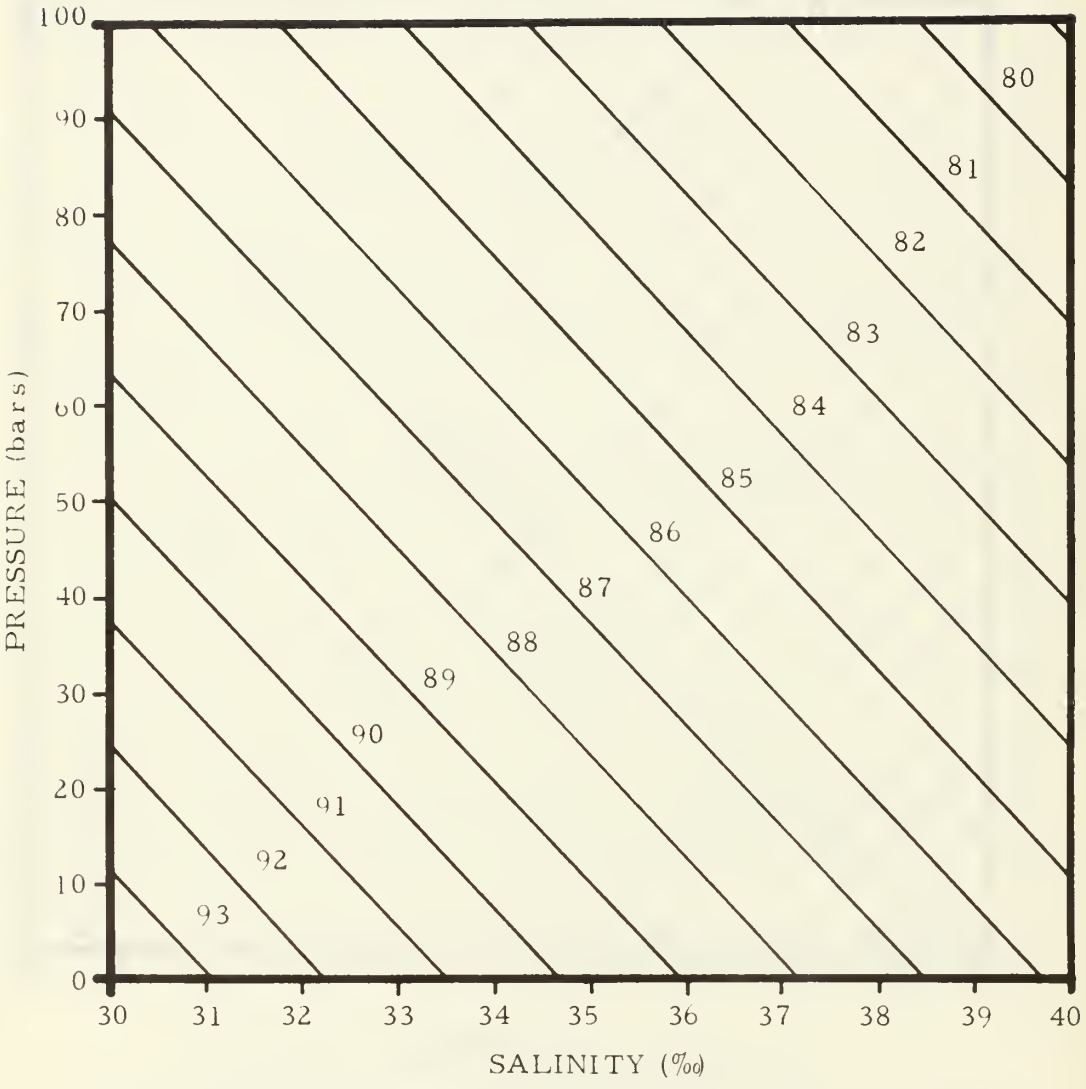

Figure 9. $2B(S, P) \times 10^7$ as a function of salinity and pressure

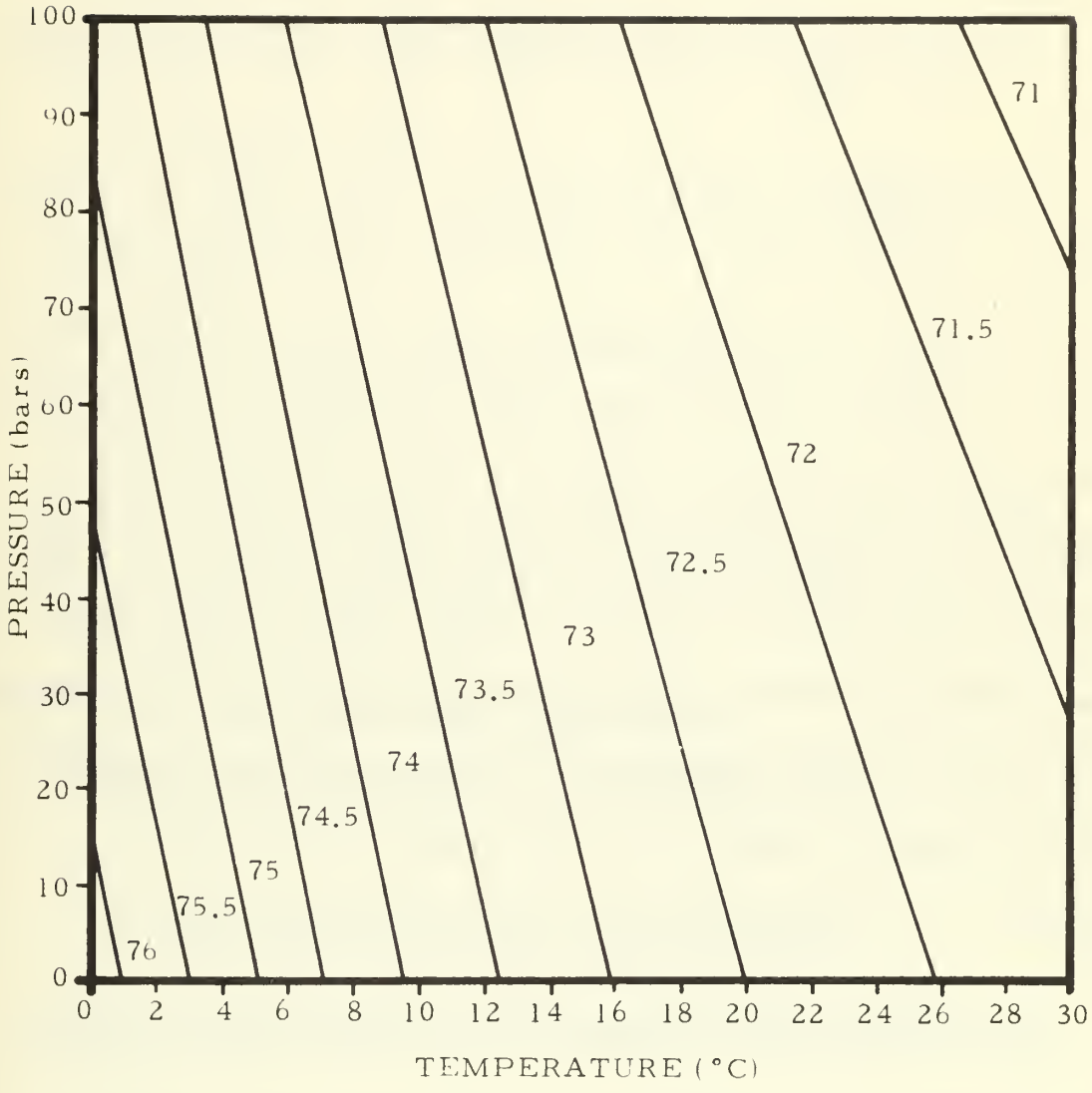

Figure 10. $C(T, P) \times 10^5$ as a function of temperature and pressure.

simplified expression for computing geostrophic currents:

$$(V_1 - V_2) = \frac{1}{f} \int_{P_1}^{P_2} \left[A(S, P) \frac{dT}{dn} + 2B(S, P)\overline{T} \frac{dT}{dn} - C(T,P)\frac{dS}{dn} \right]_p dp \quad (30)$$

Using Equation 30 geostrophic flow through a dynamic section can be computed without computing specific volume as required in the classical Helland-Hansen Equation. Only the measured temperature and salinity gradients along isobaric surfaces, and the coefficients $A(S, P)$, $2B(S, P)$ and $C(T, P)$ which can be obtained from Appendix I or Figures 8, 9 and 10 respectively are required to compute the geostrophic flow through a section. Because of the clear relationship between the measured temperature and salinity gradients, and for lack of better, Equation 30 will be referred to as the Temperature-Salinity Gradient method or simply the T-S Gradient method.

Computational Form of Temperature-Salinity Gradient Scheme

Equation 30 is rewritten in terms of finite differences for computation:

$$(V_1 - V_2) = \frac{1}{f\Delta n} \Sigma_i \left[\overline{A}_i \Delta T_i + 2\overline{B}_i \overline{T}_i \Delta T_i - \overline{C}_i \Delta S_i \right]_p \Delta P_i \quad (31)$$

where

$\overline{A}_i$ = the average value of A(S, P) over the i^{th} pressure interval (cgs units)

$2\overline{B}_i$ = the average value of 2B(S, P) over the i^{th} pressure interval (cgs units)

$\overline{C}_i$ = the average value of C(T, P) over the i^{th} interval (cgs units)

ΔT_i = the average horizontal temperature difference in the i^{th} pressure interval (°C)

$\overline{T}_i$ = the average temperature in the i^{th} pressure interval (°C)

ΔS_i = the average horizontal salinity difference in the i^{th} pressure interval (‰)

ΔP_i = the i^{th} pressure interval (dynes/cm^2)

Δn = the horizontal separation of the stations (cm)

Advantages of the Temperature-Salinity Gradient Scheme of Computing Geostrophic Currents

If Equation 30 is to be used over the standard geostrophic scheme (Equation 4) it should represent some advantage. The advantages realized in using Equation 30 are: (1) simplicity of computation, (2) speed of computation, and (3) additional insight into the individual significance of the temperature and salinity structure in geostrophic flow in the ocean. Since the much simpler expressions

for $\alpha(T)_{S,P}$ and $\alpha(S)_{T,P}$ reproduce values of specific volume to the accuracy of the experimental measure of this quantity, these advantages would seem to be gained without loss of accuracy over the range of temperature, salinity and pressure considered in this study. Furthermore the method is completely general and can be used under any circumstances that the standard method can be applied.

The computational simplification of the T-S Gradient scheme is apparent since no density computations are needed. Neither the relatively involved tables commonly used to calculate specific volume (or specific volume anomaly), nor the equations of state previously discussed need to be used. Those properties that are directly measured in the ocean (temperature and salinity as a function of depth) can be used to compute the geostrophic flow. Only the three coefficients $A(S,P)$, $2B(S,P)$ and $C(T,P)$ are needed.

The speed advantage of the T-S Gradient calculations on a digital computer was established on an IBM 360 digital computer. The time to compute the geostrophic flow through a section consisting of two stations, by the standard method and by the T-S Gradient method was measured. Only the actual time to carry out the mathematical computations was determined. The average time to compute the geostrophic flow for a single station pair was 0.25 μsec for the T-S Gradient method, and 1.80 μsec for the classical method.

Therefore, the T-S Gradient method is approximately seven times faster than the standard method using this digital computer.

Another significant advantage of the T-S Gradient scheme is the potential for separating the thermal and haline contributions to the geostrophic flow. The interaction that takes place between the thermal and haline contributions to the flow is through A(S, P), B(S,P) and C(T, P). Therefore, at least to first order, the first two terms in Equation 30 can be considered the thermal contribution to the geostrophic flow, and the last term the haline contribution.

VI. APPLICATIONS OF THE T-S GRADIENT METHOD

Introduction

It has been shown that the T-S Gradient scheme is simpler to use than the standard geopotential scheme. It remains to evaluate the T-S Gradient scheme for making geostrophic computations over large ocean areas, say over the North Pacific.

Clearly, additional advantage is gained in these calculations if the average value of the coefficients $A(S, P)$, $2B(S, P)$ and $C(T, P)$ relative to a selected reference level did not vary greatly over the ocean such that average values could be used and Equation 31 written:

$$(V_1 - V_2) = \frac{1}{f\Delta n}\left[\overline{K}_1 \sum_i T_i \Delta P_i + \overline{K}_2 \sum_i \overline{T}_i \Delta T_i \Delta P - \overline{K}_3 \sum_i \Delta S_i \Delta P_i\right] \qquad (32)$$

where

$\overline{K}_1$, $\overline{K}_2$ and $\overline{K}_3$ = weighted mean values of $A(S, P)$, $B(S, P)$ and $C(T, P)$ respectively between the surface and the selected reference level (cgs units).

If the T-S Gradient scheme can be applied using Equation 32 then only the three fixed value coefficients and the measured temperature and salinity structure would be needed to make geostrophic computations. To determine if Equation 32 is applicable, three questions must be answered:

1. What reference level should be used?
2. Relative to the selected reference level, what is the spatial variation in the weighted mean values of the coefficients (A(S, P), 2B(S, P) and C(T, P)?
3. Relative to the selected reference level, what is the time variation of the weighted mean values of the coefficients A(S, P), 2B(S, P) and C(T, P)?

Selection of the Reference Level

The question of the proper reference level to select is open to question (Defant, 1961, and Fomin, 1964). Hopefully the level selected would be a level of little or no motion. Many reference levels have been used to compute surface currents (Neumann and Pierson, 1966). FNWC uses 200 m over the entire Northern Hemisphere oceans (Hubert and Laevastu, 1967). Reid (1958) used a reference level of 500 db in the California Current region, and 1,000 db reference level in his investigation (1961) of the dynamic topography in the entire Pacific Ocean. Reed and Laird (1966) used 1,000 db for dynamic computations in a section off central California. Reed and Taylor (1965) used 1,000 db for geostrophic calculations in the Alaska Stream. Stommel (1965) summarizes the problem of selecting a reference level (page 20):

> Thus the choice of the reference level for geostrophic calculations becomes mostly a matter of taste, and we should admit that that is ultimately intolerable. The determination of the level of no motion is not a matter for debate, but for direct measurement.

There are simply not sufficient direct current measurements in the oceans to select suitable reference levels. However, Fomin (1964) shows that it may be better to select a shallow reference level of low velocity than a substantially deeper level where the velocity may approach zero, thus reducing the computational errors. He points out that in some cases the selection of a deep reference level may completely distort the computed currents.

For this study a level of 1,000 db is selected as this is possibly near an average value for the oceans. Furthermore, more hydrographic data is available over most of the ocean to 1,000 db than to deeper levels. Lastly, to go to a deeper reference level could introduce computational errors that may overcome any better approximation to no motion. Stommel (1965) states (page 19) "Fortunately, the choice of reference level has less effect upon velocity in the very surface layer than on those of deep water."

Determination of the Weighted Mean Value of $\overline{K}_1$, $\overline{K}_2$ and $\overline{K}_3$ Relative to 1,000 db in the Summer and Winter for the Pacific Ocean

Determination of $\overline{K}_1$, $\overline{K}_2$ and $\overline{K}_3$ relative to any reference level requires that the distribution of temperature and salinity be

known to this level. These distributions are available from historical data deposited at oceanographic data centers. However, it requires a great quantity of data to accomplish oceanic coverage. As a first approximation, atlas values of temperature and salinity over the Pacific Ocean were used to determine weighted mean values of the coefficients relative to the 1,000 db level.

One of the most comprehensive atlases of temperature and salinity distributions of the entire Pacific Ocean is that by Muromotsev (1963). This atlas gives the fields of temperature and salinity at selected levels between the sea surface and the deepest part of the ocean. Fields are given for summer and winter conditions at the following levels: 0, 10, 25, 50, 100, 150, 200, 300, 400 and 500 m. Below 500 m the seasonal variations are considered negligible and only single fields of temperature and salinity are available at each level: 600, 800, 1,000, 1,200, 1,500 m, and thereafter every 500 m to the bottom. In all 30,000 deep water hydrographic stations were used to compile the atlas supplemented in the upper layers by other temperature data.

The values of $\overline{K}_1$, $\overline{K}_2$ and $\overline{K}_3$ were determined for summer and winter conditions by interpolating the Muromotsev atlas temperature and salinity fields at the following levels: 0, 10, 25, 50, 100, 150, 200, 300, 400, 500, 600, 800 and 1,000 m at the intersection of the lines of latitude and longitude given in Figure 11. The

resulting weighted mean values of $\overline{K}_1$, $\overline{K}_2$ and $\overline{K}_3$ for summer and winter are shown in Figures 11 and 12, 13 and 14, and 15 and 16 respectively. It can be seen from these Figures that the variation in the coefficients over the entire ocean, or from season to season does not change by more than a few percent. Using fixed values of $\overline{K}_1$, $\overline{K}_2$ and $\overline{K}_3$ over the entire ocean relative to the selected reference level of 1,000 db should lead to only a small percent error which is certainly acceptable in the geostrophic computation. The values of the coefficients selected are:

$$\overline{K}_1 = 81.0 \times 10^{-6} \text{ (cgs units)}$$
$$\overline{K}_2 = 86.5 \times 10^{-7} \text{ (cgs units)}$$
$$\overline{K}_3 = -74.0 \times 10^{-5} \text{ (cgs units)}$$

At most an error of five percent will be introduced into the geostrophic surface current relative to 1,000 db in the Pacific by the selection of these values.

The Significance of Water Structure

The use of fixed value coefficients relative to the 1,000 db reference level in the Pacific appears to be justified. To further support this hypothesis, station pairs were selected in various regions of the world oceans and geostrophic calculations using the standard method and the T-S Gradient method using fixed values of

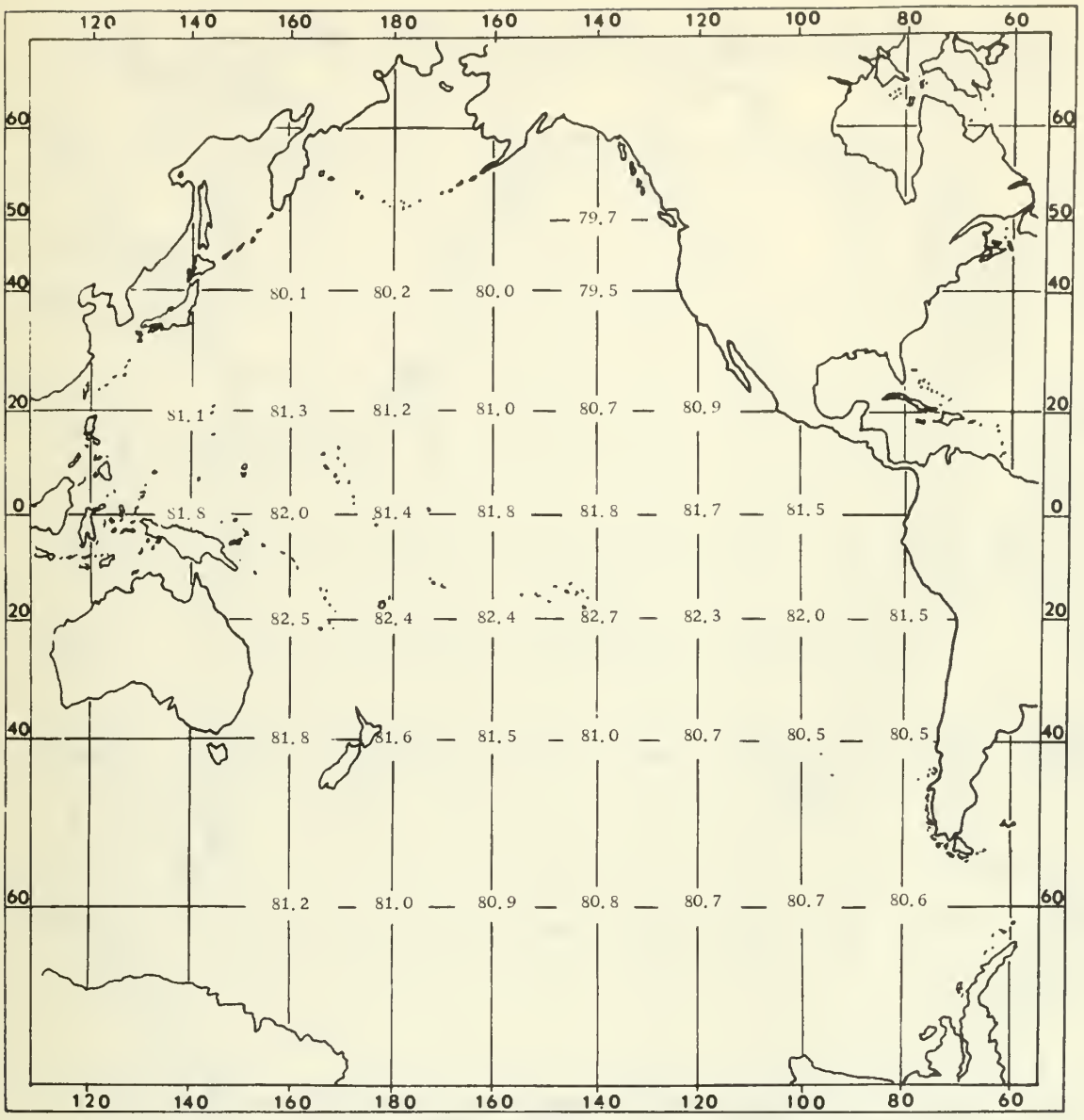

Figure 11. Variation of $\overline{K}_1$ over the Pacific Ocean in the summer

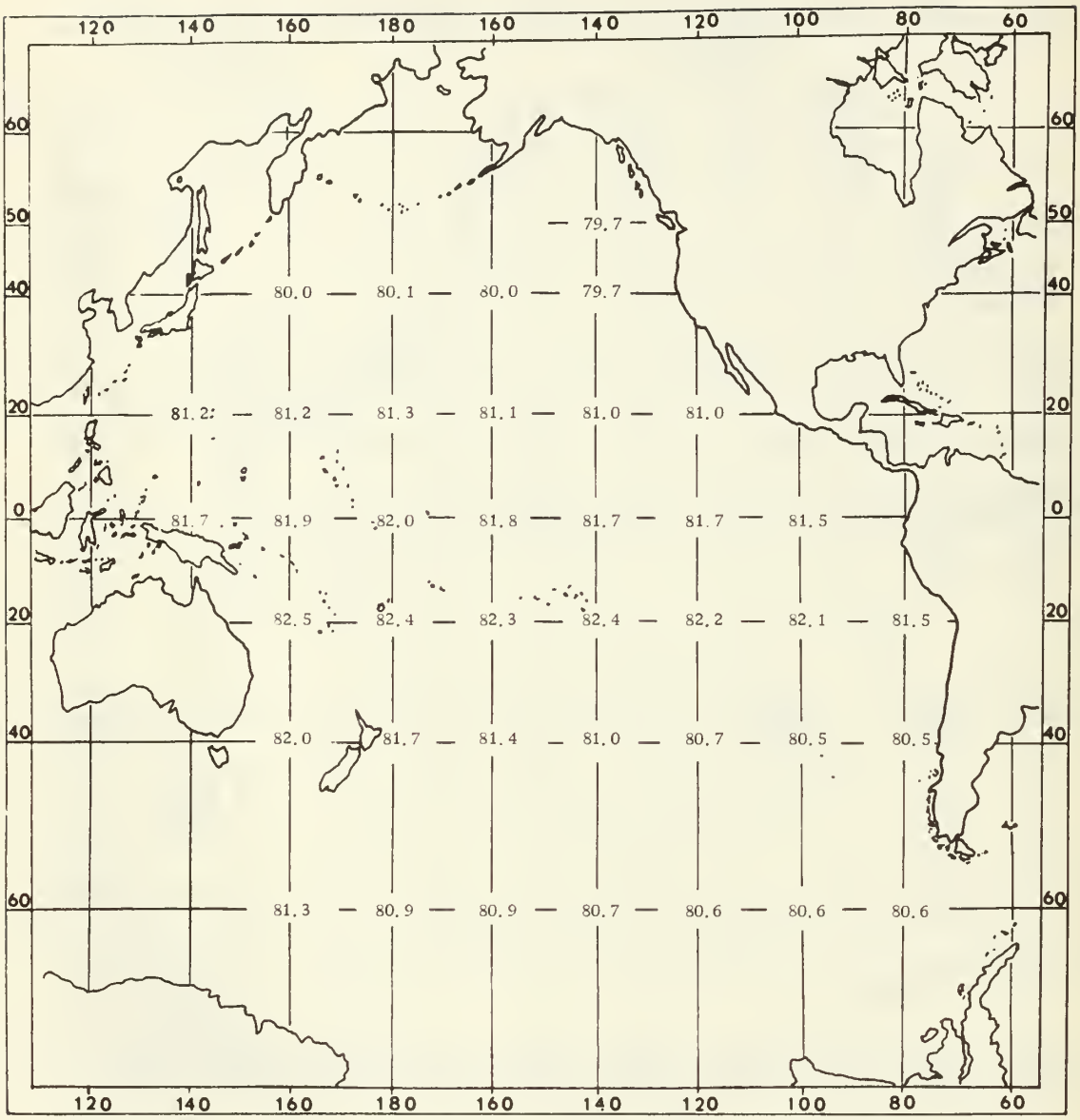

Figure 12. Variation of $\overline{K}_1$ over the Pacific Ocean in the winter

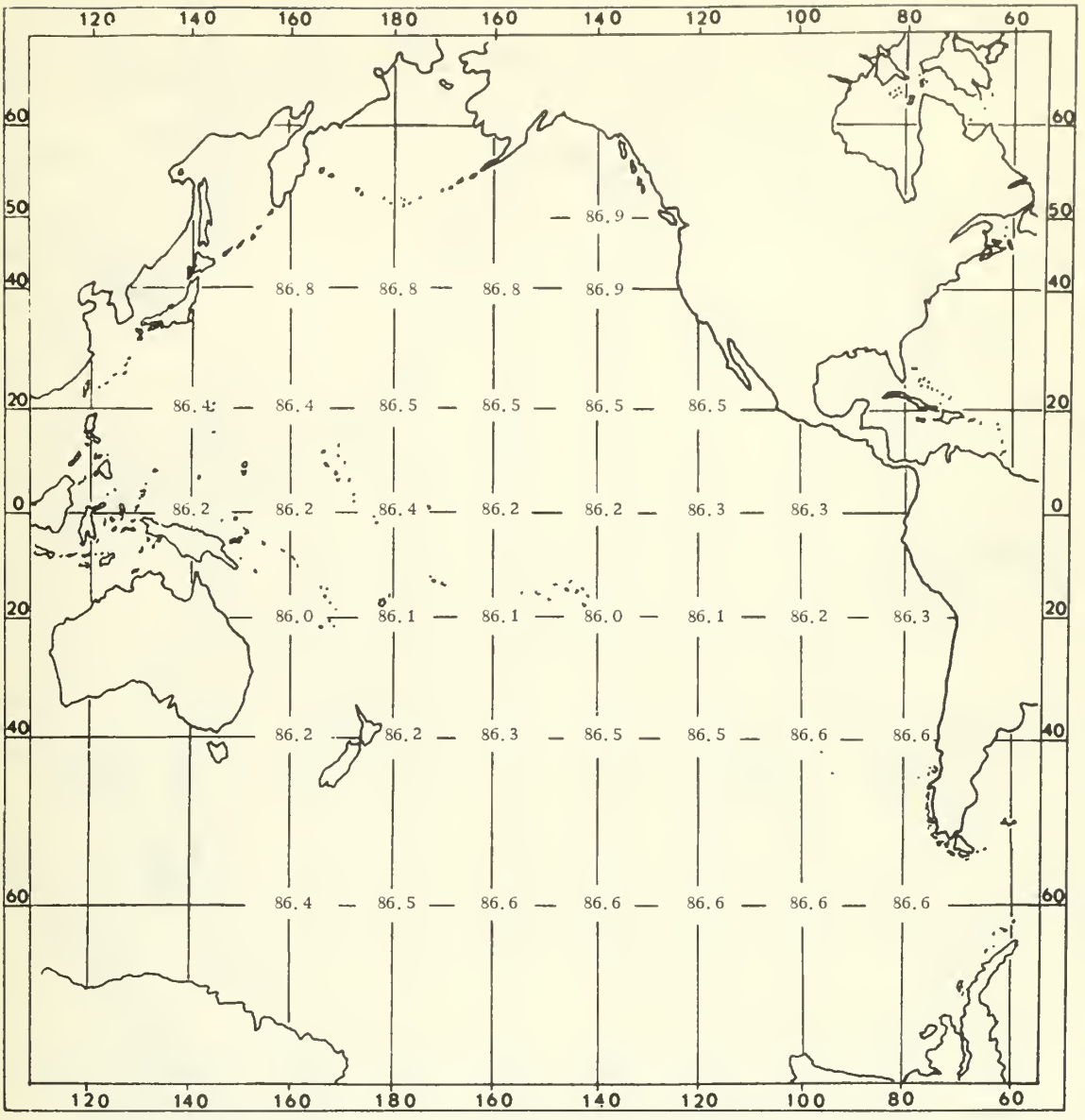

Figure 13. Variation of $\overline{K}_2$ over the Pacific Ocean in the summer

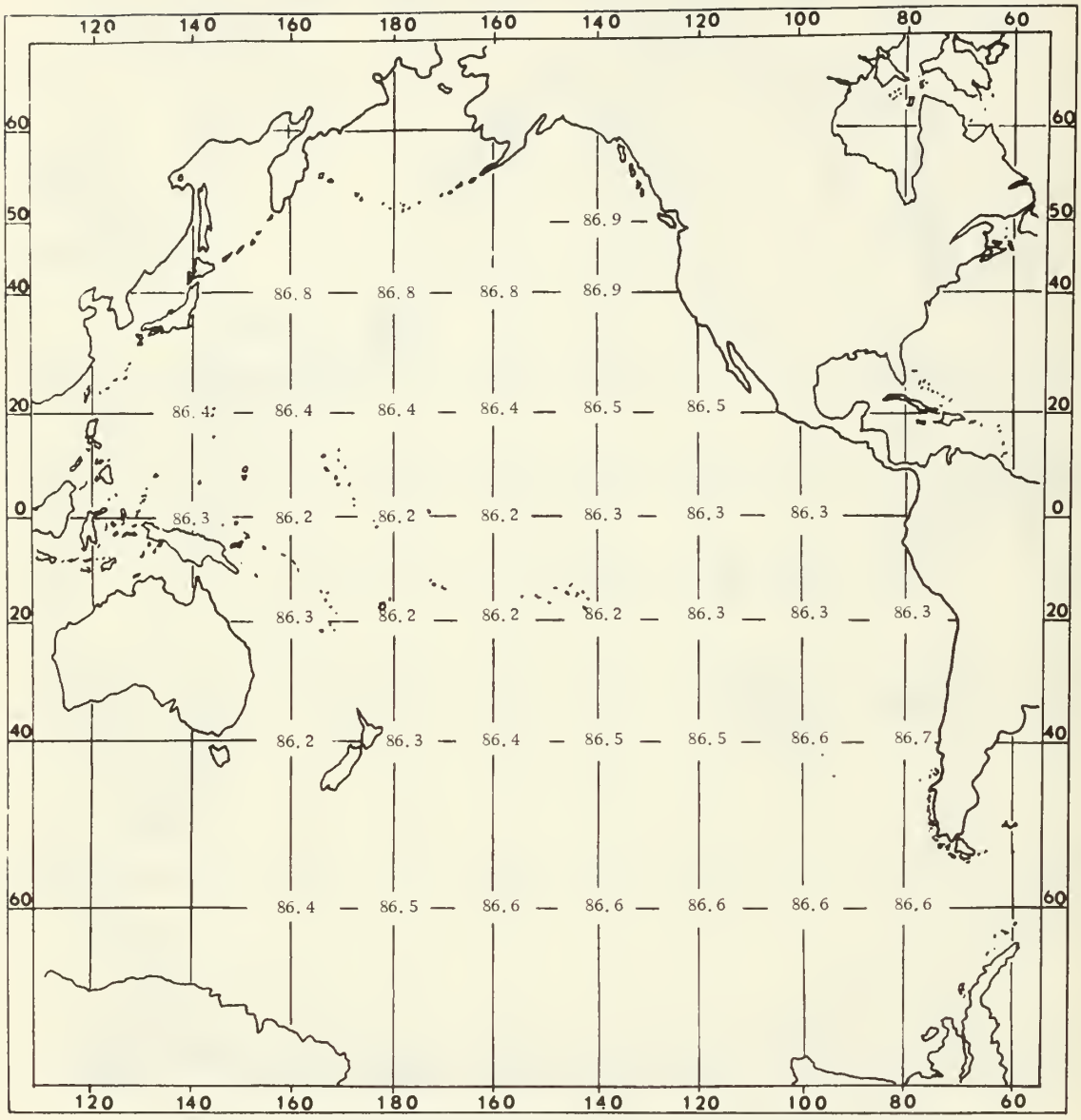

Figure 14. Variation of $\overline{K}_2$ over the Pacific Ocean in the winter

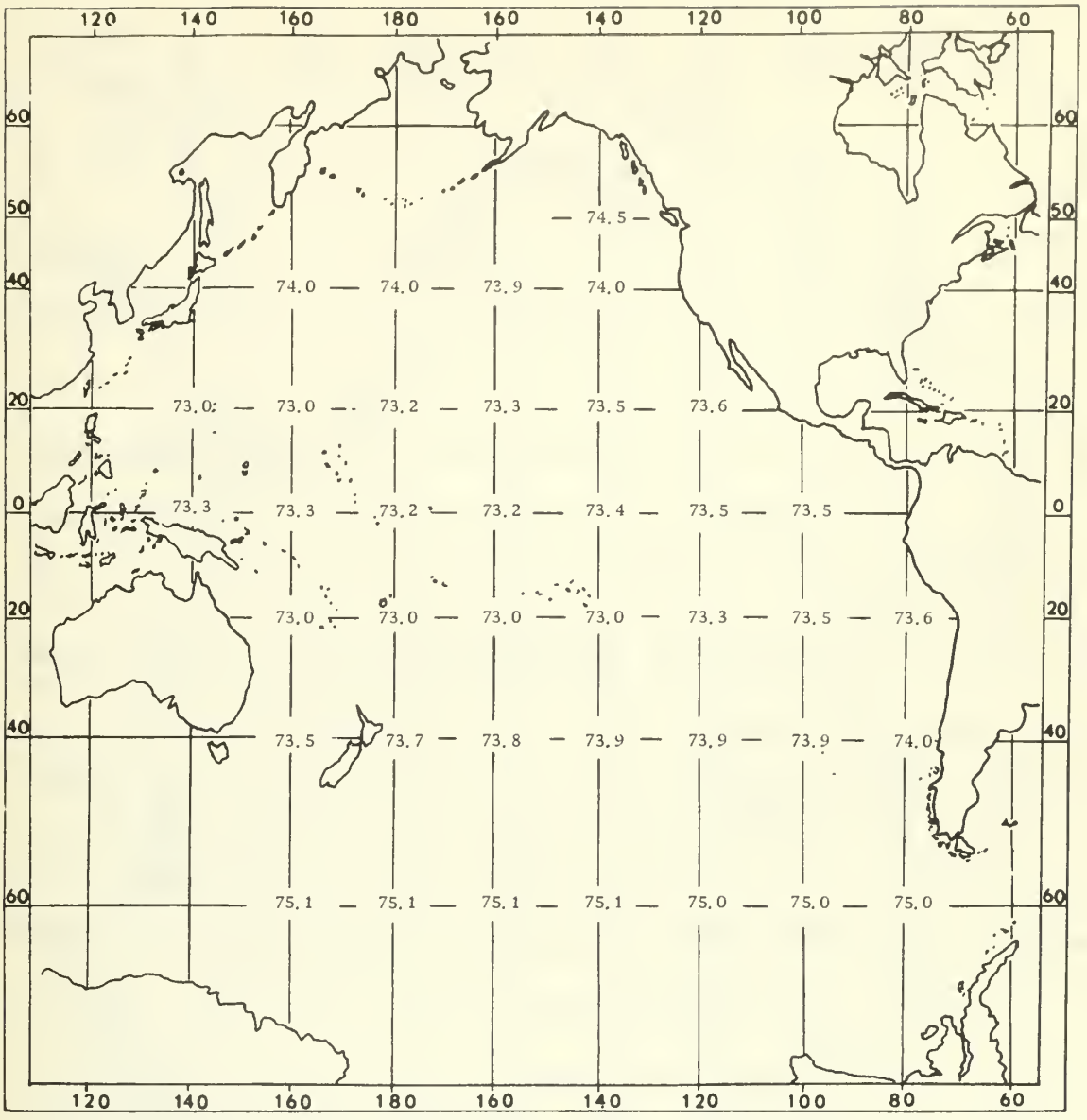

Figure 15. Variation of $\overline{K}_3$ over the Pacific Ocean in the summer

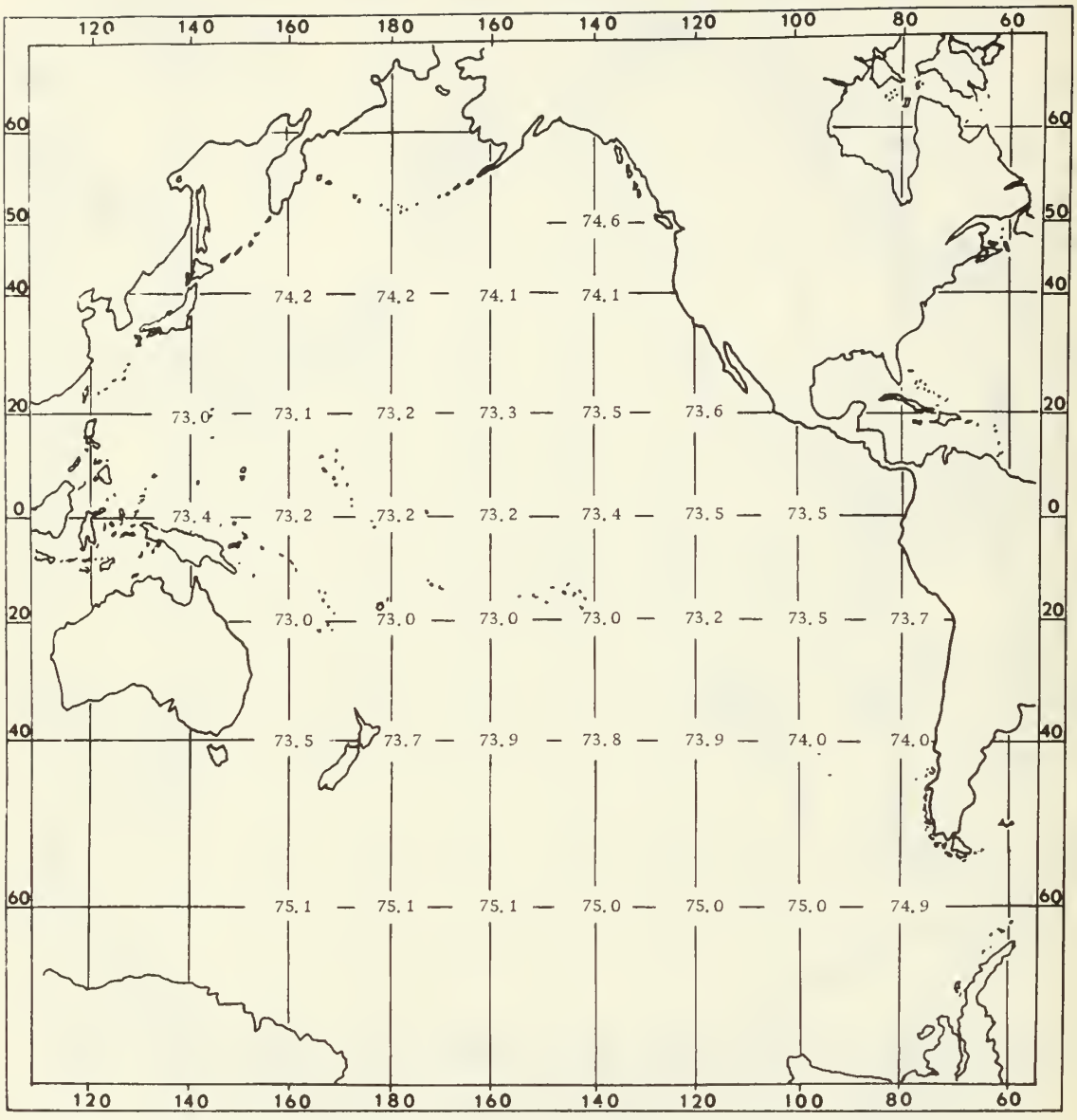

Figure 16. Variation of $\overline{K}_3$ over the Pacific Ocean in the winter

the coefficients. Lack of agreement would indicate that adjustment of the coefficients is required in some water masses.

Stations used are shown in Table 5 where region, station identification, latitude and longitude, and the computed surface speed by each method are listed. The stations were selected to be approximately perpendicular to the mean flow in each region. The complete velocity profile between the surface and the selected reference level shows small and generally not significant deviations between the two methods. The velocity profiles computed by both methods are given in Appendix II. The velocity profiles for each station pair computed by the two methods agree to better than ten percent at all depths.

The comparison made in Table 5 shows the agreement required between geostrophic surface currents computed by the two methods. None of the values computed by the T-S Gradient method disagree by more than five percent from the values computed by the standard method. Therefore, the use of average coefficients in the T-S Gradient method to calculate geostrophic flow in the surface layer relative to the 1,000 db reference level is justified. These results are encouraging. However, the need for direct verification of indirectly computed currents is great. Very few attempts to verify indirectly computed currents have been made, some are reviewed in Chapter II of this thesis. Clearly, more experiments are needed to establish the relationship between indirectly computed currents

Table 5. Comparison of geostrophic surface currents computed by the standard method and the T-S gradient method.

Ocean Region	Ship/Cruise	Station	Latitude (°)	Longitude (°)	T-S Gradient (cm/sec)	Standard (cm/sec)	Remarks
Subarctic Pacific	Explorer	5904	51°45'N	174°22'W	72.0	71.9	
		5905	51°41'N	173°24'W			
Western North Pacific	Chofu Maru	E-7	28°43'N	132°13'E	13.3	13.4	
		E-8	28°29'N	132°26'E			
Eastern South Pacific	Horizon Step 1	28	15°40'S	77°20'W	22.7	22.5	
		29	15°56'S	77°51'W			
Equatorial Pacific	Horizon Eastropac	24	09°00'N	111°25'W	27.8	28.0	
		25	08°00'N	111°33'W			
Equatorial Pacific	H. M. Smith-31	135	04°33'N	139°14'W	11.3	10.8	
		136	03°31'N	139°15'W			
Subantarctic Pacific	Ob-3	391	52°25'S	159°51'W	5.3	5.2	
		392	50°21'S	159°50'W			
Eastern North Pacific	NPGS-A1	2A	36°50'N	122°36'W	4.5	4.5	
		2B	36°20'N	123°12'W			
Western North Pacific	Inuna Maru	13	39°01'N	153°00'E	3.5	3.6	
		14	38°56'N	153°17'E			
Equatorial Atlantic	Crawford-10	122	15°52'S	37°36'W	4.9	5.0	
		123	15°55'S	36°46'W			

Table 5. Continued.

Ocean Region	Ship/Cruise	Station	Latitude (°)	Longitude (°)	T-S Gradient (cm/sec)	Standard (cm/sec)	Remarks
Equatorial Atlantic	Crawford-17	361	15° 38'N 16° 26'N	73° 56'W 73° 57'W	34. 3	35. 1	
Western North Atlantic	Atlantis	2298 2299	36° 23'N 36° 15'N	73° 45'W 73° 29'W	195. 1	204. 2	As cited in Neumann and Pierson, 1966 (p. 134-135)
North Atlantic		A B	54° 02'N 54° 06'N	24° 34'W 23° 00'W	12. 7	12. 9	As cited in Proudman, 1953 (p. 64-65)
Equatorial Indian	Norsel	25 26	09° 00'S 06° 06'S	75° 00'E 75° 01'E	12. 7	12. 5	

and actual observed currents.

Verification of Indirectly Computed Currents

Two field experiments were performed to investigate the approximation of computed geostrophic surface currents to measured currents. These experiments are discussed in some detail in Appendix V. The surface currents computed by the classical scheme, the T-S Gradient scheme and by FNWC were compared to the measured surface currents.

In both experiments the surface currents computed by the T-S Gradient scheme were identical with those computed by the classical scheme. In the first experiment the FNWC computed currents were in the opposite direction to the measured surface currents and the currents computed by both the T-S Gradient scheme and the standard geostrophic scheme. FNWC currents are heavily weighted toward the wind drift component. The computed geostrophic currents (4.0 to 9.5 cm/sec) were only about half as great as the observed currents (7.1 to 14.1 cm/sec) but they were in the correct direction.

In the second experiment as in the first the computed currents and measured currents agree in direction, but the geostrophic computed currents were again slower (5.4 cm/sec) than the measured currents (9.7 cm/sec to 16.8 cm/sec). The FNWC computed currents were the same speed (12.7 cm/sec to 25.5 cm/sec) and

direction as the measured currents.

Thus in both experiments the geostrophic currents were nearly half the directly measured currents. This might be completely explained by the fact that the mass structure was not sensed at the same time as the currents were measured. Even though these measurements were only separated by approximately 24 hours the mass structure may have changed or in fact never been in balance with the local currents. Furthermore, the geostrophic currents were calculated from the average mass structure over at least a 48 hour period, and one would expect the average gradients to be less than the maximum gradient. One fact these experiments show is the need for more field experiments to establish the validity of indirectly computed currents.

In both experiments the T-S Gradient method and the standard geostrophic computations lead to essentially the same currents. That is, the simpler T-S Gradient computations give equivalent results to the standard geostrophic computations and the advantages of simplicity are gained without giving up accuracy. Another advantage of the T-S Gradient scheme is the separation of the thermal and saline contributions to the flow. An example of this advantage is presented in the next section.

The Relationship Between the Thermal Component of the Geostrophic Surface Velocity and the Total Geostrophic Surface Velocity in the Gulf Stream Water on the Grand Banks

One of the advantages of the T-S Gradient method over standard geostrophic computations is the capability to separate the first order thermal and haline components of the geostrophic flow. To illustrate this feature of the method the thermal component and the total geostrophic surface velocities were computed for 33 station pairs of the U. S. Coast Guard, International Ice Patrol stations in the Gulf Stream water (Kollmeyer, 1966) off the Grand Banks (Appendix IV). The linear correlation of the thermal component and the total geostrophic velocity for the 33 station pairs was determined (Moynihan, 1968):

$$V_g = 0.39V_t + 2.84$$

where

V_g = the total geostrophic velocity (cm/sec)

V_t = the thermal component of the geostrophic velocity (cm/sec)

The standard deviation of the total geostrophic current from the linear correlation function between it and the thermal component is less than four (4) cm/sec. Therefore, in this water mass total geostrophic currents might be determined using only temperature data through the relationship above.

VII. HEMISPHERIC COMPUTER APPLICATION

Introduction

The Fleet Numerical Weather Central, Monterey, California is the only facility attempting to determine surface currents on a hemispheric scale. The background of their computational technique has been given in an earlier section of this thesis (Chapter IV). For lack of any other hemispheric fields the FNWC 63 x 63 grid fields will be used in this study. The following fields are available through FNWC over their 63 x 63 grid:

1. Synoptic temperature fields between the surface and 1, 200 feet at 100 foot intervals.
2. Climatological (monthly means) temperature fields between the surface and 1, 200 feet at 100 foot intervals.
3. Climatological (summer and winter) temperature and salinity fields in the Pacific and Atlantic, derived from published atlases (Muromtsev, 1963 and Bohnecke, 1936).

Attempts were made in this study to use these fields to investigate the geostrophic flow through the T-S Gradient computations in the surface layers of the North Pacific.

Synoptic Fields

During April, 1968, Equation 33 was programed on the Naval Postgraduate School IBM 360 digital computer to run over the FNWC synoptic temperature field for 0000 GMT, March 5, 1968. The program is found in Appendix III. While the program will calculate the salinity term in Equation 32, a constant salinity of 35 ‰ was assumed for lack of a salinity field. The output of the program is the i and j components of the velocity between the grid points, and the vector sum of these components at the southwest grid point of a four-point element as is shown in Figure 17. The direction of the total current was determined by hand computation from the ratio of the i, j components. Because of the large number of points (3889) in the 63 x 63 grid only those in the North Pacific will be considered. However, since the major oceanic circulation features are thought to be common to all oceans (Sverdrup, 1942) any conclusions drawn for the Pacific Ocean should be valid in the other oceans.

For comparative purpose the FNWC Current Transport and Stream Function maps for the same period are shown in Figures 18 and 19 respectively. Recall that these maps represent the sum of their geostrophic and wind driven components. Independent control for the geostrophic currents is provided by Tully (1964 after Reid, 1961) who gives the surface geostrophic flow relative to 1,000 db

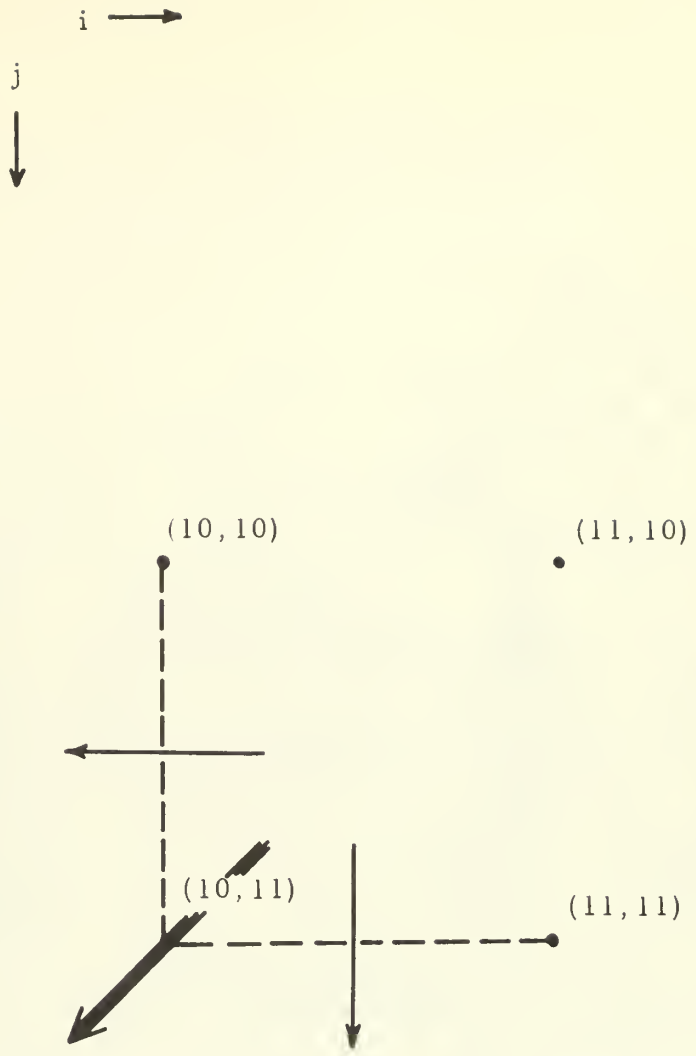

Figure 17. Resolution of the i and j components of the velocity

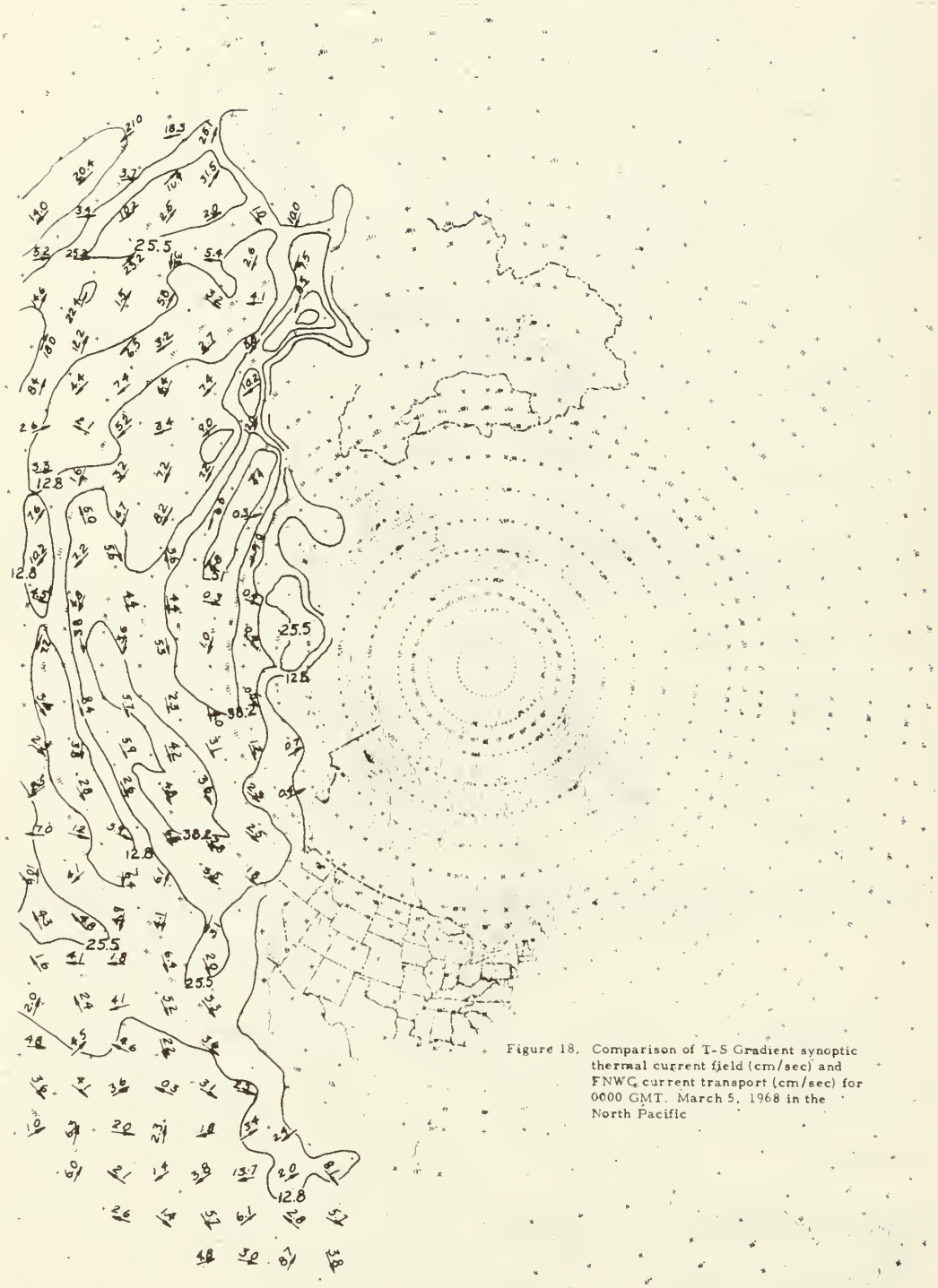

Figure 18. Comparison of T-S Gradient synoptic thermal current field (cm/sec) and FNWC current transport (cm/sec) for 0000 GMT, March 5, 1968 in the North Pacific

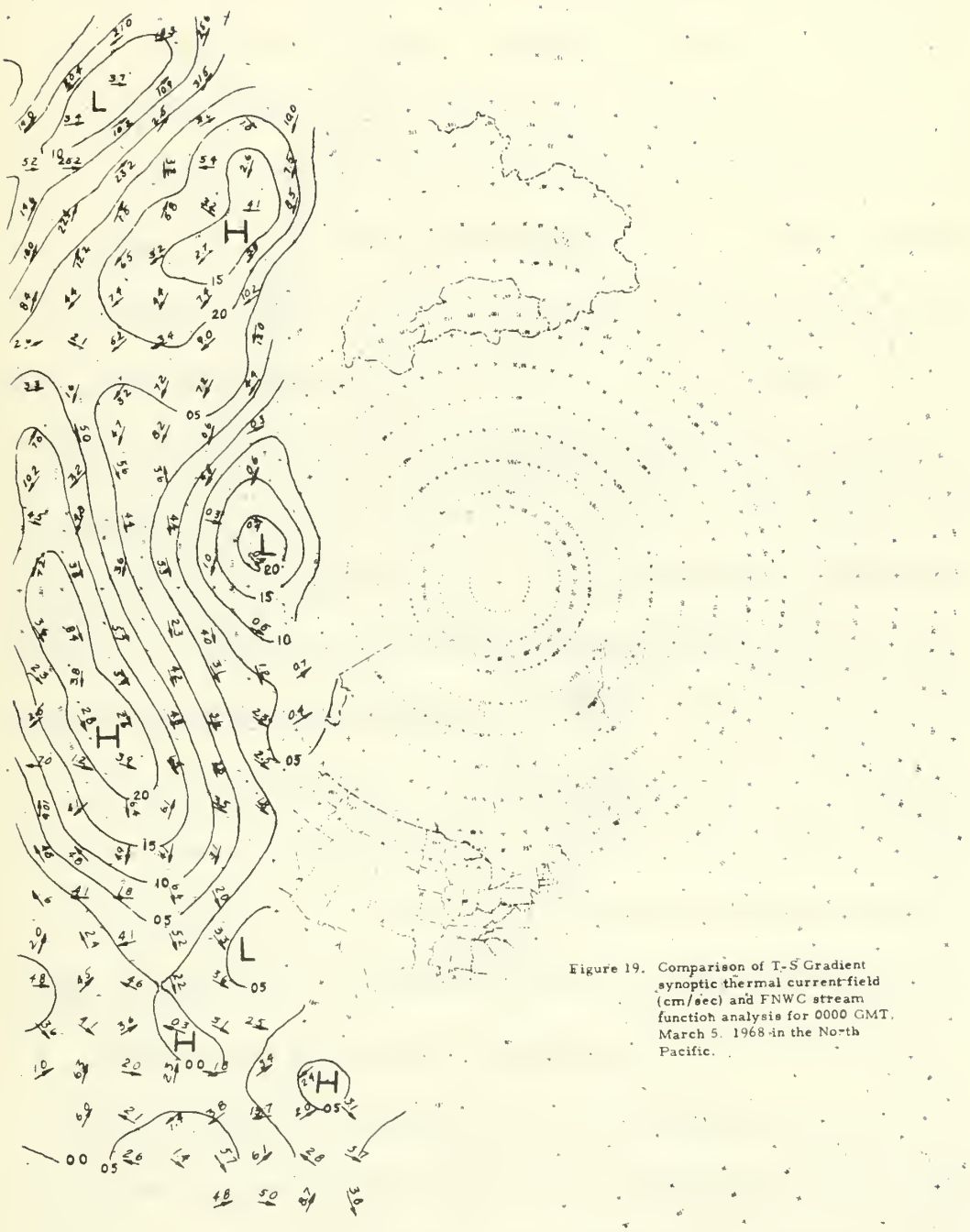

Figure 19. Comparison of T-S Gradient synoptic thermal current field (cm/sec) and FNWC stream function analysis for 0000 GMT, March 5, 1968 in the North Pacific.

(Figure 20).

First, in Figure 19 the FNWC currents display many features of the established mean circulation in the North Pacific (Figure 20), i. e., the subarctic gyre, subtropic gyre, and tropic gyre. Beginning at the Equator the equatorial system is shown, including the North Equatorial, South Equatorial, and Equatorial Counter Currents. The Kuroshio appears as a high speed flow and the Oyashio Current is present. The North Pacific Drift is apparent as is the separation of this flow into a northerly flow, providing the Gulf of Alaska circulation, and a southerly flow, the California Current. The magnitude of the recognized currents is reasonable, but in general the values are low in the narrow, concentrated streams such as the Kuroshio, and high in the regions of wide slow flows like the California Current.

The currents computed with Equation 32 are plotted at selected grid points in Figures 18, 19, and 20. While some of the major circulation patterns can be identified, the current speeds are consistently low over the entire ocean. The computed currents are in poorest agreement in the western boundary area of the Kuroshio. Here Equation 33 over the 1, 200 foot temperature field gives a value which is low by an order of magnitude. The values in the North Pacific Drift are in agreement with those given by Tully (7 cm/sec to 10 cm/sec). The speeds in the Alaska stream also are low by an order of magnitude. The agreement is best in the California

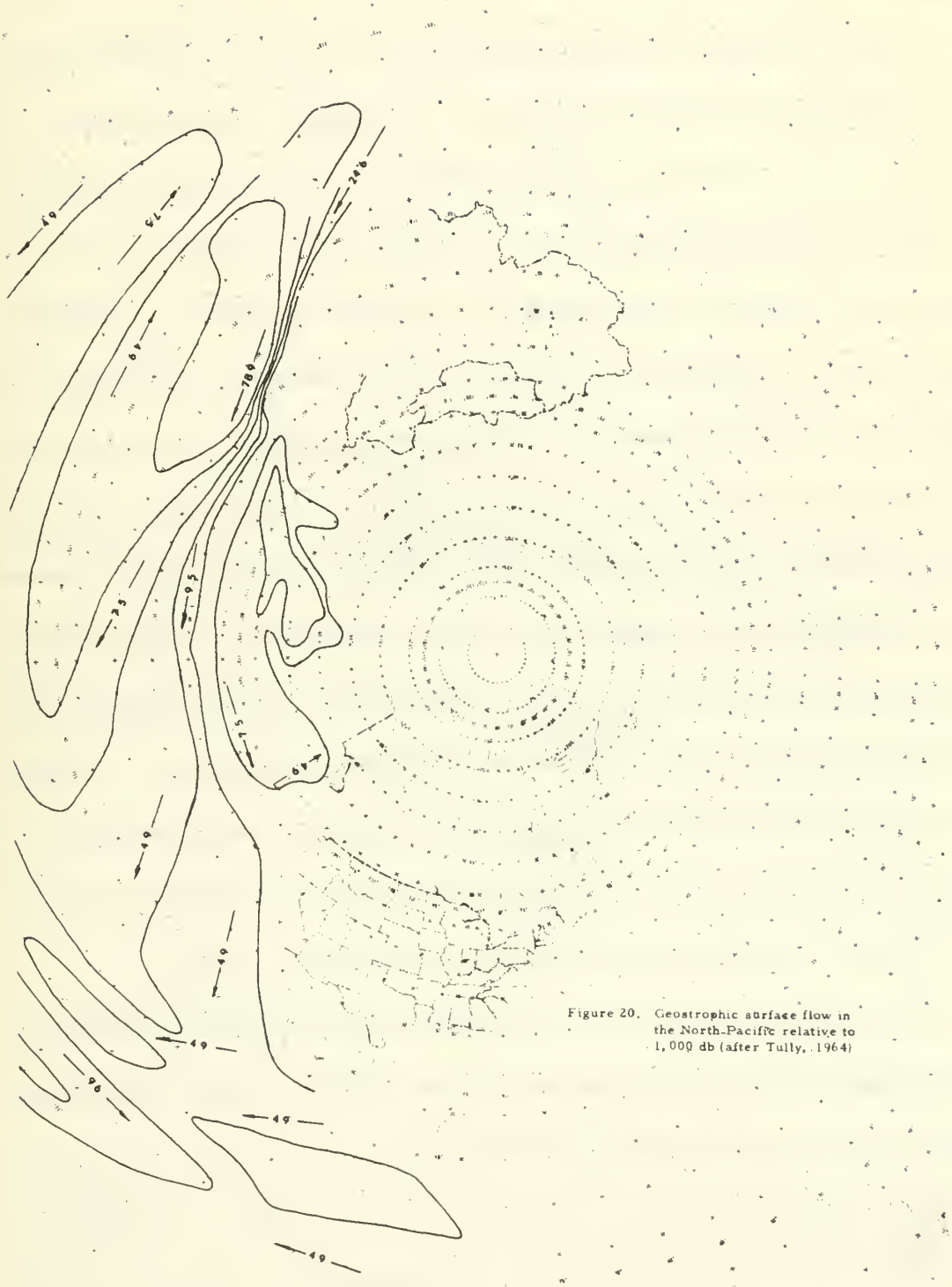

Figure 20. Geostrophic surface flow in the North Pacific relative to 1,000 db (after Tully, 1964)

Current. Some of the features of the equatorial current system appear, but the speeds are high in the North Equatorial Current compared to those given by Tully.

Several possible explanations are apparent for the low current speeds in the Kuroshio Current and in the Alaska Current. First these currents are narrow high speed flows. The grid spacing used in these calculations is so large as to completely straddle the currents. Geostrophic computations assume that the velocity is uniform between any two stations in a section. The statement that any particular stream is in geostrophic balance is meaningful only within the boundaries of the stream. If one station of a station pair is removed from the stream (and in many cases grid points used to calculate the velocity in a stream lie outside the stream boundaries) then geostrophic computations cannot be expected to be representative of the stream velocity. For this reason alone one would expect the geostrophic velocity to be low in most cases since the mass gradients are rarely sensed at their maximum. Secondly, in both these flows a 1, 200 foot reference level is clearly too shallow. Lastly, only the thermal component of the current has been computed. Possibly the last two of these problems can be corrected by using the climatological temperature and salinity fields.

Climatological Fields

To investigate the magnitude of the problems suggested in the previous section Equation 32 was programmed to run over the FNWC atlas climatological temperature and salinity fields on the FNWC CDC 3600 computer. The program is found in Appendix III. Since the atlas temperature fields were not digitized between the surface and 400 m, either the synoptic or the monthly climatological temperature fields must be used for temperatures above this depth. Thus fields from different sources are combined to make the calculations. The compatability of the fields at any level and between levels has not been investigated. A reference level of 1,000 m was selected as the average coefficients in Equation 32 had previously been determined for that reference level (Chapter VI). Furthermore, this was the reference level used by Reid (1961). The flow computed is shown in Figure 21 where isotachs indicate the surface current speed and arrows indicate the direction.

The currents exhibit few of the features of the geostrophic circulation as given by Tully (1964), and many anomalies exist. In particular, there is a high transport region shown extending off the Japanese islands but the magnitude is too low by nearly half an order of magnitude. There is some indication of a westerly drift across the north Pacific, a southerly flow off the west coast of the United

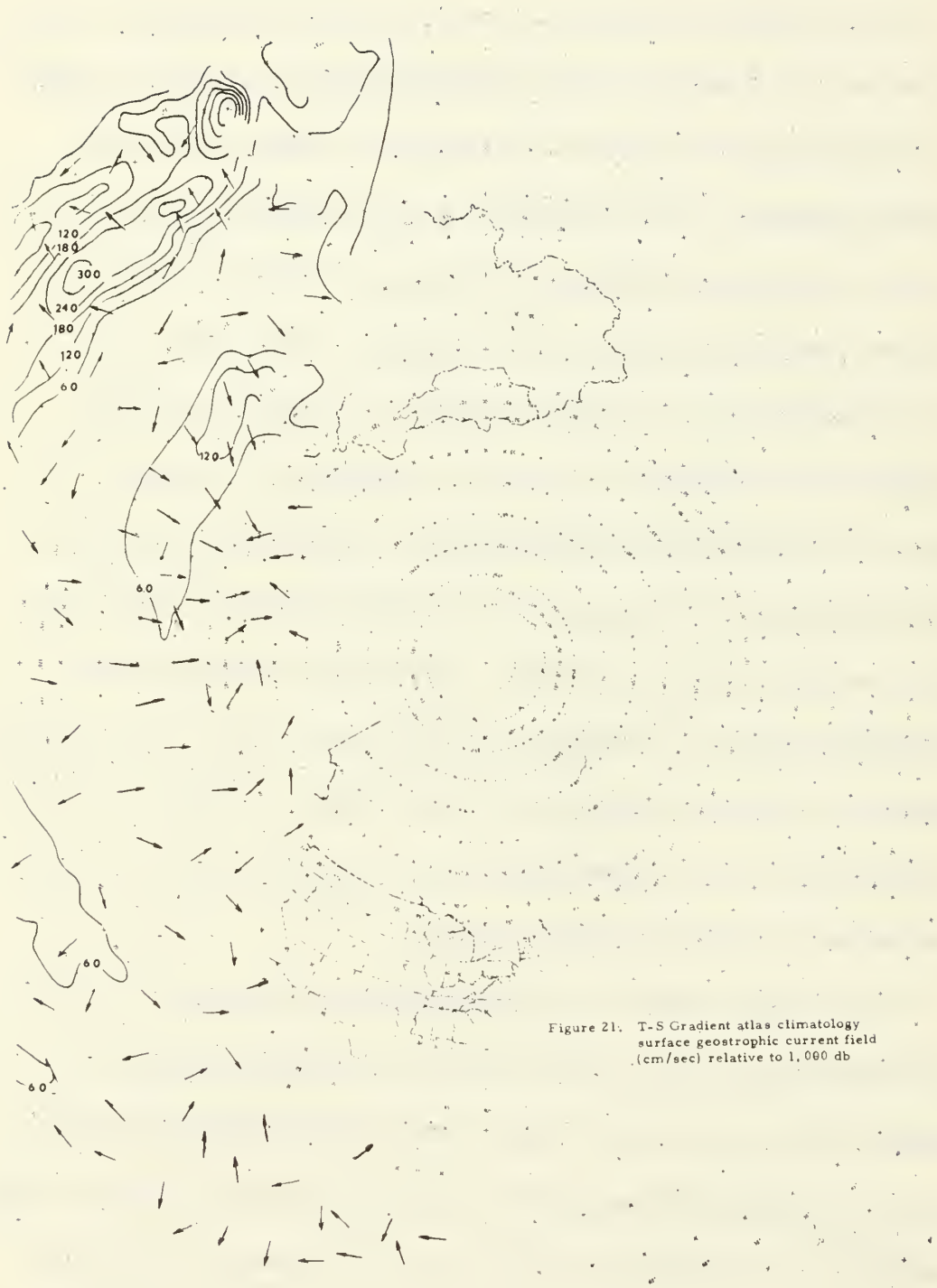

Figure 21. T-S Gradient atlas climatology surface geostrophic current field (cm/sec) relative to 1,000 db

States and Mexico, and a cyclonic gyre in the Gulf of Alaska. The magnitude of the computed currents are in most reasonable agreement in the California Current region where values of a few centimeters per second appear. In general the central portion of the subtropic gyre shows a strong northerly component which is not in agreement with known geostrophic circulation. Furthermore, the high transport in the western equatorial region is not in agreement with Tully.

Remarks and Recommendations

Remarks

Equation 33 has been programed to run over the available 63 x 63 fields of FNWC. The results of these computations have been compared to surface current computations presently made by FNWC and with geostrophic flow relative to 1, 000 m given by Tully (1964) for the North Pacific. These comparisons show clearly that acceptable geostrophic surface currents cannot be computed from the existing fields. While indications of accepted flow patterns appear, several limitations of the available fields are clear.

For the synoptic fields one of the chief limitations is the fact that these fields only extend to 1, 200 feet. This is too shallow for a reference level over much of the ocean. Obviously, a second

limitation is the lack of salinity fields to complete the computations. Another limitation of the synoptic fields is the coarseness of the grid system. In many areas the grid spacing is larger than the known width of the existing currents.

Using the existing climatological fields, the computations can be extended to 1,000 db. Unfortunately, in the Pacific these fields do not represent adequately the mass field for geostrophic computations. Derived from atlases, the fields are smoothed in an undetermined way. Furthermore, since the atlases present the temperature and salinity as horizontal fields at each level, the interpolation of these fields to the grid points undoubtedly will contribute errors. A further problem with the existing climatological fields is the requirement to use monthly climatological temperature fields in the upper 400 m along with atlas salinity fields, without establishing the compatability of the two fields. Again the coarseness of the available 63 x 63 grid is not appropriate for geostrophic computations in the narrow current regions. If these computations are to be made then several adjustments must be made in the available fields.

Clearly the available fields and coarse grid restrict geostrophic computations over the ocean by <u>any</u> method. The more acceptable agreement between currents computed by FNWC and "accepted" currents is due to their capability to "tune" the flow. This same procedure could be used to adjust the geostrophic flow

computed by the T-S Gradient scheme using the synoptic temperature fields which appear from this study to be the best available fields. However, "tuning" the ocean to an arbitrary standard seems questionable. Geostrophic computations should be objective and the use of arbitrary "tuning" factors removes this objectivity. Several recommendations are obvious which should be considered as possible improvements, hopefully leading eventually to the capability of computing actual geostrophic flow over the world oceans.

Recommendations

First, the 63 x 63 Northern Hemisphere grid used by FNWC gives a grid spacing of 373 nmi at the equator, 200 nmi at 60° N latitude, and 186 nmi at the pole. This grid spacing is too large for geostrophic computations over most of the oceans. The minimum spacing suggested by Reed and Laird (1965) for 160°W and 175°W longitude is an indication of more acceptable spacing. Their values are shown in Table 6. The basis for their recommendations is that the dynamic height difference should be five times the error in dynamic height computations. However, a grid spacing too much larger than this will lead to poor results. Since the dynamic height represents an integral of the water structure a grid should be developed for geostrophic computations using the dynamic height gradient as one criterion in constructing a new grid and temperature

and salinity fields.

Table 6. Minimum station spacing along 160° W and 175° W in the North Pacific (from Reed and Laird, 1965).

Current	Optimum Station Spacing (km) along approx. 160° W	Optimum Station Spacing (km) along approx. 175° W
Alaska Stream	16	8
Subarctic	183	110
West Wind Drift	61	39
Gyre	> 137	> 137
Kuroshio Extension	55	34

Another justification for altering the grid spacing considers the distribution of data. The smallest grid spacing is found at the poles where the lowest data density is available, while in the tropical regions the grid spacing is largest although this is where data is relatively more abundant (Wolff, 1964). Therefore, where the most data are available and the smallest scale features could be shown in the data, the grid scale is coarsest and these features are lost.

New fields must be constructed if geostrophic computations are to be made. The best approach to the construction of these new fields would be to work with actual hydrographic data available from depositories of these data i. e., the National Oceanographic Data Center, Washington, D. C. The requirements of geostrophic computations should be used as a guideline in construction of new fields.

VIII. SUMMARY AND CONCLUSIONS

This study has examined schemes for simplifying geostrophic computations. Several schemes have been previously proposed to simplify these computations, but except for the use of the thermosteric anomaly proposed by Montgomery and Wooster (1954) none are satisfactory over the entire ocean.

A simplification is proposed here which represents a significant simplification of dynamic computations without loss of accuracy. The scheme expresses the geostrophic velocity as three terms involving the observed variables, temperature and salinity. Only three coefficients are needed. These coefficients have been determined and are given in graphical and tabular form. If a fixed reference level of 1,000 db is used it has been shown that fixed values of the coefficients can be used for geostrophic surface current computations over the entire Pacific Ocean without introducing more than a five percent error. The name T-S Gradient scheme is proposed for the simplification. It provides the following advantages over other schemes:

1. Computations show no loss in accuracy from the classical scheme for most practical purposes.

2. The computation of geostrophic currents is substantially simplified.

3. The scheme is general and can be used in any region of the ocean where the temperature, salinity and pressure fall within the range for which the coefficients have been determined.

4. The scheme requires only the observed variables, temperature, salinity and pressure, and the coefficients A(S, P), 2B(S, P) and C(T, P).

5. The first order thermal and haline structure contributions to the geostrophic flow can be determined independently.

6. The scheme is computationally faster than the classical scheme (seven times faster on the IBM 360).

7. The scheme is particularly well suited to use onboard ships with small digital computers as involved equations of state are not used.

The proposed scheme was used to compute surface geostrophic flow over the 63 x 63 FNWC northern hemisphere fields, the only hemispheric fields available at this time. The resulting computed surface currents were compared to surface currents in the North Pacific Ocean computed by FNWC, and by Tully (1964) from Reid's (1961) investigation of the geopotential topography of the 0 db level relative to the 1000 db level. These comparisons lead to the conclusions that the FNWC 63 x 63 fields are unsuited to geostrophic computations for the following reasons:

1. The grid spacing is too large even at its smallest spacing.

2. The atlas derived fields do not adequately depict the mass distribution in the ocean.

3. The synoptic temperature fields do not extend to deep enough level to reasonably approximate level of little or no motion. The computations over the 63 x 63 fields do show, however, that it is practical to make actual geostrophic computations over such a large ocean area on a synoptic basis if the desired fields are available.

Two proposals are made to improve geostrophic computations over hemispheric grids. First, that a new grid should be constructed in which the grid spacing is compatible with geostrophic computational requirements; second, new temperature and salinity fields be constructed from the available hydrographic data to replace the atlas climatological fields presently available.

The T-S Gradient method can be used to compute independently the first order thermal and haline contributions to the geostrophic flow. It has been shown that the correlation of the first order thermal geostrophic surface current (V_T) with the geostrophic surface current (V_g) in the Gulf Stream water off the Grand Banks can be expressed by a simple linear relationship. This relationship is useful for the determination of the total geostrophic surface current from temperature measurements alone.

The reliability of the T-S Gradient scheme was tested by

comparing T-S Gradient and standard geostrophic computations in several differing water masses. The current velocity structure was nearly exactly the same in both cases (Appendix II). Never were the computations in disagreement by more than ten percent even though fixed coefficients were used.

Two field tests were performed to investigate the approximation of computed geostrophic surface currents (Appendix IV) to measured surface currents. The currents were measured prior to the hydrographic measurements using parachute drogues. Geostrophic currents were computed from the measured temperature and salinity by both the classical geostrophic method and the T-S Gradient method, and FNWC currents were obtained from their Current Transport and Stream Function maps for the periods of the experiments. On the second experiment the geostrophic computations were also made with the reversing thermometer temperatures replaced by the expendable bathythermograph temperatures.

The geostrophic currents computed by both methods were identical for both experiments. The substitution of expendable bathythermograph temperatures raised the computed surface velocity by both methods approximately one cm/sec. The computed geostrophic surface velocity was approximately half the observed current in both experiments. The FNWC currents were in the opposite direction to the observed flow in the first experiment but agreed

with the observed flow in the second.

Certainly two experiments should not be considered as verification or condemnation of any scheme. The results of the experiments do show the need for additional experimentation before a great deal of confidence can be placed in any indirectly computed currents.

It is proposed that this research be continued to further investigate the relationships between indirectly computed surface currents and observed currents (see Appendix V).

BIBLIOGRAPHY

Bierknes, V. and J. W. Sandstrom. 1910. Dynamic meteorology and hydrography, Part I. Statics. Washington, D. C., Carnegie Institution of Washington. 146 p. (Publication 88)

Bisset-Berman Corporation. 1968. 9040 Salinity-temperature-depth system. San Diego. n. p. (Specifications brochure)

Bowden, K. F. 1953. Measurement of wind currents in the sea by methods of towed electrodes. Nature 171(4356):735-736.

Broida, S. 1966. Interpretation of geostrophy in the straits of Florida. Ph. D. thesis. Coral Gables, Florida, University of Miami. 107 numb. leaves.

Brown, N. L. 1968. An in situ salinometer for use in the deep ocean. In: Marine sciences instrumentation, ed. by Fred Alt. Vol. 4. Proceedings of the Fourth National Instrument Society of America Marine Sciences Instrumentation Symposium, Coca Beach, Florida, 1968. New York, Plenum. p. 563-577.

Cox, C. S. 1962. Internal waves. Part I. In: The sea, ed. by M. N. Hill. Vol. 2. New York, Interscience. p. 752-763.

Defant, A. 1950. Reality and illusion in oceanographic surveys. Journal of Marine Research 9(2):120-138.

_____ 1961. Physical oceanography. Vol. 1 New York, Pergamon. 725 p.

Denner, W. W., T. Green and W. H. Snyder. 1968. Large scale oceanic drogue diffusion. Nature 219(5152):361-362.

Eckart, C. 1958. Properties of water. Part III. The equation of state of water and sea water at low temperatures and pressures. American Journal of Science 256:225-240.

Ekman, V. W. 1908. Die Zusammendrückbarkeit des Meerwassers. Publications de Circonstance du Conseil Permanent International pour L'Exploration de la Mer 43:1-47.

Fofonoff, N. P. 1962. Physical properties of sea-water. In: The sea, ed. by M. N. Hill. Vol. 2. New York, Interscience. p. 3-28.

Fomin, L. M. 1964. The dynamic method in oceanography. New York, Elsevier. 212 p.

Forsch, C., M. Knudsen and S. P. L. Sorensen. 1902. Berichte uber die Konstantenbestimmungen zur Aufsellung der hydrographischen Tabellen. Kongelige Danske Videnskabernes Selskab Skrifter, Naturvidenskabelig og Mathematisk Afdeling 12(1):1-151.

Gibson, B. W. 1962. Sea surface temperature synoptic analysis. Washington, D. C., U. S. Naval hydrographic office. 17 p. (Antisubmarine Warfare Environmental Prediction System Report no. 7)

Groen, P. 1967. The waters of the sea, Princeton, New Jersey, Van Nostrand. 316 p.

Haltiner, G. J., and F. L. Martin. 1957. Dynamical and physical meterology. New York, McGraw-Hill. 470 p.

Haurwitz, B., H. Stommel and W. H. Munk. 1959. On the thermal unrest in the ocean. In: The atmosphere and the sea in motion, ed. by Bert Bolin. New York, Rockefeller Institute in association with Oxford University. p. 74-94. (Rossby Memorial Volume)

Hubert, W. E. 1964. Computer produced synoptic analysis of surface currents and their application for navigation. Navigation 12(2):101-107.

Hubert, W. E. and T. Laevastu. 1967. Synoptic analysis and forecasting of surface currents. Norfolk, U. S. Navy Weather Research Facility. 55 p. (Report no. 36-0667-127)

Interstate Electronics Corporation. 1968. Critical evaluation of geostrophic current prediction techniques for ASWEPS. Anaheim, California. 125 p. (Unpublished report)

James, R. W. 1966. Ocean thermal structure forecasting. Washington, D. C. U. S. Naval Oceanographic Office. 217 p. (Antisubmarine Warfare Manual no. 5)

Jones, T. B. 1939. An introduction to Hispanic American history. New York, Harper. 577 p.

Knudsen, M. 1901. Hydrographic tables. Copenhagen, G. C. E. Gad. 63 p.

Kollmeyer, R. C. 1964. An examination of errors in dynamic height determinations. Washington, D. C., U. S. Coast Guard, Oceanographic Unit. 23 p.

_____ 1966. Oceanography of the Grand Banks region of Newfoundland in 1965. Washington, D. C., U. S. Coast Guard, Oceanographic Unit. p. 157. (Report no. CG373-11)

LaFond, E. C. 1949. The use of bathythermograms to determine ocean currents. Transactions of the American Geophysical Union 30(2):231-237.

_____ 1951. Processing oceanographic data. Washington, D. C., U. S. Hydrographic Office. 113 p.

Lenczyk, R. E. 1962. Report of the International Ice Patrol Service in the North Atlantic Ocean. Washington, D. C., U. S. Coast Guard. 109 p. (Bulletin no. 50)

Li, Yuan-Hui. 1967. Equation of state of water and sea water. Jounral of Geophysical Research 72(10):2665-2678.

Magnavox Corporation. MX/702/hp Shipboard navigation system. Fort Wayne, Indiana. n. p. Specification brochure TP 67-1947)

Montgomery, R. B. and W. S. Wooster. 1954. Thermosteric anomaly and analysis of serial oceanographic data. Deep sea research 2:63-70.

Montgomery, R. B. and E. D. Stroup. 1962. Equatorial waters and currents at 150° W in July-August 1952. Baltimore, Johns Hopkins Press. 88 p. (Johns Hopkins Oceanography Studies no. 1)

Moynihan, M. J. 1968. Investigation of Geostrophic current calculations on the Grand Banks. Master's thesis. Monterey, U. S. Naval Postgraduate School. 62 numb. leaves.

Neumann, G. and W. J. Pierson, Jr. 1966. Principles of physical oceanography. Englewood Cliffs, New Jersey, Prentice-Hall. 545 p.

Newton, M. S. and G. C. Kennedy. 1965. An experimental study of the P-V-T-S relations of sea water. Journal of Marine Research 23(2):88-103.

Proudman, J. 1953. Dynamical oceanography. London, Methuen. 409 p.

Rattray, M. 1962. Interpolation errors and oceanographic sampling. Deep Sea Research 9:25-37.

Reed, R. K. and N. E. Taylor. 1965. Some measurements of the Alaska Stream with parachute drogues. Deep Sea Research 12:777-784.

Reed, R. K. and N. B. Laird. 1966a. On the reliability of geostrophic flow determinations across a section of the North Pacific Ocean. Paper presented at the Northwest Regional Meeting of the American Geophysical Union, Corvallis, Oregon, August. 7 numb. leaves.

_____ 1966b. An oceanographic section off the California coast, February, 1966. Seattle, Environmental Science Services Administration, Pacific Oceanographic Laboratory. 51 p. (Technical Memorandum IER TM-POL-s)

Reid, J. L., Jr., G. I. Roden and J. G. Wyllie. 1958. Studies of the California Current system. In: Progress report of the California Cooperative Oceanic Fisheries Investigations, July 1, 1956, to January 1, 1958. [Sacramento] p. 27-57.

Reid, J. L. 1961. On the geostrophic flow at the surface of the Pacific Ocean with respect to the 1, 000 decibar surface. Tellus 13(4):489-502.

Reid, R. O. 1959. Influence of some errors in the equation of state or in observations on geostrophic currents. In: Proceedings of a Conference of Physical and Chemical Properties of Sea Water. Washington, D. C., (National Research Council. p. 10-29. (Publication 600)

Sandstrom, J. W. and B. Helland-Hansen. 1903. Uber die Berechnung von Meerströmungen. Bergen, Norway. 43 p. (Report on Norwegian Fisheries and Marine Investigation. Vol. 2. No. 4)

Smith, E. H. 1931. Arctic ice with special reference to its distribution to the North Atlantic Ocean. Washington, D. C. U. S. Coast Guard. 221 p. (The Marion Expedition, 1928. Bulletin 19, part 3)

Stommel, H. 1947. Note on the use of the T-S correlation for dynamic height anomaly computations. Journal of Marine Research 6:85-92.

Stommel, H. 1965. The Gulf Stream, a physical and dynamical description. Berkeley, University of California. 248 p.

Sverdrup, H. U., M. W. Johnson and R. H. Fleming. 1942. The oceans: their physics, chemistry and general biology. Englewood Cliffs, New Jersey, Prentice-Hall. 1087 p.

Sverdrup, H. U. 1947. Wind-driven currents in a baroclinic ocean, with application to the equatorial currents of the Eastern Pacific. Proceedings of the National Academy of Sciences 33:318-236.

Tully, J. P. 1964. Oceanographic regions and assessment of temperature structure in the seasonal zone of the North Pacific Ocean. Journal of the Fisheries Research Board of Canada 21:941-969.

Volkman, G., J. Knauss and A. Vine. 1956. The use of parachute drogues in the measurement of subsurface ocean currents. Transactions of the American Geophysical Union, 37(5):573-577.

von Arx, W. S. 1962. An introduction to physical oceanography. Reading, Massachusetts, Addison-Westley. 422 p.

Warriner, B. 1958. Application of NNSS to marine navigation. In: Marine sciences instrumentation, ed. by Fred Alt. Vol. 4. Proceedings of the Fourth National Instrument Society of America Marine Sciences Instrumentation Symposium, Coca Beach, Florida, 1968. New York, Plenum. p. 168-188.

Werenskiold, W. 1937. Die Berechnung von Meeresströmungen. In: Annual hydrographic report on maritime meteorology. Berlin, Hamburg Marine Observatory. p. 68-72.

Wilson, W. and D. Bradley. 1968. Specific volume of sea water as a function of temperature, pressure, and salinity. Deep Sea Research and Oceanographic Abstracts 15:355-364.

Wolff, P. 1964. Operational analyses and forecasting of ocean temperature structure. Monterey, California, U. S. Navy Fleet Numerical Weather Facility. 24 p. (Unpublished report)

Wooster, W. S. and B. A. Taft. 1958. On the reliability of field measurements of temperature and salinity in the ocean. Journal of Marine Research 17:552-556.

Wüst, G. 1924. Florida und Antillenstrom. Veröffentlichungen des Institutes für meereskunde and dem universitat. Berlin, University of Berlin. 48 p.

Yao, N. 1967. Analysis of hydrographic techniques--A study of different effects on geostrophic current computations by using various hydrographic data processing methods. Master's thesis. Corvallis, Oregon State University. 70 numb. leaves.

Yausi, M. 1955. On the rapid determination of the dynamic depth anomaly in the Kuroshio area. Records of Oceanographic Works in Japan 2(2):90-95.

_____ 1957. On the rapid estimation of the dynamic topography in the seas adjacent to Japan. Records of Oceanographic Works in Japan 3(1):8-15.

APPENDIX I

Tables of A(S, P), B(S, P) and C(T, P)

Table AI-1. $\alpha_o(S, P)$, 10^6 A(S, P), the error in A(S, P) [$10^6 \epsilon_{A(S, P)}$], 10^7 B(S, P), the error in B(S, P)[$10^7 \epsilon_{B(S, P)}$] and the standard deviation of $10^5 \sigma(T)_{S,P}$ as a function of salinity (‰) and pressure (db). (cgs units)

S (‰)	A(S, P)	ϵ_A	B(S, P)	ϵ_B	Sigma
		P = 0 db			
30	56.09	2.06	46.97	0.66	2.00
31	58.89	2.04	46.55	0.66	1.99
32	61.65	2.03	46.14	0.65	1.97
33	64.41	2.01	45.72	0.65	1.95
34	67.14	2.00	45.31	0.64	1.95
35	69.85	1.99	44.90	0.64	1.94
36	72.55	1.98	44.49	0.64	1.92
37	75.23	1.97	44.08	0.63	1.92
38	77.89	1.96	43.67	0.63	1.91
39	80.53	1.96	43.27	0.63	1.90
40	83.16	1.95	42.87	0.63	1.90
		P = 100 db			
30	58.72	2.03	46.58	0.65	1.98
31	61.49	2.01	46.16	0.65	1.96
32	64.23	2.00	45.75	0.64	1.95
33	66.96	1.99	45.34	0.64	1.93
34	69.67	1.97	44.93	0.64	1.92
35	72.36	1.96	44.52	0.63	1.91
36	75.03	1.95	44.11	0.63	1.90
37	77.69	1.94	43.71	0.62	1.89
38	80.32	1.94	43.31	0.62	1.88
39	82.94	1.93	42.90	0.62	1.88
40	85.55	1.92	42.50	0.62	1.87

Table AI-1. Continued.

S (‰)	A(S, P)	ϵ_A	B(S, P)	ϵ_B	Sigma
		P = 200 db			
30	61.33	2.01	46.19	0.64	1.95
31	64.07	1.99	45.77	0.64	1.93
32	66.80	1.97	45.37	0.63	1.92
33	69.50	1.96	44.96	0.63	1.91
34	72.18	1.95	44.55	0.63	1.89
35	74.85	1.94	44.15	0.62	1.88
36	77.50	1.93	43.74	0.62	1.87
37	80.13	1.92	43.34	0.62	1.86
38	82.74	1.91	42.94	0.61	1.86
39	85.34	1.90	42.55	0.61	1.85
40	87.91	1.90	42.15	0.61	1.85
		P = 300 db			
30	63.93	1.98	45.80	0.64	1.92
31	66.64	1.96	45.40	0.63	1.91
32	69.34	1.95	44.98	0.63	1.89
33	72.01	1.93	44.58	0.62	1.88
34	74.68	1.92	44.18	0.62	1.87
35	77.32	1.91	43.78	0.61	1.86
36	79.94	1.90	43.38	0.61	1.84
37	82.55	1.89	42.98	0.61	1.84
38	85.14	1.88	42.59	0.61	1.83
39	87.71	1.88	42.19	0.61	1.82
40	90.27	1.87	41.80	0.60	1.82

Table AI-1. Continued

S (‰)	A(S, P)	ϵ_A	B(S, P)	ϵ_B	Sigma
		P = 400 db			
30	66.50	1.95	45.41	0.63	1.90
31	69.19	1.94	45.01	0.62	1.88
32	71.86	1.92	44.60	0.62	1.87
33	74.52	1.90	44.21	0.61	1.85
34	77.15	1.89	43.81	0.61	1.84
35	79.77	1.88	43.41	0.60	1.83
36	82.37	1.87	43.01	0.60	1.82
37	84.95	1.86	42.62	0.60	1.81
38	87.52	1.86	42.23	0.60	1.80
39	90.07	1.85	41.84	0.60	1.80
40	92.60	1.85	41.45	0.59	1.79
		P = 500 db			
30	69.05	1.92	45.03	0.62	1.87
31	71.72	1.91	44.63	0.61	1.85
32	74.37	1.89	44.23	0.61	1.84
33	77.00	1.88	43.84	0.60	1.82
34	79.61	1.86	43.44	0.60	1.81
35	82.20	1.85	43.05	0.60	1.80
36	84.78	1.84	42.65	0.60	1.79
37	87.34	1.84	42.26	0.59	1.78
38	89.88	1.83	41.88	0.59	1.78
39	92.41	1.82	41.49	0.59	1.77
40	94.92	1.82	41.10	0.59	1.77

Table AI-1. Continued.

S (‰)	A(S, P)	ϵ_A	B(S, P)	ϵ_B	Sigma
		P = 600 db			
30	71.59	1.90	44.65	0.61	1.84
31	74.23	1.88	44.26	0.60	1.83
32	76.85	1.86	43.86	0.60	1.81
33	79.46	1.85	43.47	0.60	1.80
34	82.05	1.84	43.08	0.59	1.79
35	84.62	1.83	42.69	0.59	1.78
36	87.17	1.82	42.30	0.58	1.77
37	89.71	1.81	41.91	0.58	1.76
38	92.22	1.80	41.53	0.58	1.75
39	94.73	1.80	41.14	0.58	1.75
40	97.22	1.79	40.76	0.58	1.74
		P = 700 db			
30	74.01	1.87	44.28	0.60	1.82
31	76.72	1.85	43.89	0.60	1.80
32	79.32	1.84	43.49	0.59	1.79
33	81.91	1.82	43.10	0.59	1.77
34	84.47	1.81	42.72	0.58	1.76
35	87.02	1.80	42.32	0.58	1.75
36	89.55	1.79	41.94	0.58	1.74
37	92.06	1.78	41.56	0.57	1.73
38	94.56	1.77	41.18	0.57	1.72
39	97.04	1.77	40.80	0.57	1.72
40	99.50	1.76	40.42	0.57	1.72

Table AI-1. Continued.

S (‰)	A(S, P)	ϵ_A	B(S, P)	ϵ_B	Sigma
		P = 800 db			
30	76.60	1.84	43.91	0.59	1.79
31	79.20	1.82	43.52	0.59	1.77
32	81.77	1.81	43.13	0.58	1.76
33	84.33	1.80	42.74	0.57	1.75
34	86.87	1.78	42.36	0.57	1.73
35	89.40	1.77	41.94	0.57	1.72
36	91.90	1.76	41.59	0.57	1.71
37	94.40	1.75	41.21	0.56	1.70
38	96.87	1.75	40.83	0.56	1.70
39	99.32	1.74	40.45	0.56	1.69
40	101.77	1.74	40.08	0.56	1.69
		P = 900 db			
30	79.08	1.81	43.54	0.58	1.76
31	81.65	1.80	43.15	0.58	1.75
32	84.21	1.79	42.76	0.57	1.73
33	86.74	1.77	42.38	0.57	1.72
34	89.26	1.76	42.00	0.56	1.71
35	91.76	1.74	41.62	0.56	1.70
36	94.24	1.74	41.24	0.56	1.69
37	96.71	1.73	40.87	0.56	1.68
38	99.16	1.72	40.49	0.55	1.67
39	101.60	1.72	40.12	0.55	1.67
40	104.02	1.71	39.75	0.55	1.66

Table AI-1. Continued.

S (‰)	A(S, P)	ϵ_A	B(S, P)	ϵ_B	Sigma
		P = 1000 db			
30	81.55	1.79	43.18	0.58	1.74
31	84.09	1.77	42.79	0.57	1.72
32	86.62	1.76	42.40	0.56	1.71
33	89.13	1.74	42.03	0.56	1.69
34	91.63	1.73	41.65	0.56	1.68
35	94.01	1.72	41.27	0.55	1.67
36	96.57	1.71	40.90	0.55	1.66
37	99.01	1.70	40.53	0.55	1.65
38	101.44	1.69	40.15	0.54	1.65
39	103.85	1.69	39.78	0.54	1.64
40	106.25	1.68	39.41	0.54	1.64
		P = 1100 db			
30	83.99	1.76	42.81	0.57	1.71
31	86.51	1.74	42.43	0.56	1.69
32	89.02	1.73	42.06	0.56	1.68
33	91.51	1.71	41.68	0.55	1.67
34	93.98	1.70	41.30	0.55	1.65
35	96.43	1.69	40.93	0.54	1.64
36	98.87	1.69	40.56	0.54	1.64
37	101.29	1.67	40.19	0.54	1.62
38	103.70	1.67	39.82	0.54	1.62
39	106.09	1.66	39.45	0.53	1.61
40	108.46	1.66	39.09	0.53	1.61

Table AI-1. Continued.

S (‰)	A(S, P)	ϵ_A	B(S, P)	ϵ_B	Sigma
		P = 1200 db			
30	86.41	1.73	42.46	0.56	1.68
31	88.91	1.72	42.08	0.55	1.67
32	91.40	1.70	41.70	0.55	1.65
33	93.86	1.69	41.33	0.54	1.64
34	96.31	1.67	40.96	0.54	1.63
35	98.74	1.66	40.59	0.53	1.61
36	101.16	1.65	40.22	0.53	1.61
37	103.56	1.65	39.85	0.53	1.60
38	105.94	1.64	39.49	0.53	1.60
39	108.31	1.63	39.12	0.53	1.59
40	110.66	1.63	38.76	0.52	1.58
		P = 1300 db			
30	88.82	1.70	42.10	0.55	1.66
31	91.29	1.69	41.73	0.54	1.64
32	93.76	1.67	41.35	0.54	1.63
33	96.20	1.66	40.98	0.53	1.61
34	98.63	1.65	40.61	0.53	1.60
35	101.04	1.64	40.25	0.53	1.60
36	103.43	1.63	39.88	0.52	1.58
37	105.81	1.62	39.52	0.52	1.57
38	108.17	1.61	39.16	0.52	1.57
39	110.51	1.61	38.80	0.52	1.56
40	112.84	1.60	38.44	0.52	1.56

Table AI-1. Continued.

S (‰)	A(S, P)	ϵ_A	B(S, P)	ϵ_B	Sigma
		P = 1400 db			
30	91.21	1.68	41.75	0.54	1.63
31	93.66	1.66	41.38	0.53	1.61
32	96.10	1.65	41.01	0.53	1.60
33	98.52	1.63	40.64	0.52	1.59
34	100.92	1.62	40.28	0.52	1.57
35	103.31	1.61	39.91	0.52	1.56
36	105.68	1.60	39.55	0.51	1.55
37	108.04	1.59	39.19	0.51	1.55
38	110.38	1.58	38.83	0.51	1.54
39	112.70	1.58	38.47	0.51	1.54
40	115.01	1.58	38.12	0.51	1.53
		P = 1500 db			
30	93.58	1.65	41.40	0.53	1.60
31	96.01	1.63	41.03	0.52	1.59
32	98.43	1.62	40.67	0.52	1.57
33	100.82	1.60	40.30	0.52	1.56
34	103.20	1.59	39.94	0.51	1.55
35	105.57	1.58	39.58	0.51	1.54
36	107.92	1.57	39.22	0.51	1.53
37	110.25	1.56	38.86	0.50	1.52
39	112.57	1.56	38.51	0.50	1.51
39	114.87	1.55	38.15	0.50	1.51
40	117.16	1.55	37.80	0.50	1.51

Table AI-1. Continued.

S (‰)	A(S, P)	ϵ_A	B(S, P)	ϵ_B	Sigma
		P = 1600 db			
30	95.93	1.62	41.06	0.52	1.58
31	98.34	1.61	40.69	0.52	1.56
32	100.73	1.59	40.33	0.51	1.55
33	103.11	1.58	39.97	0.51	1.53
34	105.47	1.57	39.61	0.50	1.52
35	107.81	1.56	39.25	0.50	1.51
36	110.14	1.54	38.89	0.50	1.50
37	112.49	1.54	38.54	0.49	1.49
38	114.74	1.53	38.19	0.49	1.49
39	117.03	1.53	37.84	0.49	1.48
40	119.29	1.52	37.49	0.49	1.48
		P = 1700 db			
30	98.27	1.60	40.71	51.32	1.55
31	100.65	1.58	40.35	50.79	1.54
32	103.02	1.56	39.99	50.30	1.52
33	105.38	1.55	39.63	49.86	1.51
34	107.71	1.54	39.28	49.47	1.50
35	110.04	1.53	38.92	49.13	1.49
36	112.34	1.52	38.57	48.82	1.48
37	114.63	1.51	38.22	48.57	1.47
38	116.90	1.50	37.87	48.36	1.46
39	119.16	1.50	37.52	48.19	1.46
40	121.41	1.49	37.17	48.07	1.45

Table AI-1. Continued.

S (‰)	A(S, P)	ϵ_A	B(S, P)	ϵ_B	Sigma
		P = 1800 db			
30	100.59	1.57	40.38	0.50	1.52
31	102.95	1.55	40.02	0.50	1.51
32	105.30	1.54	39.66	0.49	1.49
33	107.63	1.52	39.31	0.49	1.48
34	109.94	1.51	38.95	0.49	1.47
35	112.24	1.50	38.60	0.48	1.46
36	114.53	1.49	38.25	0.48	1.45
37	116.79	1.48	37.90	0.48	1.44
38	119.05	1.48	37.56	0.47	1.43
39	121.29	1.47	37.21	0.47	1.43
40	123.51	1.47	36.87	0.47	1.43
		P = 1900 db			
30	102.89	1.54	40.04	0.50	1.50
31	105.23	1.53	39.69	0.49	1.48
32	107.55	1.51	39.33	0.49	1.47
33	109.86	1.50	38.98	0.48	1.45
34	112.16	1.48	38.63	0.48	1.44
35	114.43	1.47	38.28	0.47	1.43
36	116.69	1.46	37.93	0.47	1.42
37	118.94	1.46	37.59	0.47	1.42
38	121.17	1.45	37.25	0.47	1.41
39	123.39	1.45	36.90	0.46	1.40
40	125.59	1.44	36.56	0.46	1.40

Table AI-1. Continued.

S (‰)	A(S, P)	ϵ_A	B(S, P)	ϵ_B	Sigma
		P = 2000 db			
30	105.17	1.51	39.71	0.49	1.47
31	107.49	1.50	39.36	0.48	1.46
32	109.79	1.48	39.00	0.48	1.44
33	112.08	1.47	38.65	0.47	1.42
34	114.35	1.46	38.31	0.47	1.42
35	116.61	1.45	37.96	0.47	1.41
36	118.85	1.44	37.62	0.46	1.40
37	121.07	1.43	37.28	0.46	1.39
38	123.28	1.42	36.94	0.46	1.38
39	125.48	1.42	36.60	0.46	1.38
40	127.66	1.41	36.26	0.45	1.37

Table AI-2. 10^5 C(T, P), 10^5 $\epsilon_{C(T,P)}$ and the standard deviation of $10^5 a(S)_{T,P}$ as a function of temperature (°C) and pressure (db).

T(°C)	C(T, P)	ϵ_C	Sigma	T(°C)	C(T, P)	ϵ_C	Sigma	T(°C)	C(T, P)	ϵ_C	Sigma
	P = 0 db				P = 100 db				P = 200 db		
0	76.26	0.04	0.37	0	76.11	0.03	0.37	0	75.96	0.03	0.37
2	75.71	0.03	0.35	2	75.57	0.03	0.34	2	75.43	0.03	0.34
4	75.22	0.03	0.32	4	75.08	0.03	0.32	4	74.93	0.03	0.32
6	74.75	0.03	0.30	6	74.62	0.03	0.30	6	74.48	0.03	0.30
8	74.33	0.03	0.30	8	74.19	0.03	0.28	8	74.06	0.03	0.28
10	73.94	0.03	0.28	10	73.81	0.03	0.27	10	73.68	0.03	0.27
12	73.58	0.02	0.26	12	73.45	0.02	0.26	12	73.32	0.02	0.26
14	73.26	0.02	0.25	14.	73.13	0.02	0.25	14	73.01	0.02	0.25
16	72.96	0.02	0.24	16	72.84	0.02	0.24	16	72.72	0.02	0.24
18	72.71	0.02	0.23	18	72.59	0.02	0.23	18	72.47	0.02	0.23
20	72.48	0.02	0.22	20	72.36	0.02	0.22	20	72.22	0.02	0.22
22	72.29	0.02	0.22	22	72.17	0.02	0.21	22	72.06	0.02	0.21
24	72.12	0.02	0.20	24	72.01	0.02	0.20	24	71.89	0.02	0.20
26	71.98	0.02	0.19	26	71.87	0.02	0.19	26	71.76	0.02	0.19
28	71.88	0.02	0.18	28	71.77	0.02	0.18	28	71.66	0.02	0.17
30	71.80	0.01	0.16	30	71.69	0.02	0.16	30	71.88	0.02	0.16

Table AI-2. Continued.

T(°C)	C(T, P)	ϵC	Sigma	T(°C)	C(T, P)	ϵC	Sigma	T(°C)	C(T, P)	ϵC	Sigma
	P = 300 db				P = 400 db				P = 500 db		
0	75.81	0.03	0.36	0	75.66	0.03	0.36	0	75.51	0.03	0.36
2	75.28	0.03	0.37	2	75.14	0.03	0.33	2	75.00	0.03	0.33
4	74.80	0.03	0.31	4	74.66	0.03	0.31	4	74.52	0.03	0.31
6	74.34	0.03	0.30	6	74.21	0.03	0.29	6	74.07	0.03	0.29
8	73.93	0.03	0.28	8	73.80	0.03	0.28	8	73.67	0.03	0.27
10	73.55	0.02	0.27	10	73.42	0.03	0.26	10	73.29	0.02	0.26
12	73.32	0.02	0.26	12	73.08	0.02	0.25	12	72.95	0.02	0.25
14	72.89	0.02	0.25	14	72.76	0.02	0.24	14	72.64	0.02	0.24
16	72.60	0.02	0.24	16	72.48	0.02	0.23	16	72.37	0.02	0.23
18	72.35	0.02	0.23	18	72.24	0.02	0.23	18	72.12	0.02	0.22
20	72.13	0.02	0.23	20	72.01	0.02	0.22	20	71.90	0.02	0.21
22	71.94	0.02	0.21	22	71.83	0.02	0.21	22	71.72	0.02	0.20
24	71.78	0.02	0.20	24	71.67	0.02	0.20	24	71.56	0.02	0.19
26	71.65	0.02	0.19	26	71.54	0.02	0.19	26	71.43	0.02	0.18
28	71.55	0.02	0.17	28	71.44	0.02	0.17	28	71.33	0.02	0.17
30	71.47	0.01	0.16	30	71.36	0.01	0.16	30	71.26	0.01	0.15

Table AI-2. Continued.

T(°C)	C(T, P)	ϵ_C	Sigma	T(°C)	C(T, P)	ϵ_C	Sigma	T(°C)	C(T, P)	ϵ_C	Sigma
	P = 600 db				P = 700 db				P = 800 db		
0	75.36	0.03	0.35	0	75.22	0.03	0.35	0	75.07	0.03	0.34
2	74.85	0.03	0.33	2	74.71	0.03	0.32	2	74.57	0.03	0.32
4	74.38	0.03	0.31	4	74.24	0.03	0.30	4	74.10	0.03	0.30
6	73.94	0.03	0.29	6	73.81	0.03	0.28	6	73.67	0.03	0.28
8	73.54	0.03	0.27	8	73.41	0.03	0.27	8	73.28	0.03	0.27
10	73.16	0.02	0.26	10	73.04	0.02	0.26	10	72.91	0.03	0.25
12	72.83	0.02	0.25	12	72.70	0.02	0.25	12	72.58	0.02	0.24
14	72.52	0.02	0.24	14	72.40	0.02	0.24	14	72.28	0.02	0.23
16	72.25	0.02	0.23	16	72.13	0.02	0.23	16	72.01	0.02	0.23
18	72.00	0.02	0.22	18	71.89	0.02	0.22	18	71.77	0.02	0.22
20	71.79	0.02	0.21	20	71.67	0.02	0.21	20	71.56	0.02	0.21
22	71.61	0.02	0.20	22	71.49	0.02	0.20	22	71.38	0.02	0.20
24	71.45	0.02	0.19	24	71.34	0.02	0.19	24	71.23	0.02	0.19
26	71.32	0.02	0.18	26	71.21	0.02	0.18	26	71.10	0.02	0.18
28	71.22	0.02	0.17	28	71.11	0.02	0.17	28	71.01	0.02	0.16
30	71.15	0.01	0.15	30	71.04	0.01	0.15	30	70.93	0.01	0.15

Table AI-2. Continued.

T(°C)	C(T, P)	ϵC	Sigma	T(°C)	C(T, P)	ϵC	Sigma	T(°C)	C(T, P)	ϵC	Sigma
	P = 900 db				P = 1000 db				P = 1100 db		
0	74.93	0.03	0.34	0	74.78	0.03	0.33	0	74.64	0.03	0.34
2	74.42	0.03	0.32	2	74.29	0.03	0.31	2	74.15	0.03	0.31
4	73.97	0.03	0.30	4	73.83	0.03	0.29	4	73.69	0.03	0.29
6	73.54	0.03	0.28	6	73.41	0.03	0.28	6	73.28	0.03	0.27
8	73.15	0.03	0.26	8	73.02	0.02	0.26	8	72.89	0.02	0.26
10	72.79	0.02	0.25	10	72.66	0.02	0.25	10	72.54	0.02	0.25
12	72.49	0.02	0.24	12	72.34	0.02	0.24	12	72.21	0.02	0.24
14	72.16	0.02	0.23	14	72.04	0.02	0.23	14	71.92	0.02	0.23
16	71.89	0.02	0.22	16	71.78	0.02	0.22	16	71.66	0.02	0.22
18	71.66	0.02	0.21	18	71.54	0.02	0.21	18	71.43	0.02	0.21
20	71.46	0.02	0.21	20	71.34	0.02	0.21	20	71.23	0.02	0.20
22	71.27	0.02	0.20	22	71.16	0.02	0.19	22	71.05	0.02	0.19
24	71.12	0.02	0.18	24	71.01	0.02	0.19	24	70.90	0.02	0.19
26	71.00	0.02	0.18	26	70.89	0.02	0.18	26	70.78	0.02	0.17
28	70.90	0.02	0.16	28	70.79	0.02	0.16	28	70.69	0.02	0.16
30	70.83	0.01	0.15	30	70.72	0.01	0.15	30	70.62	0.01	0.15

Table AI-2. Continued.

T(°C)	C(T, P)	ϵC	Sigma	T(°C)	C(T, P)	ϵC	Sigma	T(°C)	C(T, P)	ϵC	Sigma
	P = 1200 db				P = 1300 db				P = 1400 db		
0	74.49	0.03	0.33	0	74.35	0.03	0.33	0	74.21	0.03	0.33
2	74.01	0.03	0.31	2	73.87	0.03	0.31	2	73.73	0.03	0.30
4	73.56	0.03	0.28	4	73.42	0.03	0.28	4	73.29	0.03	0.28
6	73.14	0.03	0.27	6	73.01	0.03	0.27	6	72.88	0.03	0.26
8	72.76	0.02	0.26	8	72.63	0.02	0.25	8	72.51	0.02	0.25
10	72.41	0.02	0.24	10	72.29	0.02	0.24	10	72.16	0.02	0.24
12	72.09	0.02	0.23	12	71.97	0.02	0.23	12	71.85	0.02	0.23
14	71.80	0.02	0.22	14	71.69	0.02	0.22	14	71.57	0.02	0.22
16	71.55	0.02	0.22	16	71.43	0.02	0.21	16	71.32	0.02	0.21
18	71.32	0.02	0.21	18	71.20	0.02	0.21	18	71.09	0.02	0.20
20	71.11	0.02	0.20	20	71.00	0.02	0.20	20	70.89	0.02	0.20
22	70.09	0.02	0.19	22	70.83	0.02	0.19	22	70.72	0.02	0.19
24	70.79	0.02	0.18	24	70.69	0.02	0.18	24	70.58	0.02	0.18
26	70.67	0.02	0.17	26	70.57	0.02	0.17	26	70.46	0.02	0.17
28	70.58	0.02	0.16	28	70.48	0.02	0.16	28	70.37	0.02	0.16
30	70.51	0.01	0.15	30	70.41	0.01	0.14	30	70.30	0.01	0.14

Table AI-2. Continued.

T(°C)	C(T, P)	ϵC	Sigma	T(°C)	C(T, P)	ϵC	Sigma	T(°C)	C(T, P)	ϵC	Sigma
	P = 1500 db				P = 1600 db				P = 1700 db		
0	74.07	0.03	0.32	0	73.92	0.03	0.32	0	73.78	0.03	0.32
2	73.59	0.03	0.30	2	73.46	0.03	0.30	2	73.32	0.03	0.29
4	73.16	0.03	0.27	4	73.02	0.03	0.28	4	72.89	0.03	0.27
6	72.75	0.02	0.26	6	72.62	0.02	0.26	6	72.50	0.02	0.26
8	72.38	0.02	0.25	8	72.25	0.02	0.25	8	72.13	0.02	0.24
10	72.04	0.02	0.24	10	71.92	0.02	0.23	10	71.80	0.02	0.23
12	71.73	0.02	0.23	12	71.61	0.02	0.22	12	71.49	0.02	0.22
14	71.45	0.02	0.22	14	71.34	0.02	0.22	14	71.22	0.02	0.21
16	71.20	0.02	0.21	16	71.09	0.02	0.21	16	70.97	0.02	0.21
18	70.98	0.02	0.20	18	70.87	0.02	0.20	18	70.76	0.02	0.20
20	70.78	0.02	0.20	20	70.67	0.02	0.19	20	70.56	0.02	0.19
22	70.61	0.02	0.19	22	70.51	0.02	0.19	22	70.40	0.02	0.18
24	70.47	0.02	0.18	24	70.37	0.02	0.18	24	70.26	0.02	0.18
26	70.36	0.02	0.17	26	70.25	0.02	0.17	26	70.15	0.02	0.17
28	70.27	0.01	0.16	28	70.16	0.01	0.15	28	70.06	0.01	0.15
30	70.20	0.01	0.14	30	70.09	0.01	0.14	30	69.99	0.01	0.14

Table AI-2. Continued.

T(°C)	C(T, P)	ϵC	Sigma	T(°C)	C(T, P)	ϵC	Sigma	T(°C)	C(T, P)	ϵC	Sigma
	P = 1800 db				P = 1900 db				P = 2000 db		
0	73.64	0.03	0.31	0	73.50	0.03	0.31	0	73.37	0.03	0.31
2	73.19	0.03	0.29	2	73.05	0.03	0.29	2	72.91	0.03	0.28
4	72.76	0.03	0.27	4	72.63	0.03	0.27	4	72.50	0.03	0.26
6	72.37	0.02	0.25	6	72.24	0.02	0.25	6	72.11	0.02	0.25
8	72.01	0.02	0.24	8	71.88	0.02	0.24	8	71.76	0.02	0.23
10	71.68	0.02	0.23	10	71.56	0.02	0.23	10	71.44	0.02	0.22
12	71.38	0.02	0.22	12	71.26	0.02	0.22	12	71.14	0.02	0.21
14	71.10	0.02	0.21	14	70.99	0.02	0.21	14	70.87	0.02	0.21
16	70.86	0.02	0.20	16	70.75	0.02	0.20	16	70.64	0.02	0.20
18	70.64	0.02	0.20	18	70.53	0.02	0.19	18	70.42	0.02	0.19
20	70.46	0.02	0.19	20	70.35	0.02	0.19	20	70.23	0.02	0.19
22	70.29	0.02	0.18	22	70.19	0.02	0.18	22	70.08	0.02	0.18
24	70.15	0.02	0.17	24	70.05	0.02	0.17	24	69.95	0.02	0.17
26	70.04	0.02	0.16	26	69.94	0.02	0.16	26	69.84	0.02	0.16
28	69.96	0.01	0.15	28	69.85	0.01	0.15	28	69.75	0.01	0.15
30	69.89	0.01	0.14	30	69.79	0.01	0.14	30	69.69	0.01	0.13

APPENDIX II

Geostrophic Velocity Profile Comparison of Standard Versus T-S Gradient Method for Various Regions in the Oceans
(Stations Positions are Given in Table 5)

Note: Original scales reduced in reproduction.

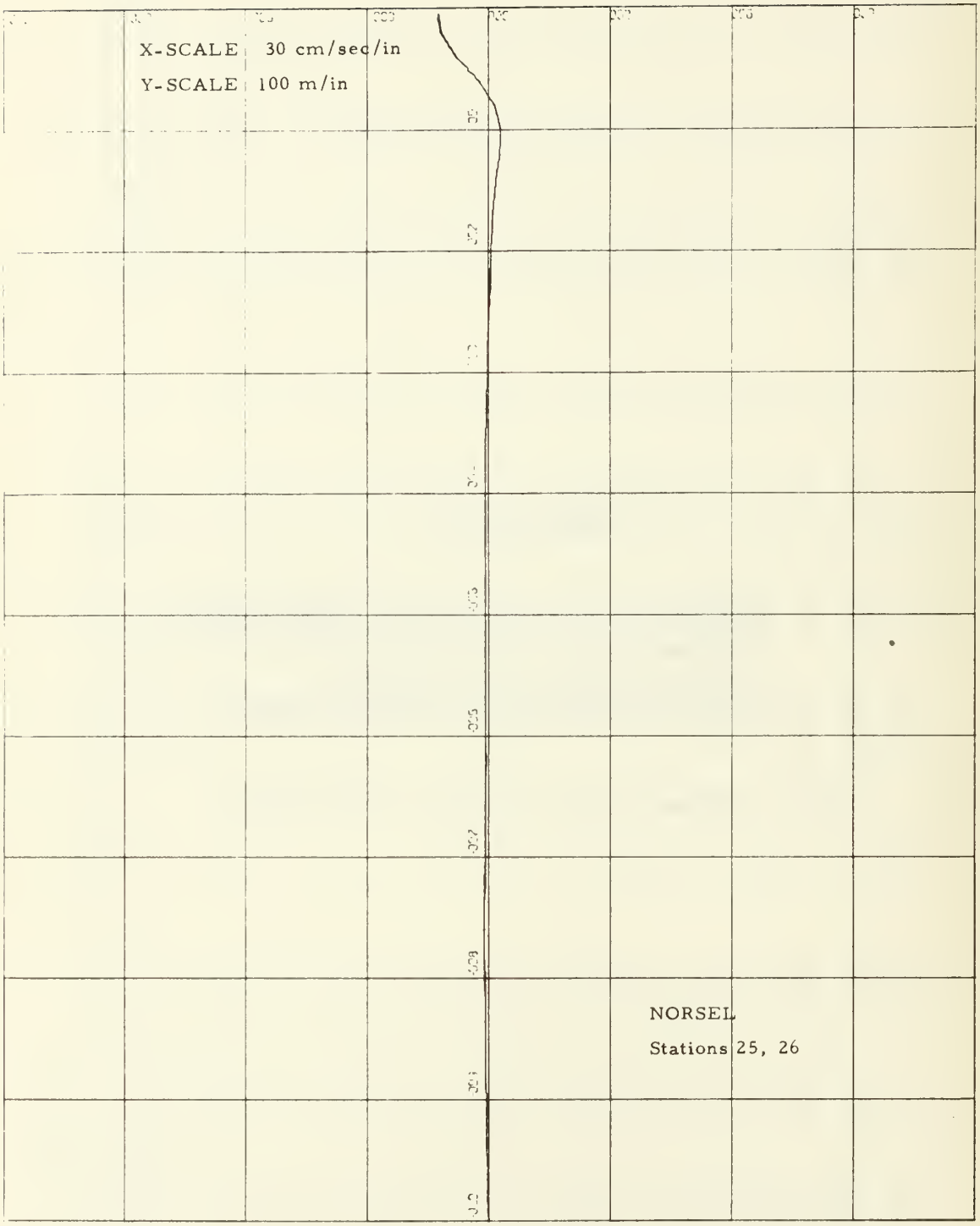
X-SCALE 30 cm/sec/in
Y-SCALE 100 m/in
NORSEL
Stations 25, 26

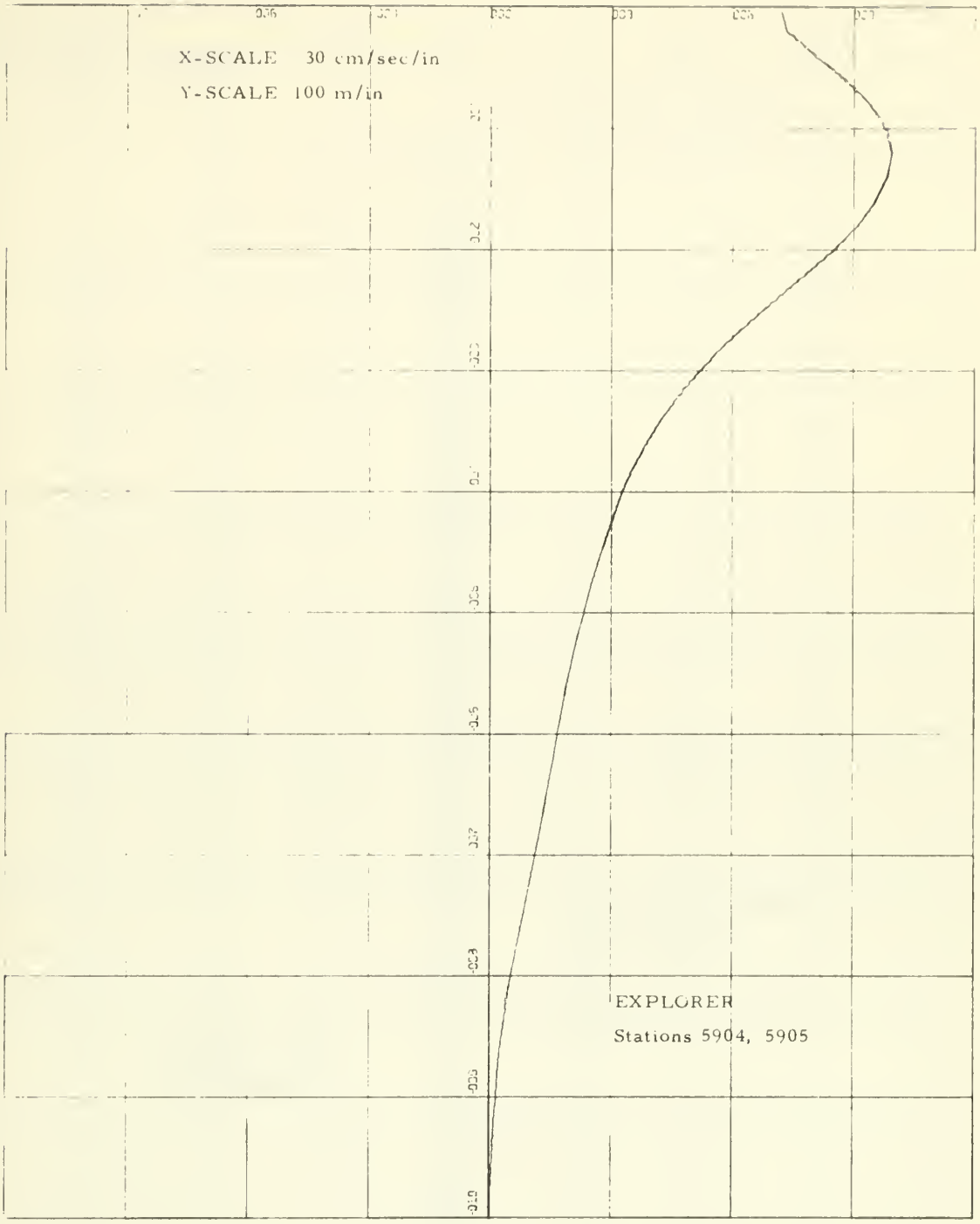
X-SCALE 30 cm/sec/in
Y-SCALE 100 m/in
EXPLORER
Stations 5904, 5905

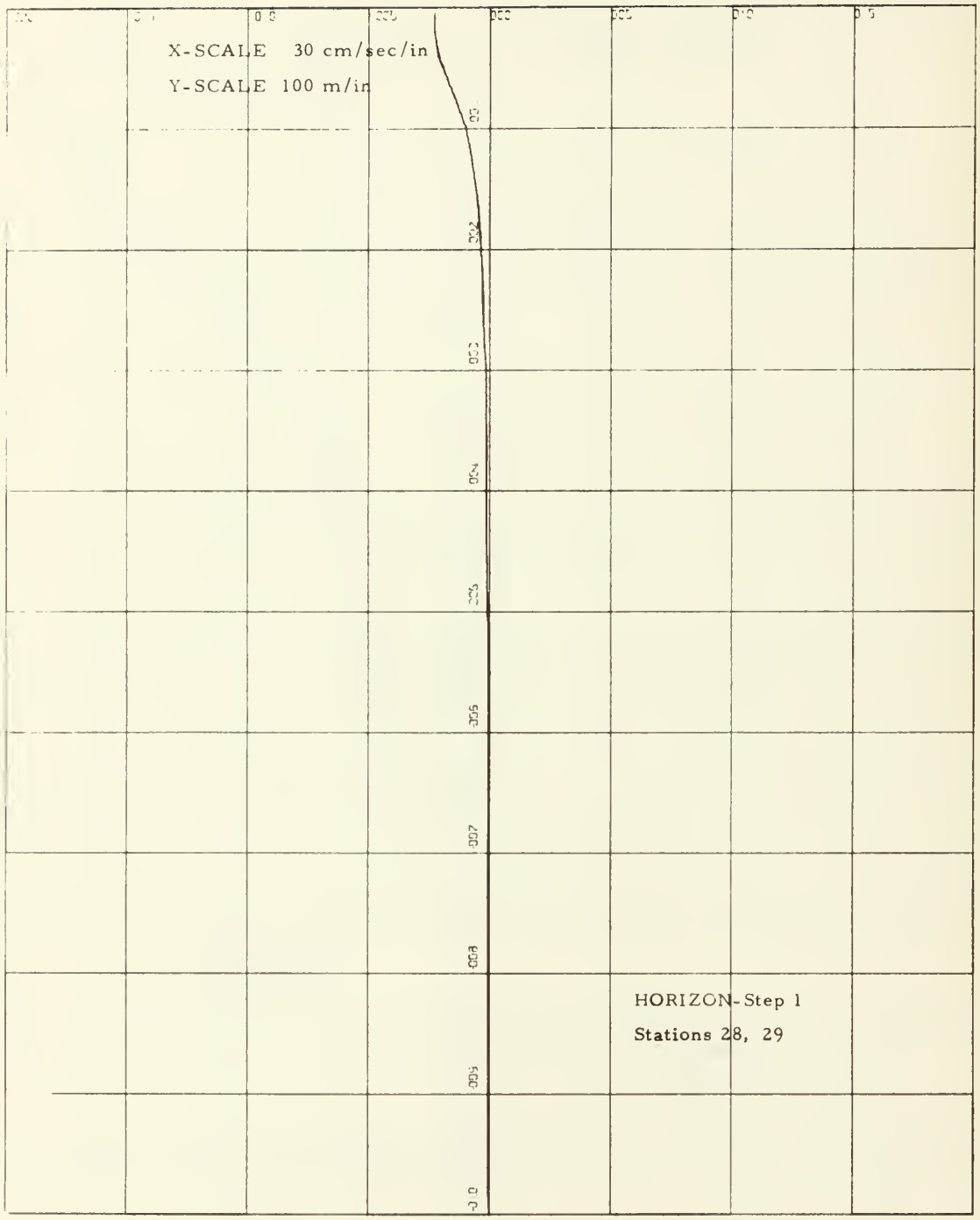
X-SCALE 30 cm/sec/in
Y-SCALE 100 m/in
HORIZON-Step 1
Stations 28, 29

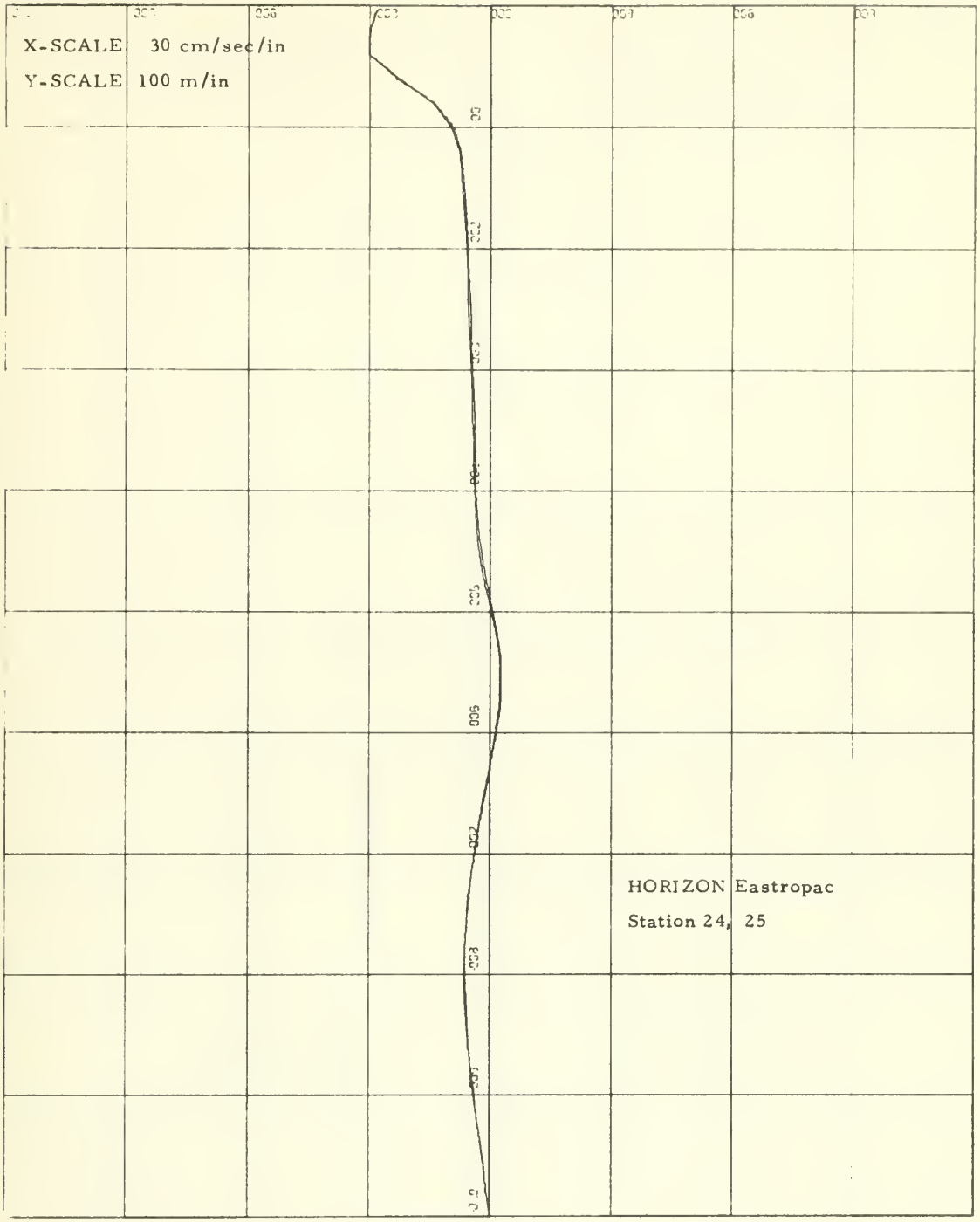
X-SCALE 30 cm/sec/in
Y-SCALE 100 m/in
HORIZON Eastropac
Station 24, 25

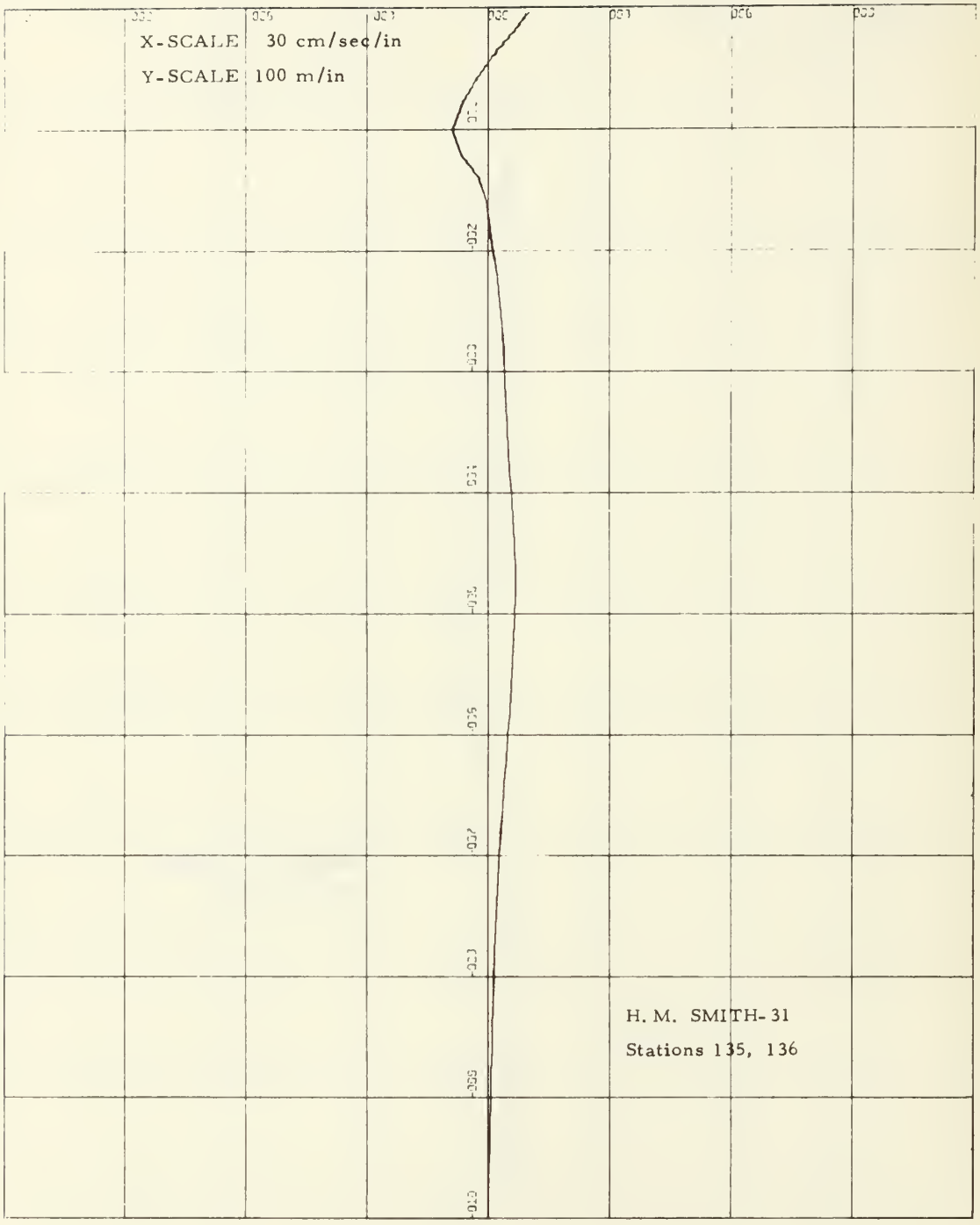
X-SCALE 30 cm/sec/in
Y-SCALE 100 m/in
H. M. SMITH-31
Stations 135, 136

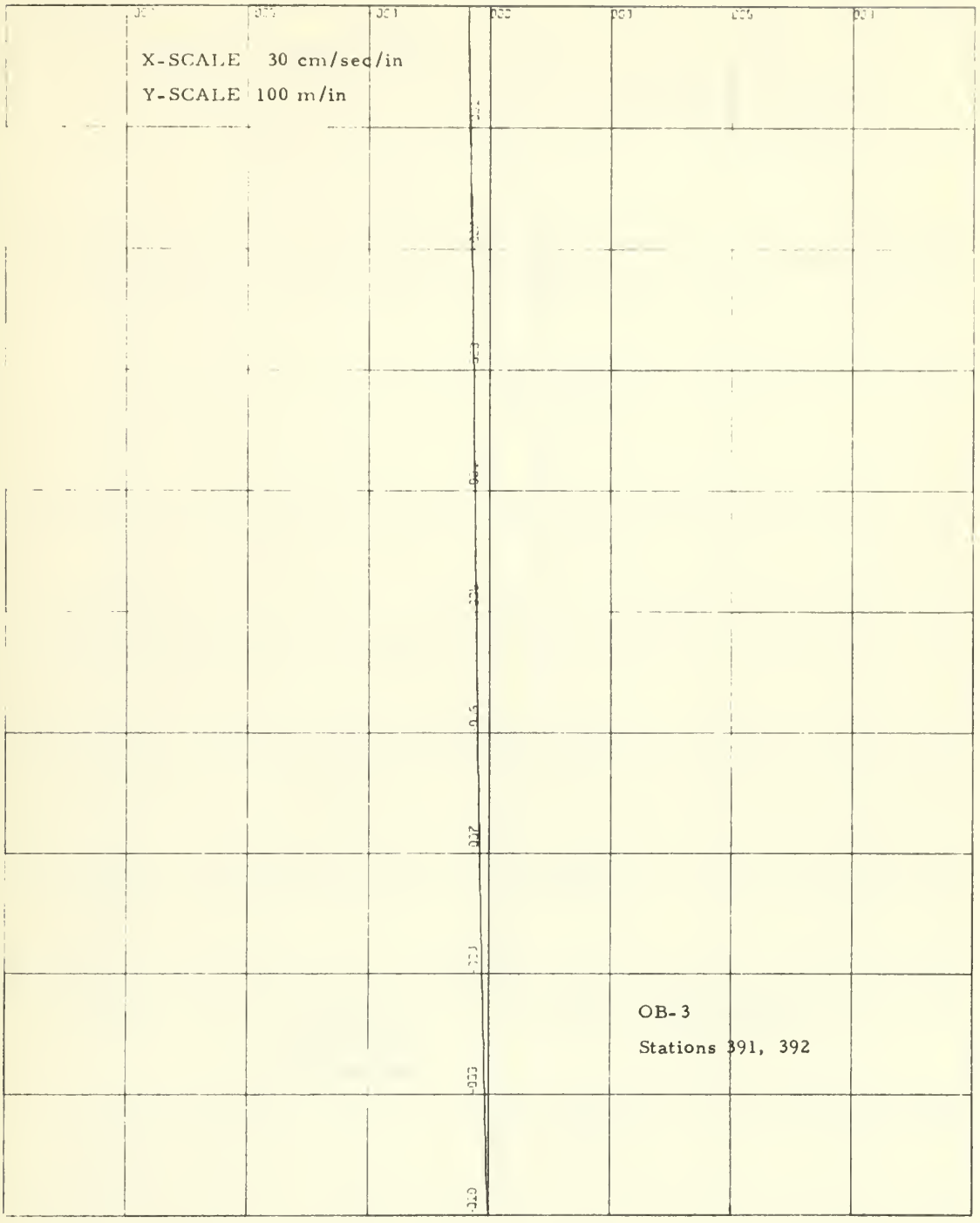
X-SCALE 30 cm/sec/in
Y-SCALE 100 m/in
OB-3
Stations 391, 392

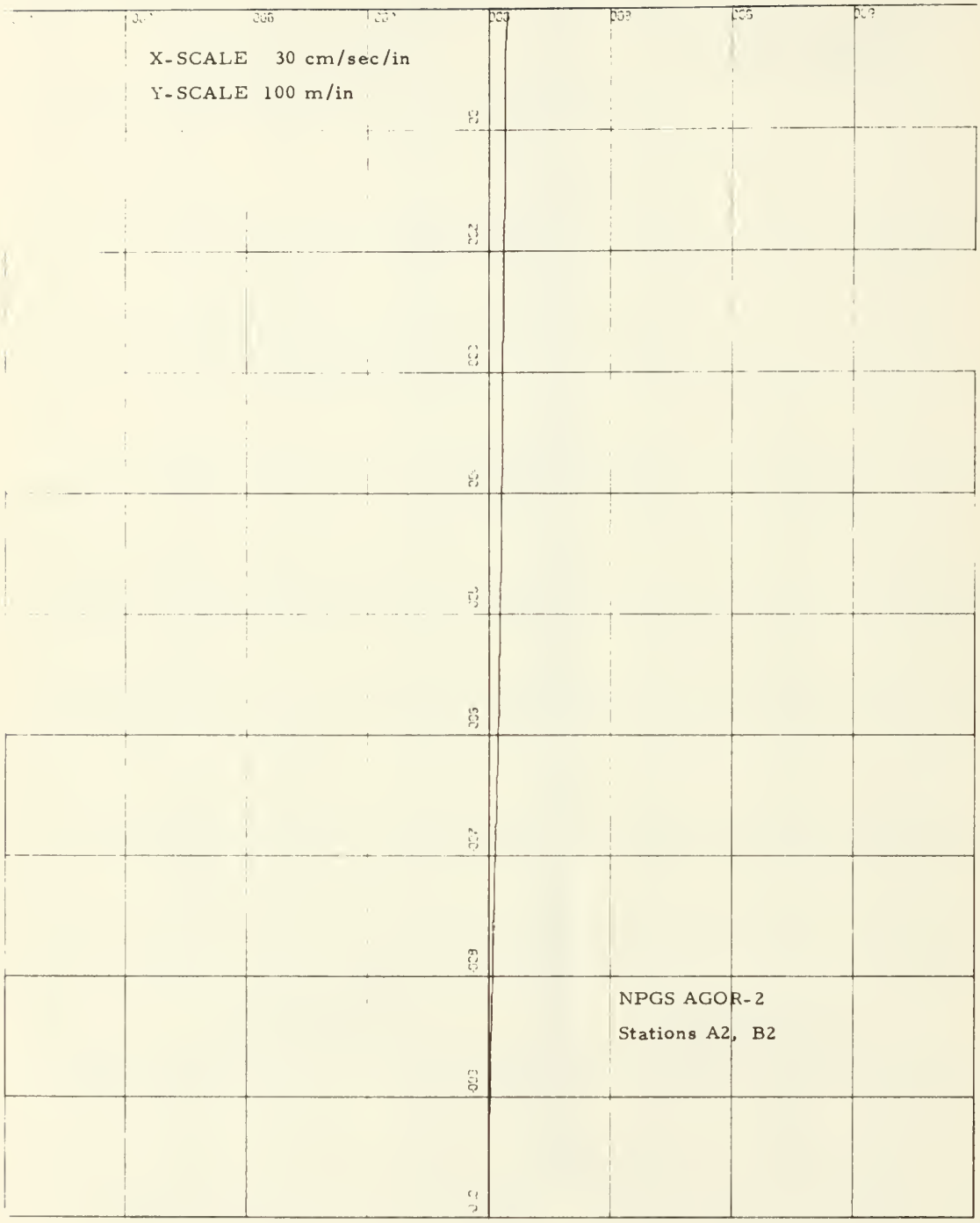
X-SCALE 30 cm/sec/in
Y-SCALE 100 m/in
NPGS AGOR-2
Stations A2, B2

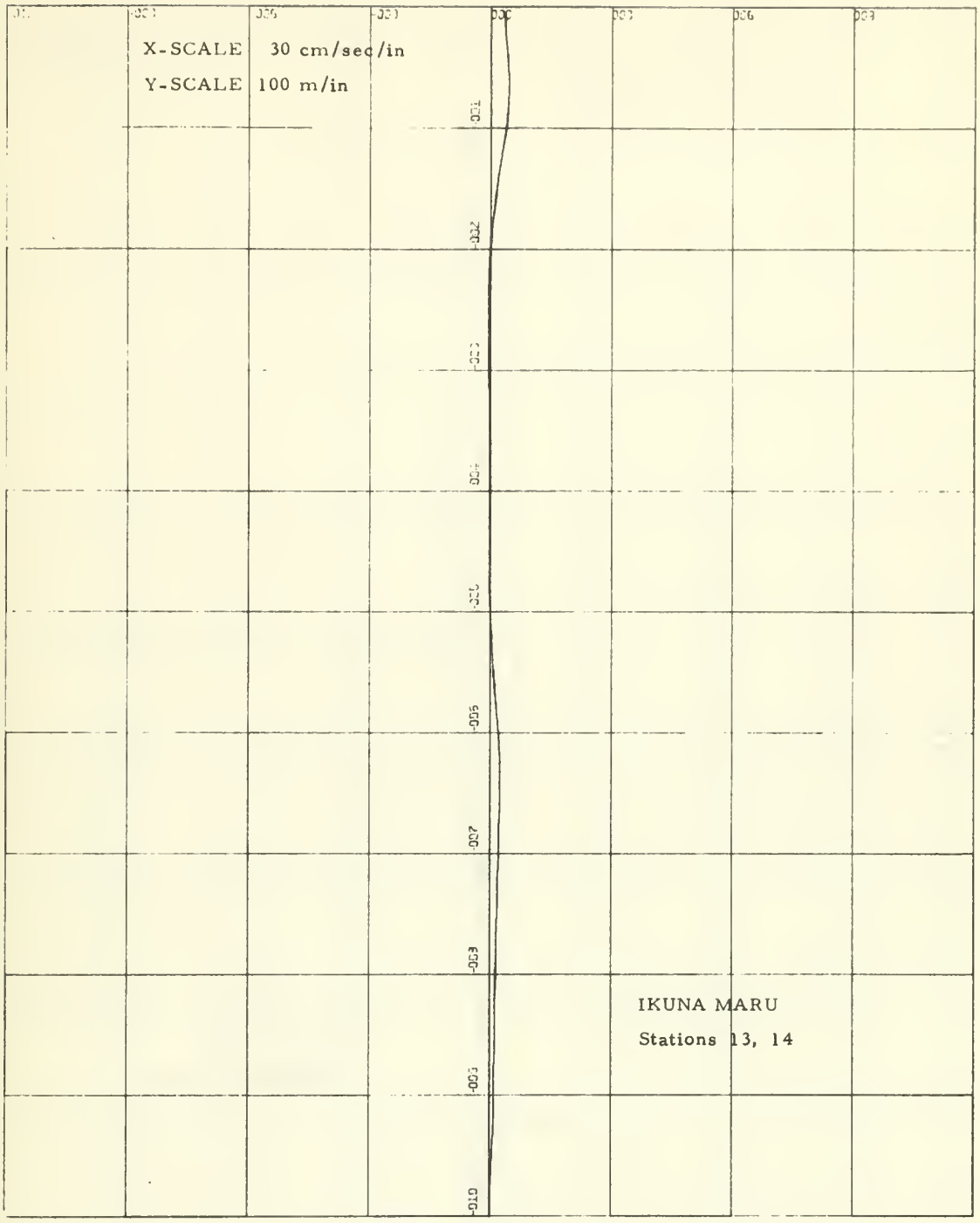
X-SCALE 30 cm/sec/in
Y-SCALE 100 m/in
IKUNA MARU
Stations 13, 14

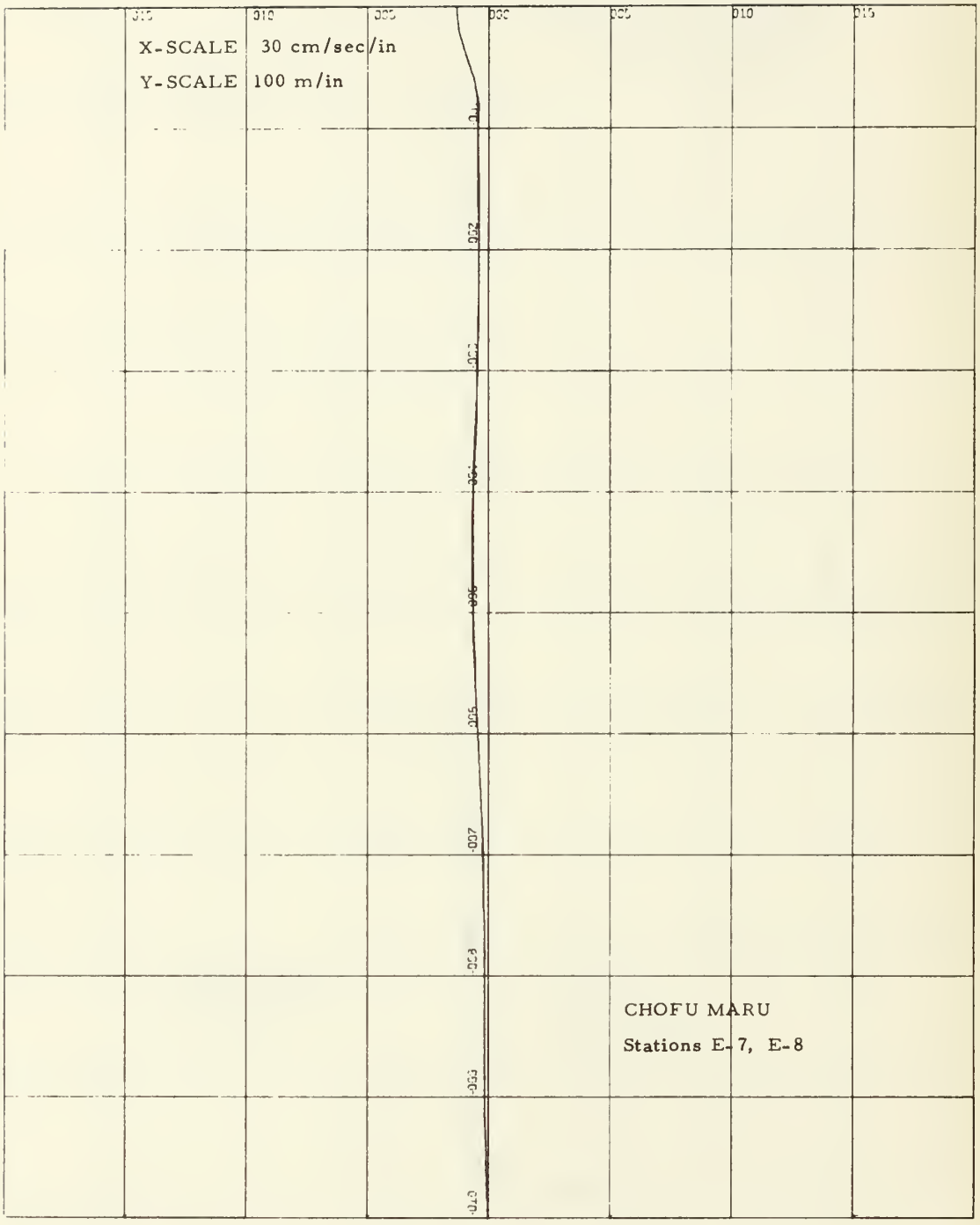
X-SCALE 30 cm/sec/in
Y-SCALE 100 m/in
CHOFU MARU
Stations E-7, E-8

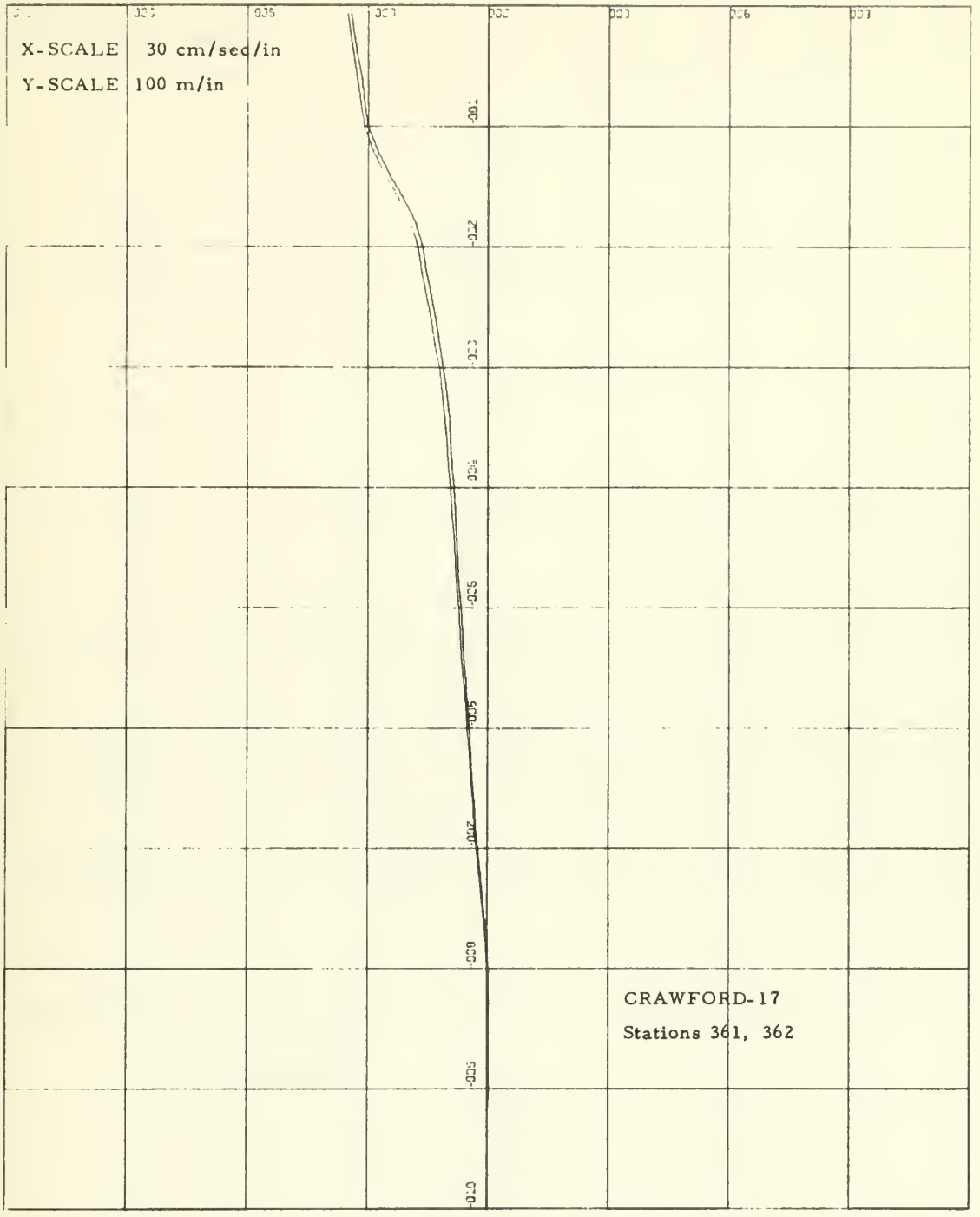
X-SCALE 30 cm/sec/in
Y-SCALE 100 m/in
CRAWFORD-17
Stations 361, 362

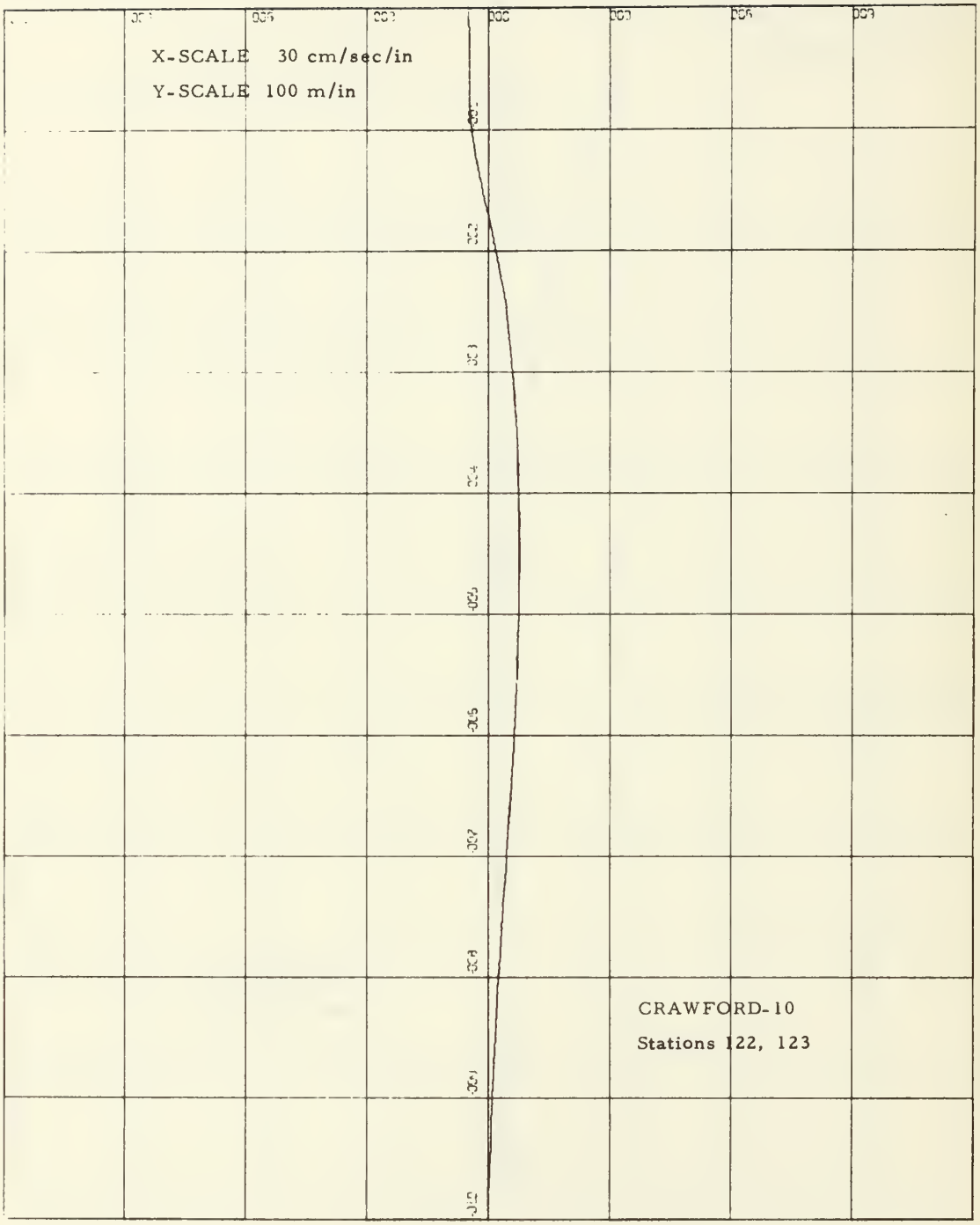
X-SCALE 30 cm/sec/in
Y-SCALE 100 m/in
CRAWFORD-10
Stations 122, 123

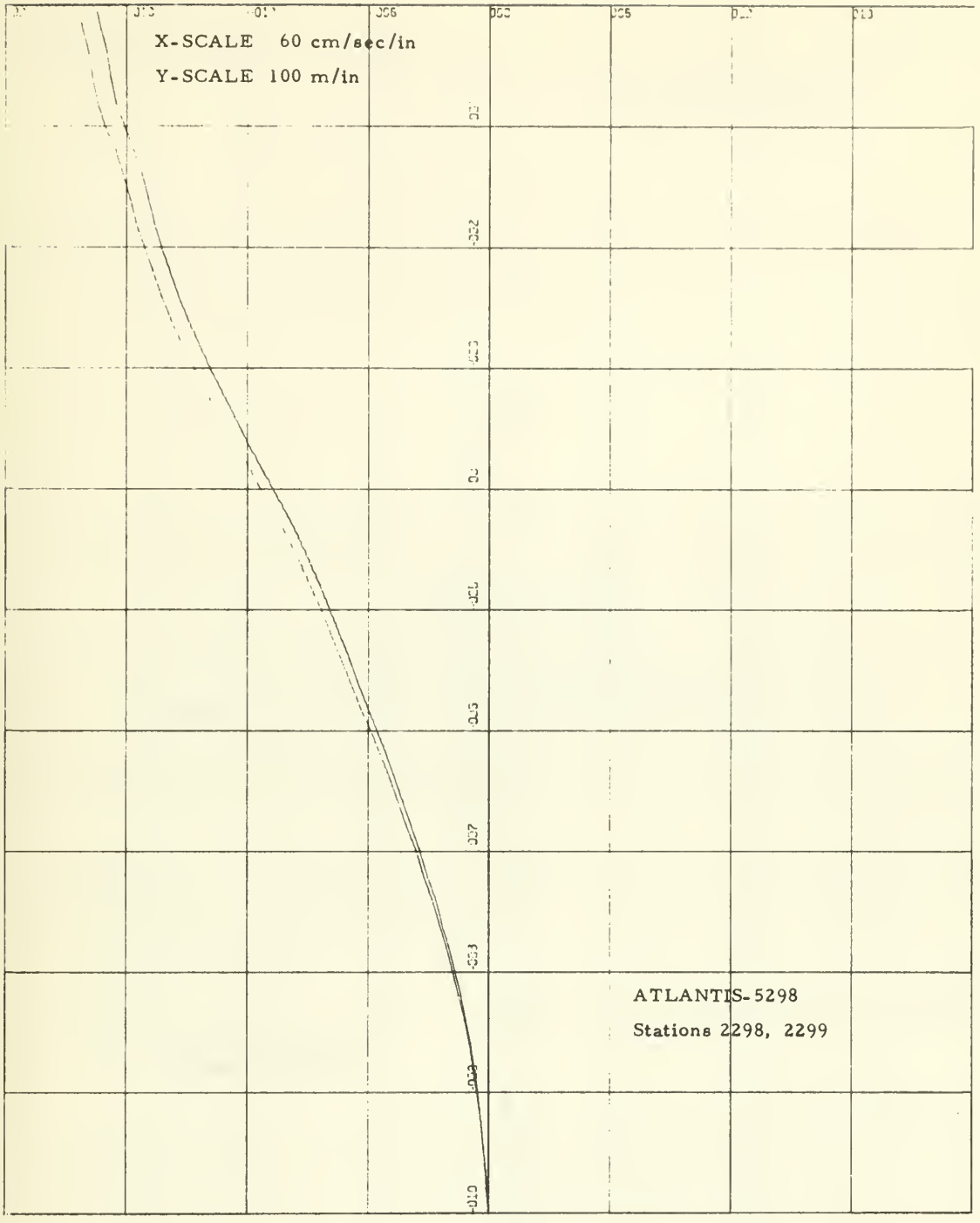
X-SCALE 60 cm/sec/in
Y-SCALE 100 m/in
ATLANTIS-5298
Stations 2298, 2299

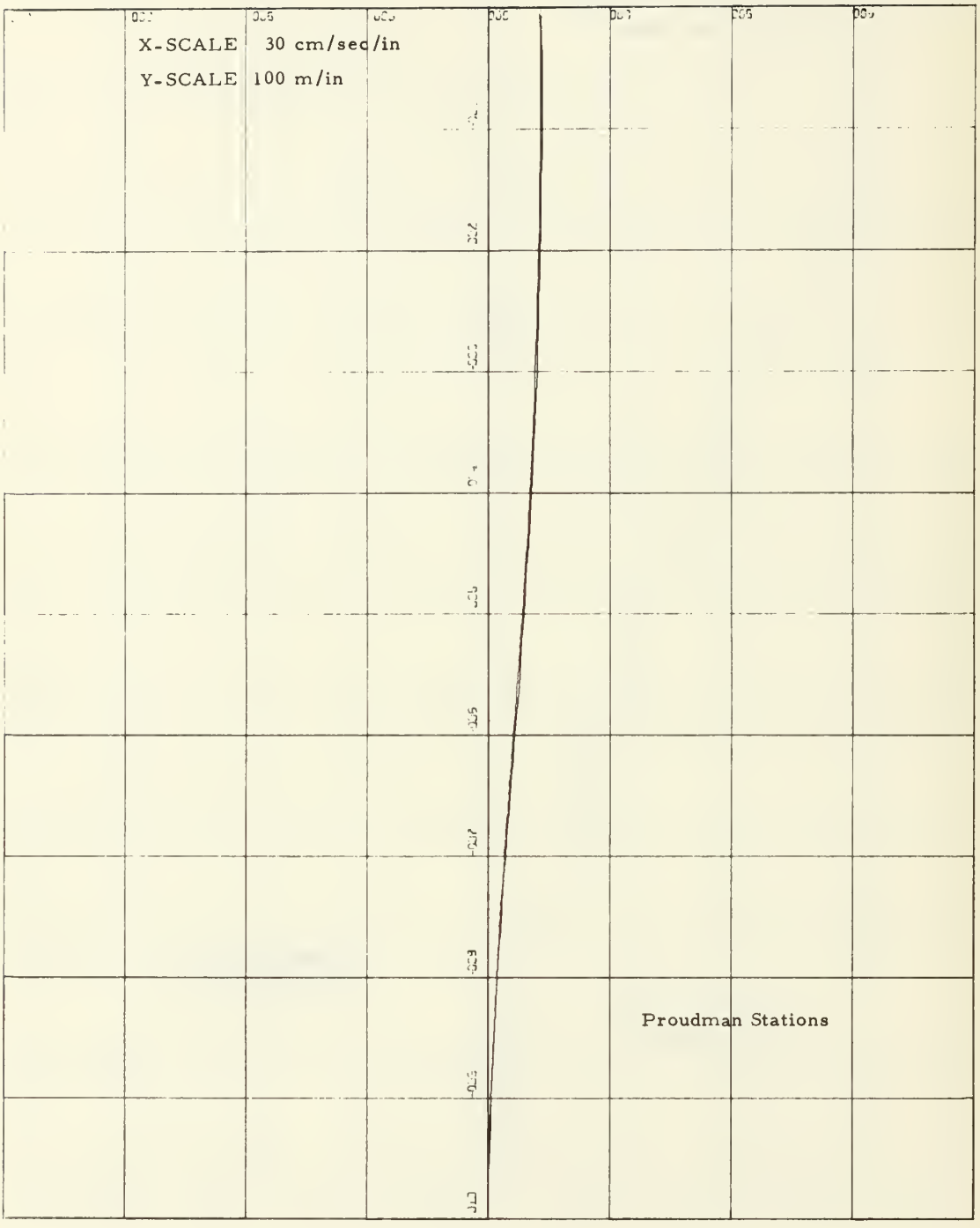
X-SCALE 30 cm/sec/in
Y-SCALE 100 m/in
Proudman Stations

APPENDIX III

Computer Programs for Hemispheric Computations

Program 1. A program to interpolate hydrographic data on the IBM/360 computer

```
      SUBROUTINE LGINTP (N,V,D,SD,CV,NN)
      DIMENSION D(100),V(1000),CV(1000),SD(1000)
  111 DO 188 J=1,500
  112 DO 186 I=1,N
      IF(SD(J)-D(N))113,115,190
  115 CV(J)=V(N)
      GO TO 190
  113 IF(SD(J)-D(I))114,114,116
  114 CV(J)=V(I)
      GO TO 188
  116 IF(SD(J)-D(I+1))120,118,186
  118 CV(J)=V(I+1)
      GO TO 188
  120 IF(I-1)132,132,126
  126 XA=(SD(J)-D(I))*(SD(J)-D(I+1))*V(I-1)/
     1((D(I-1)-D(I))*(D(I-1)-D(I+1)))
      XB=(SD(J)-D(I-1))*(SD(J)-D(I+1))*V(I)/
     1((D(I)-D(I-1))*(D(I)-D(I+1)))
      XC=(SD(J)-D(I-1))*(SD(J)-D(I))*V(I+1)/
     1((D(I+1)-D(I-1))*(D(I+1)-D(I)))
      ANSU=XA+XB+XC
  132 IF ((I+2)-N)133,133,134
  133 YA=(SD(J)-D(I+1))*(SD(J)-D(I+2))*V(I)/
     1((D(I)-D(I+1))*(D(I)-D(I+2)))
      YB=(SD(J)-D(I))*(SD(J)-D(I+2))*V(I+1)/
     1((D(I+1)-D(I))*(D(I+1)-D(I+2)))
      YC=(SD(J)-D(I))*(SD(J)-D(I+1))*V(I+2)/
     1((D(I+2)-D(I))*(D(I+2)-D(I+1)))
      ANSD=YA+YB+YC
  134 ZA=(SD(J)-D(I+1))*V(I)/(D(I)-D(I+1))
      ZB=(SD(J)-D(I))*V(I+1)/(D(I+1)-D(I))
      ANSL=ZA+ZB
      IF(I-1)136,136,138
  136 CV(J)=(ANSD+ANSL)/2.
      DLL=(ANSD+ANSL+ANSL)/3.
      GO TO 188
  138 IF((I+2)-N)140,140,142
  140 CV(J)=(ANSU+ANSD+ANSL)/3.
      UD=(ANSU+ANSD)/2.
      GO TO 188
  142 CV(J)=(ANSU+ANSL)/2.
      ULL=(ANSU+ANSL+ANSL)/3.
      GO TO 188
  186 CONTINUE
  188 CONTINUE
      J=501
  190 NN=J
      RETURN
      END
```

Program 2. A program to compute specific volume anomaly from hydrographic data on the IBM/360 computer

```
      SUBROUTINE SGTSVA (T,S,D,SGT,SV,SVA)
      ST=-(((T-3.98)**2)/503.57)*((T+283.)/(T+67.26))
      CL=(S-.030)/1.805
      SO=-.069+1.4708*CL-.00157*CL**2+3.98E-5*CL**3
      AT=T*(4.7867-.098185*T+.0010843*T**2)*1.E-3
      BT=T*(18.030-.8164*T+.01667*T**2)*1.E-6
      SGT=ST+(SO+.1324)*(1.-AT+BT*(SO-.1324))
      AFST=1./(1.+SGT*1.E-3)
      A=D*AFST*1.E-9
      B=4886./(1.+1.83E-5*D)
      C=227.+28.33*T-.551*T**2+.004*T**3
      E=D*1.E-4
      G=(SO-28.)/10.
      H=147.3-2.72*T+.04*T**2
      U=105.5+9.5*T-.158*T**2
      V=1.5*D**2*T*1.E-8
      W=32.4-.87*T+.02*T**2
      X=4.5-.1*T
      Y=1.8-.06*T
      SV=AFST-A*(B-C+E*U-V-G*(H-E*W)+G**2*(X-E*Y))
      AZ=.972643
      YA=-227.+.01055*D
      YB=.0126*(147.3-.00324*D)
      AP=AZ-D*AZ*(B+YA-YB)*1.E-9
      SVA=SV-AP
      RETURN
      END
```

Program 3. A program to compute geostrophic currents by the Helland-Hansen equation and the T-S Gradient equation on the IBM/360 computer

```
      REAL *8 IMSG
      REAL *8 ITL(12)
      DIMENSION SD(500),DA(500),TA(500),SA(500),DB(500),TB(500),SB(500)
      DIMENSION TCA(500),SCA(500),TCB(500),SCB(500),DLT(500),DLS(500)
      DIMENSION BRT(500),ANS(500),VELD(500),ASVA(500),BSVA(500)
      DIMENSION DSVA(500),TSVA(500),CSVA(500),DDS(500),VELP(500)
      DIMENSION IMSG(8),SDX(500)
      EQUIVALENCE (IMSG(1),ITL(1))
      DATA ITL(9)/'          '/,ITL(10)/'MIDDELBU'/,ITL(11)/'RG      '/
      DATA ITL(12)/'BDX 85  '/
      DATA L4/'    '/
C .500276              .00500848              -.0L0736
C   11 FORMAT (2F5.2,2I3,8A8)
   11 FORMAT (2F5.1,2I3,8A8)
   14 FORMAT (8F10.3)
   15 FORMAT (4F20.0)
      DO 43 I=1,500
   43 SD(I)=10000.
      READ (5,15) A,B,C
   44 READ (5,15) ALNM,STEP
      IF (ALNM) 300,300,45
   45 SD(1)=0.
      DO 40 I=2,500
      SD(I)=SD(I-1)+STEP
      IF(SD(I)-ALNM)40,42,42
   40 CONTINUE
   42 NN=I
      READ (5,11) DIS,PSI,NA,NB,IMSG
      DO 57 I=1,NA
      READ (5,14) DA(I),TA(I),SA(I)
      IF (TA(I)-32.)52,71,71
   71 TA(I)=(TA(I)-32.)*.55555
   52 IF(SA(I)-25.)55,55,57
   55 SA(I)=0.03+1.805*SA(I)
   57 CONTINUE
      DO 59 I=1,NB
      READ (5,14) DB(I),TB(I),SB(I)
      IF (TB(I)-32.) 54,72,72
   72 TB(I)=(TB(I)-32.)*.55555
   54 IF (SB(I)-25.)58,58,59
   58 SB(I)=0.03+1.805*SB(I)
   59 CONTINUE
      CALL LGINTP (NA,TA,DA,SD,TCA,NNA)
      CALL LGINTP (NA,SA,DA,SD,SCA,NNA)
      CALL LGINTP (NB,TB,DB,SD,TCB,NNB)
      CALL LGINTP (NB,SB,DB,SD,SCB,NNB)
      W2=1.458E-4
      PSJ=(2.*3.1415926265/360.)*PSI
      SPSI= SIN(PSJ)
      IF (SPSI.LT.0.1)SPSI=0.1
      X2= 1./(W2*SPSI*DIS)
      DO 62 I=1,NN
      DLT(I)= TCA(I)-TCB(I)
      DLS(I)= SCA(I)-SCB(I)
      BRT(I)=(TCA(I)+TCB(I))*0.5
   62 CONTINUE
      ND=NN-1
      DO 64 I=1,ND
      BDLT    =(DLT(I)+DLT(I+1))*0.5
      BDLS    =(DLS(I)+DLS(I+1))*0.5
      BTDT=BDLT*((BRT(I)+BRT(I+1))*.5)
      SDSD =SD(I+1)-SD(I)
      ABDLT = A*BDLT*SDSD
      BBTDT = B*BTDT*SDSD
      CBDLS = C*BDLS*SDSD
      SVEL = (ABDLT+BBTDT+CBDLS)*X2
   64 ANS (I)= (A*BDLT+B*BTDT+C*BDLS)*(SD(I+1)-SD(I))
      VELD(NN)=0.
      DO 66 I=2,NN
      JD=NN-(I-1)
   66 VELD(JD)=VELD(JD+1)+ANS(JD)*X2
      DO 82 I=1,NN
      TS=TCA(I)
```

```
      SS=SCA(I)
      DS=SD(I)
      CALL SGTSVA (TS,SS,DS,SGT,SV,SVA)
   82 ASVA(I)=SVA
      DO 84 I=1,NN
      TS=TCB(I)
      SS=SCB(I)
      DS=SD(I)
      CALL SGTSVA (TS,SS,DS,SGT,SV,SVA)
   84 BSVA(I)=SVA
      DO 92 I=1,NN
   92 DSVA(I)=ASVA(I)-BSVA(I)
      DO 94 I=1,ND
      TSVA(I)=(DSVA(I)+DSVA(I+1))*0.5
    4 CSVA(I)=TSVA(I)*(SD(I+1)-SD(I))
      DDS(NN)=0.
      DO 96 I=2,NN
      K=NN-(I-1)
   96 DDS(K)=DDS(K+1)+CSVA(K)
      DO 98 I=1,NN
   98 VELP(I)=DDS(I)*X2
      WRITE (6,9) IMSG
      WRITE (6,10)
   10 FORMAT (1X,'DEPTH  TEMPERATURE     SALINITY',10X,'A+2B-C     VELOCI
     1TY O   DYNAMIC     VELOCITY P'/'  M.          A       B       A       B',
     2 3X,'INTERGAL      CM/SEC        HEIGHT       CM/SEC'//)
      DO 102 I=1,ND
  102 WRITE (6,12) SD(I),TCA(I),TCB(I),SCA(I),SCB(I),VELO(I),DDS(I),
     1VELP(I),ANS(I)
   12 FORMAT (1X,F5.0,2F7.2,2F8.3,16X,1P3E12.3/40X,1PE12.3)
      WRITE (6,13) SD(NN),TCA(NN),TCB(NN),SCA(NN),SCB(NN),VELO(NN),
     1DDS(NN),VELP(NN)
   13 FORMAT (1X,F5.0,2F7.2,2F8.3,16X,1P3E12.3///)
    9 FORMAT(1H1,8A8/)
      WRITE (6,24) A,B,C,X2
   24 FORMAT ('  A = ',F12.10,'  B = ',F12.10,'  C = ',F12.10,
     1'   1/(2 OMEGA SIN PHI DIST) = ',1PE12.4)
C
C           DRAW VELOCITY PROFILES
C
      DO 210 I=1,NN
  210 SDX(I)=-SD(I)
      CALL DRAW(NN,VELO,SDX,1,0,L4,ITL,25.,100.,10,4,2,2,8,10,1,LLL)
      CALL DRAW(NN,VELP,SDX,3,0,L4,ITL,25.,100.,10,4,2,2,8,10,1,LLL)
C
      GO TO 44
   30     CONTINUE
      STOP
      END
```

Program 4. A program to compute the geostrophic surface velocity over the FNWC 63 x 63 fields on the IBM/360 computer

```
C       DIMENSION S(63,63),VCX(62,62),VCY(62,62)
        DIMENSION T(63,63),VAX(62,62),VAY(62,62),VBX(62,62),VBY(62,62)
        DIMENSION VX(62,62),VY(62,62),IT(24),D(8),IX(62),IY(62)
        DIMENSION V(62,62)
      4 FORMAT (1H1,' A = ',1PE20.5,' B = ',E20.5,' C = ',E20.5//)
      5 FORMAT (/)
      6 FORMAT (I3,13F9.2)
      7 FORMAT (1X,13I9/)
      8 FORMAT (1H1,24A4//)
      9 FORMAT (3X,13F9.2)
     11 FORMAT (3F20.10,I5)
C
C     IOUT CONTROL INTEGER IN COLUMN 65
C      IOUT = 0    PRINT VELOCITY LISTING ONLY
C      IOUT = 1    PRINT CONTOURED MAP ONLY
C      IOUT = 2    PRINT BOTH LISTING AND CONTOURED MAP
C
        READ (5,11)A,B,C,IOUT
        D(1)=0.
        D(2)=121.9
        D(3)=61.0
        D(4)=61.0
        D(5)=30.5
        D(6)=30.5
        D(7)=30.5
        D(8)=30.5
        DO 41 I=1,62
        IY(I)=I
   41   IX(I)=I
C       DO 10 I=1,63
C       DO 10 J=1,63
C  10   S(I,J)=35.
        DO 15 K=1,8
        READ (8) ((T(I,J),I=1,63),J=1,63)
        READ (8) IT
        IF (K.EQ.1.) GO TO 13
        GO TO 23
   13   DO 22 J=1,62
        DO 22 I=1,62
        VX(I,J)=0.
        VY(I,J)=0.
        VAX(I,J)=T(I,J)-T(I+1,J)
        VAY(I,J)=T(I,J)-T(I,J+1)
        VBX(I,J)=(T(I,J)+T(I+1,J))*.5*VAX(I,J)
        VBY(I,J)=(T(I,J)+T(I,J+1))*.5*VAY(I,J)
C       VCX(I,J)=S(I,J)-S(I+1,J)
C       VCY(I,J)=S(I,J)-S(I,J+1)
   22   CONTINUE
        GO TO 15
   23   DO 24 J=1,62
        DO 24 I=1,62
        DTX=T(I,J)-T(I+1,J)
        DTY=T(I,J)-T(I,J+1)
        BDX=(T(I,J)+T(I+1,J))*.5*DTX
        BDY=(T(I,J)+T(I,J+1))*.5*DTY
C       DSX=S(I,J)-S(I+1,J)
C       DSY=S(I,J)-S(I,J+1)
        DAX=(VAX(I,J)+DTX)*.5
        DAY=(VAY(I,J)+DTY)*.5
        DBX=(VBX(I,J)+BDX)*.5
        DBY=(VBY(I,J)+BDY)*.5
C       DCX=(VCX(I,J)+DSX)*.5
C       DCY=(VCY(I,J)+DSY)*.5
        CALL CORFOR (I,J,CFL)
        VX(I,J)=VX(I,J)+((DAX*A+DBX*B        )*D(K)*CFL)
        VY(I,J)=VY(I,J)+((DAY*A+DBY*B        )*D(K)*CFL)
        V(I,J)= SQRT(VX(I,J)**2+VY(I,J)**2)
        VAX(I,J)=DTX
        VAY(I,J)=DTY
        VBX(I,J)=BDX
        VBY(I,J)=BDY
C       VCX(I,J)=DSX
C       VCY(I,J)=DSY
```

```
24 CONTINUE
   NR= 62
   NC= 62
   AMIN=-100.0
   BND= 10.
   AZ=.001
   BZ= 0.0
   IJT=0
   ICON=1
   IF (IOUT.EQ.0.OR.IOUT.EQ.2) GO TO 52
   GO TO 14
52 CONTINUE
   WRITE (6,4) A,B,C
   WRITE(6,8) IT
   WRITE(6,7) (IX(I),I=1,13)
   DO 31 I=1,62
   WRITE (6,9) (T(I,J),J=1,13)
   WRITE (6,6) IY(I),(VX(I,J),J=1,13)
   WRITE (6,9) (VY(I,J),J=1,13)
   WRITE (6,9) (V(I,J),J=1,13)
   WRITE (6,5)
31 CONTINUE
   WRITE(6,8) IT
   WRITE(6,7) (IX(I),I=14,26)
   DO 32 I=1,62
   WRITE (6,9) (T(I,J),J=14,26)
   WRITE (6,6) IY(I),(VX(I,J),J=14,26)
   WRITE (6,9) (VY(I,J),J=14,26)
   WRITE (6,9) (V(I,J),J=14,26)
   WRITE (6,5)
32 CONTINUE
   WRITE(6,8) IT
   WRITE(6,7) (IX(I),I=27,39)
   DO 33 I=1,62
   WRITE (6,9) (T(I,J),J=27,39)
   WRITE (6,6) IY(I),(VX(I,J),J=27,39)
   WRITE (6,9) (VY(I,J),J=27,39)
   WRITE (6,9) (V(I,J),J=27,39)
   WRITE (6,5)
33 CONTINUE
   WRITE(6,8) IT
   WRITE(6,7) (IX(I),I=40,52)
   DO 34 I=1,62
   WRITE (6,9) (T(I,J),J=40,52)
   WRITE (6,6) IY(I),(VX(I,J),J=40,52)
   WRITE (6,9) (VY(I,J),J=40,52)
   WRITE (6,9) (V(I,J),J=40,52)
   WRITE (6,5)
34 CONTINUE
   WRITE(6,8) IT
   WRITE(6,7) (IX(I),I=53,62)
   DO 35 I=1,62
   WRITE (6,9) (T(I,J),J=53,62)
   WRITE (6,6) IY(I),(VX(I,J),J=53,62)
   WRITE (6,9) (VY(I,J),J=53,62)
   WRITE (6,9) (V(I,J),J=53,62)
   WRITE (6,5)
35 CONTINUE
14 IF (IOUT.EQ.1.OR.IOUT.EQ.2) GO TO 54
   GO TO 15
54 CONTINUE
   CALL METMAP (V,NR,NC,IT,BND,AZ,BZ,AMIN,IJT,ICON)
15 CONTINUE
   STOP
   END
   SUBROUTINE CORFOR (I,J,CFL)
   R=(I-32)*(I-32)+(J-32)*(J-32)
   S=(973.71-R)/(973.71+R)
   IF (S-.125)4,5,5
 4 S=.125
 5 A=1.86603/(1.+S)
   D=381.0/A
   T=1.45842E-04
   CFL=1./(T*S*D)
   RETURN
   END
```

Program 5. A program to compute the geostrophic surface velocity over the FNWC 63 x 63 fields on the CDC/3600 digital computer

```
      PROGRAM GEOCUR(OUTPUT,TAPE1,TAPE2,TAPE6=OUTPUT,TAPE9)
      DIMENSION T(63,63),T1(3989),T2(3969)
      DIMENSION S(63,63),S1(3969),S2(3969),S3(3969)
      DIMENSION A(12),B(12),D(12)
      DIMENSION VAX(63,63),VAY(63,63),VBX(63,63),VCY(63,63)
      COMMON    VBY(63,63),VCX(63,63)
      DIMENSION VX(63,63),VY(63,63),V(63,63)
      DIMENSION WINDX(3989),WINDY(3989),WINDV(3969)
      DIMENSION TRANS(3989),STREAM(3989)
      DIMENSION PTAB(4),DATE(3)
      INTEGER   IX(63),IY(63),E(5),ET(8),F(3),G(5)
      EQUIVALENCE (T1(21),T),(T2,VY)
      EQUIVALENCE (S1,S),(S3,VX),(S2,VCY)
      EQUIVALENCE (VAX,WINDX(21)),(VAY,WINDY(21))
      EQUIVALENCE (VBX,WINDV)
      EQUIVALENCE (TRANS(21),V),(STREAM(21),VX)
      EQUIVALENCE (DATE,A)
      EQUIVALENCE (E,IX),(G,IX(4))
      DATA GTAB/7707700008/
      DATA(PTAB(I),I=1,4)/.5,.45,5008,0,/
C
C     A, B AND C ARE CONSTANTS, AND ARE AVERAGE VALUES FOR
C      THE PRESENT DEPTH OF CALCULATION AND THAT OF THE PRE-
C      VIOUS INTEGRATION STEP.  A AND B ARE CHOSEN AT CON-
C      STANT SALINITY OF 34.5(0/00)
      A=.0000881
      B=.00000865
      C=-.00074
C
C     D IS THE DEPTH INCREMENT IN METERS BETWEEN THE LEVEL
C      OF PRESENT CALCULATION, AND THE PRECEEDING ONE
      D(1)=0.
      D(2)= 30.48
      D(3)= 30.48
      D(4)= 30.48
      D(5)= 30.48
      D(6)= 60.94
      D(7)= 60.94
      D(8)=121.92
      D(9)= 34.2
      D(10)=200.
      D(11)=200.
      D(12)=200.
C
C     ET IS AN ARRAY CONTAINING THE ADDRESSES OF ENVE FIELDS
C-----SURFACE---------
      ET(1)=10HT  SEA
C-----100FT/30.48M----
      ET(2)=10HTS 100
C-----200FT/60.96M----
      ET(3)=10HTS 200
C-----300FT/91.44M----
      ET(4)=10HTS 300
C-----400FT/121.9M----
      ET(5)=10HTS 400
C-----600FT/182.9M----
      ET(6)=10HTS 600
```

```
C-----800FT/243.8M----
      ET(7)=10HTS 800
C-----1200FT/365.8M---
      ET(8)=10HTS1200
C
C     E IS AN ARRAY WHICH CONTAINS THE CALLING PARAMETERS
C      FOR THE SUBROUTINE RDMSTF WHEN READING FNWF FIELDS
      DATE(1)=0.
      E(1)=DATE(1)
C     E(2) IS DEFINED LATER IN THE DO LOOP
      E(3)=0
      E(4)=3H
      E(5)=5LTAPE1
C
C     ISVO IS A VELOCITY FIELD PRINTING OPTION AS FOLLOWS
C        0  COMPLETE VELOCITY FIELD PRINTOUT AT ALL DEPTHS
C        1  SURFACE VELOCITY FIELD WILL BE PRINTED ONLY
C        2  NO VELOCITY FIELD PRINTOUT WILL RESULT
      ISVO=2
C     ICO IS A CONTOUR PRINT SELECTOR AS FOLLOWS
C        0 ALL LEVELS CONTOURED
C        1 SURFACE CONTOUR(S) ONLY
C        2 NO CONTOUR(S) PRINTOUT
      ICO=2
C
      IF(ISVO.EQ.2)GO TO 26
C     IX AND IY ARE ARRAYS WHICH SERVE TO NUMBER THE ROWS
C      AND COLUMNS OF THE GRID FOR PRINTING PURPOSES
      DO 41  I=1,63
      IY(I)=I
   41 IX(I)=I
C
C     READING IN OF TEMPERATURE AND SALINITY FIELDS FOLLOWS
   26 N=11
      DO 19 K=1,N
      IF(K.GT.8)GO TO 127
      GO TO(135,136,138,140,142,144,146,148)K
  135 E(2)=ET(1)
 1351 CALL RDMSTF(T1,E)
      IF(E(3).NE.0)GO TO 1351
      READ(2) S1
      GO TO 17
C
  136 E(2)=ET(2)
 1361 CALL RDMSTF(T1,E)
      IF(E(3).NE.0)GO TO 1361
      READ(2) S1
      READ(2) S3
      DO 137 I=1,3969
  137 S1(I)=(19.52*S1(I)+5.48*S3(I))/25.
      GO TO 17
C
  138 E(2)=ET(3)
 1381 CALL RDMSTF(T1,E)
      IF(E(3).NE.0)GO TO 1381
      READ(2) S2
      DO 139 I=1,3969
  139 S1(I)=(39.04*S3(I)+10.96*S2(I))/50.
```

```
      GO TO 17
C
  140 E(2)=ET(4)
 1401 CALL RDMSTF(T1,E)
      IF(E(3).NE.0)GO TO 1401
      DO 141 I=1,3969
  141 S1(I)=(8.56*S3(I)+41.44*S2(I))/50.
      GO TO 17
C
  142 E(2)=ET(5)
 1421 CALL RDMSTF(T1,E)
      IF(E(3).NE.0)GO TO 1421
      READ(2) S3
      DO 143 I=1,3969
  143 S1(I)=(28.08*S2(I)+21.92*S3(I))/50.
      GO TO 17
C
  144 E(2)=ET(6)
 1441 CALL RDMSTF(T1,E)
      IF(E(3).NE.0)GO TO 1441
      READ(2) S2
      DO 145 I=1,3969
  145 S1(I)=(17.12*S3(I)+32.88*S2(I))/50.
      GO TO 17
C
  146 E(2)=ET(7)
 1461 CALL RDMSTF(T1,E)
      IF(E(3).NE.0)GO TO 1461
      READ(2)T2
      READ(2) S3
      DO 147 I=1,3969
  147 S1(I)=(156.16*S2(I)+43.84*S3(I))/200.
      GO TO 17
C
  148 E(2)=ET(8)
 1481 CALL RDMSTF(T1,E)
      IF(E(3).NE.0)GO TO 1481
      DO 149 I=1,3969
  149 S1(I)=(34.24*S2(I)+165.76*S3(I))/200.
      GO TO 17
C
  127 READ(2)(T1(I),I=21,3989)
      READ(2)S1
C     THE FIELDS ARE WRITTEN ON DISK
   17 WRITE(9)T,S
      IF(K.EQ.8)WRITE(9)T2,S3
   19 CONTINUE
      REWIND 9
C
C     THE ACTUAL CALCULATION BEGINS HERE.  THE FIRST CALCU-
C      LATION INITIALIZES COMPONENTS AT THE LEVEL OF ASSUM-
C      ED MOTION
      READ(9)T,S
   13 DO 22 J=1,62
      DO 22 I=1,62
      VX(I,J)=0.
      VY(I,J)=0.
      V(I,J)=0.
```

```
      VAX(I,J)=T(I,J)-T(I+1,J)
      VAY(I,J)=T(I,J)-T(I,J+1)
      VBX(I,J)=(T(I,J)+T(I+1,J))*.5*VAX(I,J)
      VBY(I,J)=(T(I,J)+T(I,J+1))*.5*VAY(I,J)
      VCX(I,J)=S(I,J)-S(I+1,J)
   22 VCY(I,J)=S(I,J)-S(I,J+1)
C
C     THE ACCUMULATION OF COMPONENTS BEGINS HERE
      M2=N+1
      DO 15 K=2,M2
      READ(9)T,S
   23 DO 24 J=1,62
      DO 24 I=1,62
      DTX=T(I,J)-T(I+1,J)
      DTY=T(I,J)-T(I,J+1)
      BDX=(T(I,J)+T(I+1,J))*.5*DTX
      BDY=(T(I,J)+T(I,J+1))*.5*DTY
      DSX=S(I,J)-S(I+1,J)
      DSY=S(I,J)-S(I,J+1)
      DAX=(VAX(I,J)+DTX)*.5
      DAY=(VAY(I,J)+DTY)*.5
      DBX=(VBX(I,J)+BDX)*.5
      DBY=(VBY(I,J)+BDY)*.5
      DCX=(VCX(I,J)+DSX)*.5
      DCY=(VCY(I,J)+DSY)*.5
C     CORFOR IS A SUBROUTINE FOR COMPUTING CORIOLIS FORCE
C      BASED ON GRID POSITION
      CALL CORFOR (I,J,CFL)
      VX(I,J)=VX(I,J)+((DAX*A+DBX*B+DCX*C)*D(K)*CFL)*.4665
      VY(I,J)=VY(I,J)+((DAY*A+DBY*B+DCY*C)*D(K)*CFL)*.4665
     1*.4665
      V(I,J)= SQRT(VX(I,J)**2+VY(I,J)**2)
      VAX(I,J)=DTX
      VAY(I,J)=DTY
      VBX(I,J)=BDX
      VBY(I,J)=BDY
      VCX(I,J)=DSX
      VCY(I,J)=DSY
   24 CONTINUE
C
C
C     FOR COMPATIBILITY WITH PLOTTING PROGRAM, VX, VY AND V
C      MUST BE EXTENDED TO 63X63 ARRAYS WITH DUMMY VALUES
      DO 40 I=1,63
      VX(63,I)=VX(62,I)
      VX(I,63)=VX(I,62)
      VY(63,I)=VY(62,I)
      VY(I,63)=VY(I,62)
      V(63,I)=V(62,I)
   40 V(I,63)=V(I,62)
C
C     CONTOUR AND PRINTING SELECTION
   18 IF(ICO.EQ.2)GO TO 16
      IF(ICO.EQ.1.AND.K.NE.N)GO TO 16
      WRITE(6,1)
      CALL CONTOUR(VX,63,63,3.,3LAVX)
      CALL CONTOUR(VY,63,63,3.,3LAVY)
   16 IF(ISVO.EQ.2) GO TO 15
```

```
      IF(ISVO.EQ.1.AND.K.NE.N) GO TO 15
C
    1 FORMAT(1H1)
    5 FORMAT (/)
    6 FORMAT (I3,13F9.4)
    7 FORMAT (1X,13I9/)
    8 FORMAT (3X,13F9.4)
    9 FORMAT (3X,13F9.2)
C
      WRITE(6,1)
      WRITE(6,7) (IX(I),I=1,13)
      DO 31 I=1,63
      WRITE (6,9) (T(I,J),J=1,13)
      WRITE (6,9) (S(I,J),J=1,13)
      WRITE (6,6) IY(I),(VX(I,J),J=1,13)
      WRITE (6,8) (VY(I,J),J=1,13)
      WRITE (6,8) (V(I,J),J=1,13)
   31 WRITE (6,5)
      WRITE(6,1)
      WRITE(6,7) (IX(I),I=14,26)
      DO 32 I=1,63
      WRITE (6,9) (T(I,J),J=14,26)
      WRITE (6,9) (S(I,J),J=14,26)
      WRITE (6,6) IY(I),(VX(I,J),J=14,26)
      WRITE (6,8) (VY(I,J),J=14,26)
      WRITE (6,8) (V(I,J),J=14,26)
   32 WRITE (6,5)
      WRITE(6,1)
      WRITE(6,7) (IX(I),I=27,39)
      DO 33 I=1,63
      WRITE (6,9) (T(I,J),J=27,39)
      WRITE (6,9) (S(I,J),J=27,39)
      WRITE (6,6) IY(I),(VX(I,J),J=27,39)
      WRITE (6,8) (VY(I,J),J=27,39)
      WRITE (6,8) (V(I,J),J=27,39)
   33 WRITE (6,5)
      WRITE(6,1)
      WRITE(6,7) (IX(I),I=40,52)
      DO 34 I=1,63
      WRITE (6,9) (T(I,J),J=40,52)
      WRITE (6,9) (S(I,J),J=40,52)
      WRITE (6,6) IY(I),(VX(I,J),J=40,52)
      WRITE (6,8) (VY(I,J),J=40,52)
      WRITE (6,8) (V(I,J),J=40,52)
   34 WRITE (6,5)
      WRITE(6,1)
      WRITE(6,7) (IX(I),I=53,63)
      DO 15 I=1,63
      WRITE (6,9) (T(I,J),J=53,63)
      WRITE (6,9) (S(I,J),J=53,63)
      WRITE (6,6) IY(I),(VX(I,J),J=53,63)
      WRITE (6,8) (VY(I,J),J=53,63)
      WRITE (6,8) (V(I,J),J=53,63)
      WRITE (6,5)
   15 CONTINUE
      REWIND 1$REWIND 2
      REWIND 9
      PAUSE 1
```

```
      M1=0
      GO TO 43
C
C     UNLOAD TEMPERATURE TAPE 1 AND SALINITY TAPE 2
C      MOUNT WIND TAPE ON UNIT 1 FOR READING
C      MOUNT CURTRANS/CURRSTRM FIELD TAPE(OUTPUT) ON UNIT 2
C       FOR WRITING
C
C     READ IN WIND COMPONENTS
   48 G(1)=0
      G(2)=10HU  W
      G(3)=0
      G(4)=36
      G(5)=5LTAPE1
   44 CALL RDMSTF(WINDX,G)
      IF(G(3).EQ.1) GO TO 44
      G(2)=10HV  W
   45 CALL RDMSTF(WINDY,G)
      IF(G(3).EQ.1) GO TO 45
C     IT IS NECESSARY TO COMPUTE A WIND DRIFT TRANSPORT,
C      SINCE ONLY THE U AND V COMPONENTS OF THE WIND DRIFT
C      ARE READ IN
      DO 47 I=21,3989
   47 WINDV(I-20)=(SQRT(WINDX(I)**2+WINDY(I)**2))*.4665
      REWIND 1
      M1=M1+1
C
C     COMBINE GEOSTROPHIC CURRENT COMPONENTS WITH WIND FIELD
C      WITH WIND FIELD COMPONENTS (USING EQUIVALENT STORAGE)
      DO 42 I=1,63
      DO 42 J=1,63
      VX(I,J)=VX(I,J)+(VAX(I,J))*.4665
      VY(I,J)=VY(I,J)+(VAY(I,J))*.4665
   42 V(I,J)=V(I,J)+VBX(I,J)
C
C     THE TRANSPORT FIELD IS NOW TO BE WRITTEN ON TAPE
   43 E(4)=40
      E(5)=5LTAPE2
      TRANS(2)=140B
      TRANS(2)=(TRANS(2).OR.DATE(1))
      TRANS(3)=10H
      TRANS(6)=10HACURTRANS
      TRANS(7)=10HCLIMATIC
      IF(M1.NE.1)TRANS(8)=10HG-STROPHIC
      IF(M1.EQ.1)TRANS(8)=10HTOTAL
      TRANS(9)=10H NM/DAY
      TRANS(10)=10H FIG 7.
   25 CALL WRMSTF(TRANS,E(3))
      IF(E(3).EQ.1) GO TO 25
C
C     COMPUTE STREAM FUNCTION USING SUBROUTINE PSNF AND PSSN
      CALL PSNF(PTAB,VX,VY,GTAB,ERR)
C
C     THE STREAM FUNCTION FIELD IS NOW TO BE WRITTEN ON TAPE
      F(1)= 0
      F(2)= 38
      F(3)= 5LTAPE2
      STREAM(2)=140B
```

```
      STREAM(2)=(STREAM(2).OR.DATE(1))
      STREAM(3)=10H
      STREAM(6)=10HACURRSTRM
      STREAM(7)=10HCLIMATIC
      IF(M1.NE.1)STREAM(8)=10HG-STROPHIC
      IF(M1.EQ.1)STREAM(8)=10HTOTAL
      STREAM(9)=10H NM/DAY
      STREAM(10)=10H FIG 7.
   28 CALL WRMSTF(STREAM,F)
      IF(F(1).EQ.1) GO TO 28
C
      IF(M1.EQ.0)GO TO 48
   29 END FILE 2
      REWIND 2
C
      STOP
      END
```

APPENDIX IV

A Determination of the Thermal Geostrophic Component in the Gulf Stream Water off the Grand Banks

A DETERMINATION OF THE THERMAL GEOSTROPHIC COMPONENT IN THE GULF STREAM WATER OFF THE GRAND BANKS

One of the important advantages of the T-S Gradient method is the possibility of identifying the significance of the thermal and haline components of the geostrophic flow. Furthermore, if the thermal or haline components can be neglected or correlated with the total geostrophic flow, then the possibility exists that only one or the other measurement need be taken. If only the thermal structure is known the first order thermal contribution to the geostrophic current can be computed:

$$(V_1 - V_2)_T = \frac{1}{f}\left[\overline{K}_{1_i} \Sigma \Delta T_i \Delta P_i + \overline{K}_2 \Sigma \overline{T}_i \Delta T_i \Delta P_i\right] \quad \text{(A. 111-1)}$$

Correlating the first order thermal current with the total geostrophic current the correlation function can then be used to determine the total geostrophic current from the temperature measurements alone.

The feasibility of accomplishing this is enhanced by the development of the expendable bathythermograph (XBT) which allows a ship to steam at full speed over a region and measure the temperature structure to 6, 000 feet. Prior to the development of the XBT, temperature structure was commonly measured by mechanical bathythermographs which were limited to 900 feet.

If this technique were possible, one application where it would

be valuable would be in the International Ice Patrol Survey of the U.S. Coast Guard in the Grand Banks region. The purpose of these surveys is to provide information on the currents in this region for iceberg drift movement during the ice season. This information is useful for safe navigation. Unfortunately, two requirements of the survey are conflicting. First is the requirement to survey a relatively large area with sufficient density to delineate the flow. Second is the requirement to complete the survey in a short enough time to give a reasonable synoptic picture. At the present time the surveys take about two weeks during which time approximately 100 hydrographic stations are occupied (Lenczyk, 1964). If even a 50 percent reduction in the number of complete hydrographic stations could be achieved by sampling these at full speed using XBT's the survey time could be reduced by several days and the currents would be far more synoptic than the present program allows. Unfortunately, this region is a region of rapid changes in water structure. The charts of dynamic topography are considered of little value after two weeks and another survey must be conducted. Several surveys are needed in a single ice season, March through June.

Three water masses have been identified in the Grand Banks region (Kollmeyer, 1966): Gulf Stream Water, Labrador Water, and mixed water, representing the boundary between the two other Waters. If the geostrophic currents are to be determined from the

thermal component alone some technique must be established for separating the water masses as a different correlation will exist between the thermal component and the total flow in each water mass.

For the purpose of testing the feasibility of establishing such a relationship 33 hydrographic station pairs in the Gulf Stream Water were selected from the U. S. Coast Guard Ice Patrol Reports (Moynihan, 1968). The stations were selected using the Coast Guard charts of dynamic topography for the survey containing each station pair. The station pairs were used to compute the thermal component of the geostrophic current using Equation A. III-1, and the total geostrophic current. The coefficients used in Equation A. IV-1 were:

$$\overline{K}_1 = 83.4 \times 10^{-6}$$

$$\overline{K}_2 = 85.8 \times 10^{-7}$$

The resulting thermal component is plotted against the total geostrophic surface velocity in Figure A. IV-1. A linear regression analysis fit in the least square sense, yields the following expression:

$$(V_1 - V_2) = 0.39\,(V_1 - V_2)_T + 2.84 \text{ (cm/sec)}$$

The variance of the total geostrophic surface velocity is 15.5 $(\text{cm/sec})^2$.

Therefore, if the water mass boundaries can be identified it

Figure AIV-1. Relationship between the total geostrophic surface current and the T-S Gradient thermal component in the Gulf Stream Water off the Grand Banks.

is possible to compute the total geostrophic surface current from the thermal component using the above expression. Hydrographic surveys of this region could be made more synoptic using XBT's to substitute for some of the standard hydrographic stations.

APPENDIX V

Field Evaluation

FIELD EVALUATION

Introduction

Based on the results of this research the T-S Gradient method should allow the computation of surface geostrophic currents in good agreement with those computed using the standard geostrophic calculations. Of course, both computations suffer from the limitations inherent in the geostrophic assumptions. Therefore, the purpose of this research to find a simplified scheme to make geostrophic computations has been met, yet the computation of currents without environmental verification is not very satisfying. However, it must be concluded that at this time current observations are too few and unreliable to be used as a quantitative measure of indirectly computed currents. This appendix reviews two attempts by the author to verify the representativeness of geostrophic currents to the actual ocean currents, and proposes some refinements of these attempts to continue the research. These two experiments are the only ones known to the author as direct efforts to verify computed surface currents in the open ocean in the slow California Current.

The major oceanic gyres appear to be revealed by geostrophic computations (Reid, 1961, and Stommel, 1965). Yet at any point or time in the ocean the geostrophic current may or may not be

representative of the instantaneous flow. As mentioned earlier, many forces act to drive the waters of the ocean, and generally the flow in the ocean will consist of both baroclinic and barotrophic components (Foffonoff, 1962). Therefore, the determination of the geostrophic current at any given time from a pair of hydrographic stations does not yield the existing current. However, if the hydrographic stations are sampled in a time-series fashion over a sufficient length of time to remove the non-geostrophic periodic components, then the resulting computed current can be expected to come into closer agreement with the average current over the period of the extended sampling.

Defant (1950) has shown that the internal oscillations in the water structure can lead to significant errors in the geostrophic currents. Particularly important in dynamic computations is the change in the water structure associated with internal waves, and the most significant periods are those of the diurnal and semidiurnal tide (Defant, 1950). LaFond (1951) also identified the semidiurnal and diurnal periods as the most significant perterbations in the water structure.

Little is known of the internal oscillations in the ocean at the present time. However, Haurwitz, et al. (1959) show that significant peaks occur in their long series of records of temperature at 50 m and 500 m offshore from Castle Harbor, Bermuda, only at the

semidiurnal and inertial or diurnal periods. Except for a broad maximum at about 0. 5 cycles per hour their spectra decreases monotonically with increasing frequency. There appears to be no statistically significant coherence between observations at 50 m and 500 m. Cox (1962) shows in observations taken from the U. S. Navy Electronics Laboratory oceanographic tower with isotherm followers that the observations between laterally-spaced sensors are coherent only at low frequencies, well below the mean value of the Väisälä frequency.

It would be advantageous to use more than one ship to determine geostrophic flow between hydrographic stations, such that the measurements applied at the same "instant" in time. In general oceanographic operations are conducted by single vessels. Single vessel hydrographic surveys are limited to two possible sampling procedures, both of which may significantly influence the resulting computed geostrophic current. The choice lies between sampling between stations, first one station then another, such that enough casts are made at each station to remove the variability; or second sampling each station in a time-series fashion a sufficient number of times to remove the variability, moving on to the next station at the completion of the first.

Rapid sampling between stations means that the samplings are almost synoptic, that is, taken under nearly the same conditions.

Furthermore, in running between stations the intervening water structure can be sampled. However, in the California current area hydrographic stations for determining geostrophic flow should be at least 35 kilometers apart. This means that a conventional oceanographic vessel traveling at ten knots will require two hours to steam between stations, and a total of four hours will be required to complete both stations. Changes in the hydrographic conditions at either station may be significant during this four hour period (Defant, 1950).

On the other hand, time-series sampling at a single station requires a sample of sufficient length and density to remove the periodic variations. At least 12 hours and preferably 24 hours of sampling should be made at each station; with a cast every two hours, 50 hours will be required to completely sample a station pair (24 hours per stations with two hours steaming). One disadvantage of single station time-series sampling is that between any two station pair only one sampling of the intervening water structure is made.

To test the two types of sampling (continuous time series sampling at one station versus alternating sampling between stations) two experiments were performed. In the first experiment the alternating sampling between stations was used. In the second, the 24 hour sampling at each station was performed.

Experiment I

The first experiment was performed from August 31, 1967 to September 4, 1967 off Santa Cruz, California.

Purpose

This experiment had a dual purpose: first, the verification of computed surface currents for this research; second, to examine the validity of Richardson's "4/3 law" for particle diffusion, at large particle separations (in this case separations in excess of six nautical miles). The results of this latter work have been previously reported (Denner, et al., 1968).

Sampling Procedure

The experiment consisted of alternate sampling between two stations A and B at intervals of every four to six hours. The location of these stations were:

A = 36° 50' N, 122° 36.2' W

B = 36° 20' N, 123° 12.0' W

Temperature and salinity measurements were made using standard hydrographic procedures. Temperatures were determined as the average of paired thermometers, and salinities were determined from water samples on a Hytech model 6210 laboratory

salinometer. Temperature structure was measured to 1,500 feet every hour on station and at three equi-distant points between stations with XBT casts. Surface currents were measured at Station A using parachute drogues (Volkmann, et al., 1956). The drogues were positioned relative to a taut reference mooring, using radar. The initial locations of Station A and Station B, and all later locations of B were made using Loran C.

Meteorological Conditions

The meteorological conditions were favorable for the entire cruise. Winds were always less than Beaufort 4 and predominantly below Beaufort 3 from 330° true, with corresponding sea states. The swell were always less than five feet from about 300° true. No difficulty was experienced in sampling or holding station due to weather conditions.

Current Measurements

Station A was established first by setting a taut moored surface reference buoy for current measurements, diffusion studies, and hydrographic casts. The drogues were seeded, as nearly as possible, in an octagonal pattern at a range of two nautical miles about the reference. Also, one drogue was placed next to the reference marker. All drogues were shallow with a 10 m line between

the float and parachute. The position of each drogue relative to the reference mooring was recorded every 30 minutes on the ships radar for seven hours with the exception of drogue Number 2, which was lost after five hours.

The movement of all drogues was consistent over the entire period except for drogues 2, 4, and 8. Drogue 2 was considered anomalous and dropped from the analysis. The final position of drogue 4 and initial position of drogue 8 were anomalous and also were neglected. The surface current was taken as the straight line distance between the initial and final accepted position divided by the time lapse. The results of this analysis are given in Table A. V-1.

Table A. V-1. Average velocity of the drogues in Experiment I.

Drogue	Displacement (n miles)	Time (hours)	Speed (knots)	Direction (degrees true)
1	2.0	6.6	0.28	340
2	-	-	-	-
3	1.2	7.2	0.17	17.5
4	1.0	7.2	0.14	347
5	1.8	7.2	0.25	336
6	1.7	7.2	0.24	336
7	2.0	7.2	0.28	334
8	1.8	6.2	0.29	350
9	1.4	7.2	0.19	2

Hydrographic Measurements

At the conclusion of the current measurements the hydrographic studies were initiated with a hydrographic cast at Station A. Station B was established 40 nmi from station A, bearing 250° true, approximately at right angles to the observed currents. Casts were taken alternately at Stations A and B. The same bottle spacings were used on each cast for convenience and the maximum sampling depth was fixed by the amount of wire out, 1,000 m. An expendable bathythermograph was launched at each cast with the messenger, and at each mid-point crossing between stations. The transit time between stations was approximately five hours, and five casts were made at each station. The hydrographic studies required 60 hours. The hydrographic data are on file at the Naval Postgraduate School, Monterey, California under NPGS Cruise A-1, 1967.

Results

The drogue-measured current was taken as the average of the results summarized in Table A. V-1, 0. 25 knots toward approximately 340° true. Geostrophic surface currents were computed from the hydrographic data for each successive station pair (A_1B_1, B_1A_2, A_2B_2, B_2A_3, etc.) using both the T-S Gradient method and the standard geostrophic method. A reference level of 700 m was

Table A. V-2. Comparison of standard and T-S gradient geostrophic surface currents, and FNWC currents for Experiment I.

Day	Time	Station Pair	Standard Method		T-S Gradient Method		FNWC		
			Speed	Direction	Speed	Direction	Time	Speed	Direction
9/1/67	11:00	$A_1 - B_1$	4.0	340°	4.0	340°	06:00	12.7	168
9/1/67	18:00	$B_1 - A_2$	4.6	340°	4.6	340°	16:00	12.7	185
9/2/67	00:00	$A_2 - B_2$	4.7	340°	4.7	340°			
9/2/67	05:30	$B_2 - A_3$	6.8	340°	6.8	340°	06:00	12.7	180
9/2/67	18:30	$A_3 - B_3$	9.5	340°	9.5	340°	16:00	12.7	180
9/3/67	01:30	$B_3 - A_4$	8.8	340°	8.8	340°			
9/3/67	03:30	$A_4 - B_4$	5.8	340°	5.8	340°	06:00	12.7	185
9/3/67	09:30	$B_4 - A_5$	6.8	340°	6.9	340°			
9/3/67	21:00	$A_5 - B_5$	4.4	340°	4.4	340°	16:00	12.7	180

selected for both calculations as this depth was achieved on each cast.

The velocity profiles indicate a steady increase in velocity relative to the 700 db reference level. The profiles obtained by the two approaches to the geostrophic computations are essentially the same. The relative geostrophic surface current was between 4 cm/sec and 9.5 cm/sec, and the values for each station pair is given in Table A.V-2. These values are low compared to the measured velocity at Station A. There are several possible explanations for the disagreement between the measured and computed velocity. First, part of the measured flow may have been in the barotrophic mode which is not revealed by geostrophic computations. Secondly, the current measurements and the hydrographic measurements were not concurrent, and the currents may have decreased after the measurements. This would have been determined by longer current measurements. In fact attempts were made to locate the drogues on each return to Station A but without success.

Also shown in Table A.V-2 are the surface current speed and direction read from the FNWC synoptic current and stream function charts. During this entire period the FNWC currents were to the south-southeast (160° to 180° true) at approximately 12.7 cm/sec. This flow is in the opposite direction to the measured currents. However, it should be noted that the FNWC currents are the sum

of their mass driven and wind driven components. FNWC uses Witting's (1909) results (Equation 17) with a wind factor of 4.8: taking the winds at 10 m/sec from 330° true, a wind drift of 15.8 cm/sec to 330° true is computed. Therefore, it appears as if the FNWC current is governed mainly by the wind component which in this case does not lead to agreement with the measured currents. This is true even though the wind was persistent over the entire period.

Conclusion

This experiment shows that under these hydrographic conditions the T-S Gradient method gives essentially identical results to the standard geostrophic computations. These results give the geostrophic current in the same direction as directly-measured currents, but at a lower speed (4.0 cm/sec to 9.5 cm/sec computed versus 12.8 cm/sec measured). Since there are many variables that could not be controlled, better agreement probably cannot be expected.

Currents computed by FNWC for this area are in the opposite direction of measured flow at about 12.8 cm/sec. Since the FNWC current consists of both geostrophic and wind components, the wind component appears to be the dominant component in this case.

Two factors might improve the confidence in these results.

First would be better navigation control than the Loran C provides in this area (± 0.5 nmi), and second, a longer period of current observations. A second experiment was designed and performed to correct these difficulties.

Experiment II

The results of the first experiment indicated that the T-S Gradient method of computing geostrophic component of the flow yielded better agreement between computed and observed currents than did FNWC techniques. Yet the navigational control was not completely satisfying. On this cruise the ship's Loran navigation was supplemented with Lorac navigation, a highly accurate system capable of providing fixes to within 0.1 nmi. Experiment II was performed 50 nmi south of Point Arguello (Station A) using the U. S. Navy Pacific Missile Range Lorac system December 4, through December 7, 1967.

Purpose

The purpose was the same as for Experiment I.

Sampling Procedure

The sampling procedure was altered from Experiment I to provide two 24 hour stations (A and B) at which one cast was taken

approximately every two hours. Each station was marked with a taut moored surface marker. Drogue current measurements were made at each station. Station B was established perpendicular to the flow measured at Station A. A savonius rotor current meter was moored at Station B at a depth of 10 m. The locations of the stations were:

A = 33° 43.8' N, 120° 45.5' W

B = 33° 28.7' N, 121° 40.0' W

Meteorological Conditions

The winds were Beaufort 3 to Beaufort 5 over the entire cruise, with Beaufort 3 prevailing at Station A and Beaufort 5 at Station B. The winds were from 230° to 340° true over the entire cruise, predominantly from 320° to 340° true. The swell and sea were predominantly from 320° true.

Current Measurements

Station A was occupied first and a reference mooring was established. Unfortunately the mooring did not hold and drifted slowly to the south-southeast. However, six drogues were seeded in an east-west line around the mooring. The movement of the drogues relative to the reference float was determined by radar. These measurements do not yield absolute currents since the

mooring was moving. However, the drogue positions were determined frequently between casts by running alongside the drogues and noting their Lorac positions. Again the surface current was determined by averaging the straight line movement between successive positions. The measurements were divided into three intervals. During the first interval drogues 1 and 6 did not move consistently with drogues 2, 3, 4, and 5 and were eliminated. During the second period all drogues moved consistently. During the third interval drogue 6 was eliminated.

During the first period, 21:33 on December 4, 1967 to 14:44 on December 5, 1967, the drogues moved at 9.8 cm/sec toward 127° true. During the second period, 14:40 to 17:40, December 5, 1967, the drogues moved at 16.2 cm/sec toward 129° true. During the last period. 17:28 on December 5, 1967 to 11:28 on December 6, 1967, they moved 13.2 cm/sec toward 163° true.

At Station B another reference mooring was set, at right angles to the flow measured at Station A, and again six drogues were seeded. On this mooring a continuous recording savonious current meter was placed at 10 m below the surface on the mooring. Several problems were encountered at this station. Radar contact with the drogues was lost after only a few hours, too short a time to determine significant movement. Attempts to position the drogues by running alongside and taking their Lorac position failed when the

Lorac signal was lost. Reliable current measurements could not be determined from the drogues. The current meter on the mooring should have provided independent measure of the currents, but the recorder paper failed to advance and the record was of no value.

Hydrographic Measurements

The hydrographic stations were established prior to the cruise. Hydrographic casts were to be initiated every two hours, however, delays of up to one hour were experienced. Only 10 casts of the 12 planned at each station were obtained. The hydrographic station data is on file at the Naval Postgraduate School, Monterey, California, under NPGS Cruise A-2, 1967. Again, the stations were approximately perpendicular to the measured drift of the drogues at Station A. The section established will give the geostrophic current components along 160/340° true. The hydrographic data at each station was averaged to remove insofar as possible any short period variations, or measurement errors.

In a second analysis of the geostrophic currents, the XBT temperatures were substituted for the reversing thermometer temperatures and the computations repeated. The purpose of this analysis was to see if the current structure derived from the XBT data would agree with the analysis from the reversing thermometer temperatures.

Results

The velocity profiles for both sets of data are shown in Figure A. V-1. Since the values of the geostrophic current computed by both the T-S Gradient and the standard method agreed at all levels to within 0. 02 cm/sec only the T-S Gradient value is given. The surface current computed by the standard method, the T-S Gradient method, FNWC, and the drogue measured current at Station A are compared in Table A. V-3.

Table A. V-3. Comparison of computed and measured geostrophic surface currents for Experiment II.

	Standard Method		T-S Gradient		FNWC	Measured
	Reversing Thermometer	XBT	Reversing Thermometer	XBT		
Current Speed (cm/sec)	3. 3	4. 5	3. 3	4. 5	12. 7 to 20. 5	9. 7 to 16. 8
Current Direction (degrees true)	160°	160°	160°	160°	150° to 160°	125° to 165°

Conclusions

The surface geostrophic current through this section is 3. 3 cm/sec by both the standard geostrophic method and the T-S Gradient method using reversing thermometer temperatures. Both methods yield 4. 5 cm/sec when the XBT temperatures are substituted for the

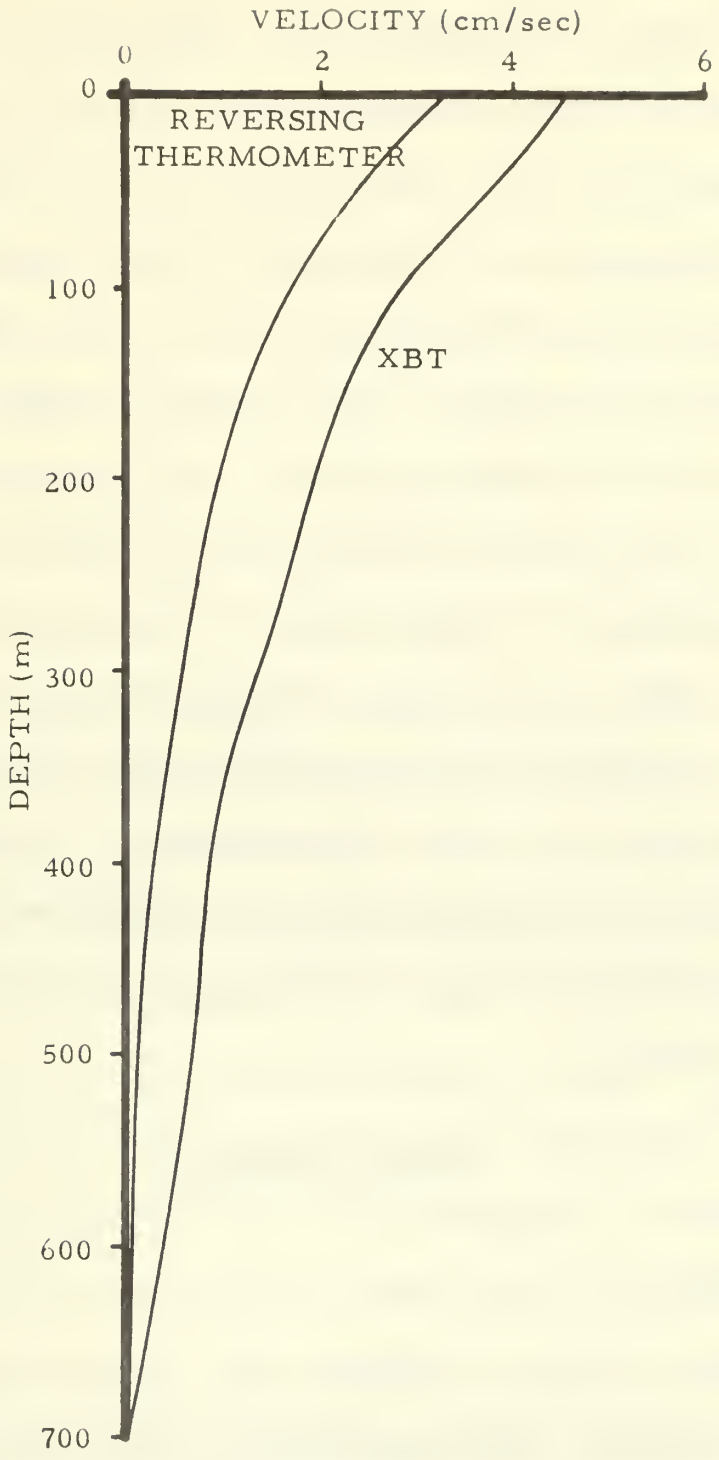

Figure AV-1. Comparison of geostrophic velocity profiles using reversing thermometer temperatures and XBT temperatures in Experiment II.

reversing thermometer temperatures. The FNWC computations yield a surface current between 12. 7 cm/sec and 20. 3 cm/sec with directions between 125° true and 165° true. These values are in substantial agreement with the drogue measurements of 9. 7 cm/sec to 16. 8 cm/sec with directions between 150° true and 165° true. If the wind drift computed according to FNWC is added to the geostrophic surface currents the currents would be increased by 18 cm/sec. This would lead to surface currents somewhat larger than those measured for the standard and T-S Gradient geostrophic computations. However, the drogue measured surface currents averaged over a depth interval of approximately eight meters around the ten meter depth of the center of the parachute. Therefore, one would expect the measured currents to be slightly lower than the current at the very surface. The influence of other factors has not been considered.

Recommendations

Introduction

Clearly the results of these two experiments cannot be considered conclusive. Much more experimental work is necessary to establish any relationship between actual currents in the ocean and those determined by indirect computation. Even though every effort was made to maintain the tightest possible experimental control

during these studies further control is necessary and possible. Two recent developments would have improved the possible control in these experiments. These developments are the commercial availability of reliable continuous profiling salinity-temperature-pressure systems (STP) (Brown, 1968), and satellite navigation systems (Warriner, 1958). In the following paragraphs another experiment is described, incorporating these developments and other improvements that occur to this researcher for the continuation of this work.

The STP provides a continuous profile of temperature and salinity as a function of depth to at least classical Nansen bottle and reversing thermometer accuracy ($\pm$ 0.02 ‰, $\pm$ 0.02°C, $\pm$ 4 m) (Bissett Berman Corporation, 1968). The continuous profile of these variables also eliminates the need to interpolate discrete Nansen data and the associated interpolation error. Another advantage of the STP over the classical Nansen approach is speed, since a cast can be completed in less than half the Nansen cast time. Finally, a distinct advantage of the STP is the repeatability of the measures. The repeatability of the STP is two times better than the absolute measurement accuracy, that is, $\pm$0.01 ‰, $\pm$ 0.01°C, and $\pm$ 2 m. Taking advantage of this repeatability very precise difference measurements necessary for geostrophic computations are possible. Thus, using the STP the measurement and computational errors in geostrophic computations could be substantially reduced.

The U. S. Navy has used satellite navigation on its vessels since 1964 (Warriner, 1968). In 1967 the system was released for private users, and receivers are now available commercially which will yield position accuracy of better than 0.1 nmi anywhere in the ocean (Magnavox Corporation, 1968). This represents at least a five-fold increase in accuracy over the best previous open ocean navigation system.

Proposed Experiment

The purpose of the experimental work discussed here is to establish the relationship between the currents at a point in the ocean and driving forces. Since currents exhibit a turbulent nature over a wide range of scales it is clear that we will never be able to specify the instantaneous velocity indirectly. However, for the purpose of contemporary forecasting this impossibility is not necessary. In the continuation of this research a modification of the experimental procedure used in this study is recommended.

Stations

Three stations should be established, initially in an area where the surface currents are not disturbed by topographic influences, such that the sections between the stations enclose a triangular region. The primary reason for the triangular array is the fact that

the three stations are the minimum number forming a closed element. Continuity considerations can be used for a closed element to help reduce ambiguities in the results. Furthermore, the geostrophic currents perpendicular to the three sections formed by the sides of the triangular station pattern will allow vector resolution of the actual current. Station locations should be marked with suitable taut moorings. Station separation should be determined by the criterion suggested by Reed and Laird (1965) that the dynamic difference between the stations be five times the error in the dynamic computations (see Chapter III). However, because of the potential repeatability of the STP and precision of the satellite navigation the station separation might be reduced from that used in Experiments I and II, keeping the transit time between stations to a minimum.

Sampling

Sampling of the following parameters should be performed at each station as outlined in the following discussion:

1. Temperature and salinity should be measured from the surface to 1,000 m.
2. Surface currents and currents at 1,000 m should be measured over the period of the study.
3. Surface wind should be measured and recorded over the period of the study.

4. Sea conditions should be measured and recorded over the period of the study.
5. Barometric pressure should be recorded over the period of the study.

Sampling should be conducted such that significant periodic variation in the structure can be identified.

Phase I - Establish Initial Conditions

At each station the taut line moor should be established, drogues with radar transponders should be set at the surface and 1,000 m, and the best satellite position obtained. Once the station has been established, two STD lowerings should be made to 1,000 db, Nansen bottles with reversing thermometers placed at 0, 500, and 1,000 db. During the period of the STD casts XBT's should be launched every ten minutes. This procedure should be followed at each station. The vessel should proceed between stations at maximum cruising speed. Between stations XBT's should be launched every one-half hour. Given a station separation of 40 km the first phase will require approximately 24 hours. Phase I establishes the stations to be used in Phase II, the initial hydrographic conditions, and the short term variability.

Phase II - Sampling

The purpose of Phase II is to establish the median conditions over the period to provide the best estimate of the factors contributing to the surface flow. Only the significant factors should be considered. Returning to each station in initial order, 24 hour time-series sampling should be initiated to the 1,000 db level. STD casts will be made every hour, with XBT probes launched every one-half hour. A parachute drogue will be established at the start of this phase at 1,000 db and at the surface, the position of the drogues in the water at each station should be established every one-half hour. As the drogues are lost, they should be replaced. The ships position will be maintained at the reference position. Again the vessel should proceed between 24 hour stations at maximum cruising speed, launching XBT's every one-half hour.

At the conclusion of the time series sampling the vessel should proceed to locate as many drogues as possible, recover the radar transponders and then the surface buoys. Approximately 96 hours would be required for Phase II exclusive of equipment recovery time.

Analysis

The currents through the array should be determined by both direct and indirect methods. The computed surface currents should

be compared to the measured surface currents. Wind data should be used to compute the wind component by various formulae to determine the best expression to use to obtain agreement between measured and computed surface currents. Significant periodic variations in the measured currents could be correlated with variations in the structure and local winds and tides to determine any relationships between these factors and the currents.

Many other questions could be answered by the data collected in this experiment. These questions should not be ignored, but the goal of the experiment is to determine the relationships between observed and computed ocean surface currents.

DISTRIBUTION LIST

	No. of Copies
Defense Documentation Center Cameron Station, Bldg. 5 Alexandria, Virginia 22314	20
Fleet Numerical Weather Center Monterey, California	20
Dean of Research Administration Naval Postgraduate School Monterey, California 93940	2
Library Naval Postgraduate School Monterey, California 93940	2
Professor Warren W. Denner Department of Oceanography Naval Postgraduate School Monterey, California 93940	25

(Abstract, Continued)

specific volume on temperature, $\alpha(T)_{S,P}$, can be expressed by a quadratic equation and the dependence of specific volume on salinity, $\alpha(S)_{T,P}$, can be expressed by a linear equation. The coefficients in the temperature dependence equation are a function of salinity and pressure, and the coefficient in the salinity dependence is a function of temperature and pressure. However, it is shown that the lack of experimental data and the presence of small errors in the data lead to inconsistencies in the values of the coefficients derived. This difficulty is corrected using Ekman's equation of state for sea water to generate P-V-T-S data.

Using derived expressions for $(\partial\alpha/\partial T)_{S,P}$ and $(\partial\alpha/\partial S)_{T,P}$ and equation is derived from the Helland-Hansen relationship and is called the Temperature-Salinity Gradient scheme for computing geostrophic currents, or simply T-S Gradient scheme. This scheme gives equivalent results to the standard geostrophic computations, yet is computationally much simpler and faster than the standard scheme. Other advantages are (1) the variables observed in the ocean, temperature and salinity structure are used directly in the computations, (2) no other quantities such as σ_o and σ_t need be computed, and (3) thermal and haline contributions to the geostrophic flow can be expressed independently.

The T-S Gradient scheme is applied to existing hemispheric fields of T and S data. It is shown that in the expressions for $(\partial\alpha/\partial T)_{S,P}$ and $(\partial\alpha/\partial S)_{T,P}$ the use of fixed coefficients over the entire Pacific Ocean relative to a reference level of 1000 db, introduces less than five percent error in the surface velocity. This application shows the feasibility of making geostrophic computations by the T-S gradient scheme. Unfortunately, it also shows the deficiencies of the available fields for hemispheric computations by any scheme. These deficiencies are (1) the inaccuracy of the data, (2) the large grid spacing, and (3) the inconsistency of the temperature and salinity fields. These must be corrected before hemispheric geostrophic computations can be made. The construction of new fields to meet the requirements of geostrophic computations using available data is discussed.

Two other aspects of current computation were investigated. First, using the capability of the T-S Gradient scheme to separate flow into thermal and haline components, the relationship between the thermal component and the total geostrophic surface current in the Gulf Stream water mass in the Grand Banks was studied. Results show that these quantities are satisfactorily related by a linear expression which allows the determination of the total geostrophic surface flow in this water mass using only temperature measurements. Such techniques may be useful in reducing survey time of the Coast Guard Ice Patrol in this region.

A second aspect investigated is the relationship between the indirectly computed currents and measured currents in the California current. Two experiments were performed in which drogue-measured surface currents were compared to indirectly computed currents given by the Fleet Numerical Weather Central and those computed by the Helland-Hansen and T-S Gradient schemes using standard hydrographic data. This investigation points out the significant need for more work on this aspect.

UNCLASSIFIED
Security Classification

DOCUMENT CONTROL DATA - R & D

Security classification of title, body of abstract and indexing annotation must be entered when the overall report is classified)

1 ORIGINATING ACTIVITY (Corporate author) Naval Postgraduate School Monterey, California	2a. REPORT SECURITY CLASSIFICATION UNCLASSIFIED 2b. GROUP

3 REPORT TITLE

The T-S Gradient Method, A New Method of Computing Geostrophic Currents over Large Ocean Areas

4 DESCRIPTIVE NOTES (Type of report and, inclusive dates)
Technical Report, 1969

5 AUTHOR(S) (First name, middle initial, last name)
Warren W. Denner

6. REPORT DATE 1 July 1969	7a. TOTAL NO. OF PAGES 201	7b. NO. OF REFS 62
8a. CONTRACT OR GRANT NO. b. PROJECT NO. Work Request 9-0011 c. d.	9a. ORIGINATOR'S REPORT NUMBER(S) NPS-58DW9072A 9b. OTHER REPORT NO(S) (Any other numbers that may be assigned this report)	

10. DISTRIBUTION STATEMENT
This document has been approved for public release and sale; its distribution is unlimited.

11. SUPPLEMENTARY NOTES This project funded by: Fleet Numerical Weather Central Monterey, California	12. SPONSORING MILITARY ACTIVITY Naval Postgraduate School Monterey, California

13. ABSTRACT

Requirements for indirect computation of geostrophic surface currents over large ocean areas are discussed. These requirements point to a need to simplify standard geostrophic computations, and to separate the first order thermal and haline contributions to geostrophic flow.

The equations of motion for geostrophic flow are reviewed and the standard geostrophic computations discussed. Errors and limitations in the geostrophic method are reviewed. Previous attempts to simplify geostrophic computations are discussed and shown to be inadequate for synoptic computation over hemispheric ocean areas.

It is shown that the Helland-Hansen equation can be rewritten such that the geostrophic velocity is composed of a temperature structure term and a salinity structure term. In order to apply this modified equation to hemispheric synoptic geostrophic computations, simple expressions are required for the dependence of specific volume on temperature at constant salinity and pressure, $(\partial\alpha/\partial T)_{S,P}$, and on salinity at constant temperature and pressure, $(\partial\alpha/\partial S)_{T,P}$. Two approaches are explored to derive these expressions, using:

1) Experimental P-V-T-S data collected in the laboratory.
2) P-V-T-S data derived from an equation of state for sea water.

Numerical fitting of the experimental P-V-T-S data shows that the dependence of

DD FORM 1 NOV 65 1473 (PAGE 1)
S/N 0101-807-6811

UNCLASSIFIED
Security Classification

A-31408

UNCLASSIFIED
Security Classification

14 KEY WORDS	LINK A		LINK B		LINK
	ROLE	WT	ROLE	WT	ROLE
Surface currents					
Geostrophic computations					
Dynamic computations					
T-S Gradient method					

DD FORM 1 NOV 65 1473 (BACK)
S/N 0101-807-6821

UNCLASSIFIED
Security Classification

A-3140